Analysis of Inorganic Carbon and pH in the Western Arm of Lake Superior

A THESIS
SUBMITTED TO THE FACULTY OF THE
UNIVERSITY OF MINNESOTA
BY

Cody James Tennant

IN PARTIAL FULFILLMENT OF THE REQUIREMENTS
FOR THE DEGREE OF
MASTER OF SCIENCE

Elizabeth Austin-Minor

May 2016

Acknowledgements

First, I would like to thank Elizabeth Austin-Minor for her time, advice, and help during my time at the Large Lakes Observatory at the University of Minnesota Duluth. This project would not have been possible without her expertise and guidance. Second, I would like to thank Erik Brown and Kathryn Schreiner for serving on my committee and providing insight along the way during my progress throughout this project. Third, I would like to thank the captain and crew of the *R/V Blue Heron* and the entire Large Lakes Observatory personnel for creating a fun, engaging, open, and joyful work atmosphere. Fourth, I would like to thank the Minor Lab Group for help with sampling and analysis. Lastly, I would like to thank the State of Minnesota Legislative-Citizen Commission on Minnesota Resources for funding this project.

Abstract

Although Lake Superior is Earth's largest lake by surface area, few studies have outlined its inorganic carbon cycle, including whether the lake is net heterotrophic (a source of CO_2 to the atmosphere) or autotrophic (a sink of atmospheric CO_2). Comparing the lake surface water pCO_2 values to atmospheric pCO_2 allows for the determination of the balance between primary production and respiration within the lake. This study expands upon previous studies by applying improved spectrophotometric pH measurement methods along with total inorganic carbon and alkalinity measurements to calculate lake surface pCO_2 and overall air-water differences in pCO_2 (ΔpCO_2) at a greater number of sampling locations and collection times in the western arm of Lake Superior. The pH measurements in this study also provide a well-characterized timepoint for determining long term trends in lake acidity as a function of climate change.

Western Lake Superior ("the western arm") was determined to be net heterotrophic in spring and approximately neutral in summer, before again turning net heterotrophic in the fall. Surface water pCO_2 values were found to be higher on average and more variable overall in the 2014 sampling season (relative to 2015) perhaps because of the harsher preceding winter. On a seasonal basis, measured pH values followed an antiphase relationship to pCO_2 with the lowest values occurring in the spring and increasing throughout the summer with a higher overall average occurring after the milder 2014-15 winter. Our data indicates that Lake Superior may provide a negative feedback loop buffering changes in local climate. This is due, in part, to the strong

dominance of heterotrophy that is observed after cold winters which delay the start of thermal stratification, ultimately outgassing more CO_2.

Table of Contents

List of Tables

List of Figures

I. Introduction

Lake Superior is the largest freshwater lake by surface area in the world and contains approximately 10% of the Earth's surface freshwater (McManus et al. 2003; Cotner et al. 2004; Bennington et al. 2012; Atilla et al. 2011). Surrounding Lake Superior and sharing its shoreline are multiple U.S. states: Michigan, Minnesota, Wisconsin, and the Ontario province of Canada (Bennington et al. 2012). Lake Superior, with an average depth of 150 m and maximum depth of over 400 m, is the coldest and deepest of the Laurentian Great Lakes (Bennington et al. 2012). Freshwater ecosystems offer many goods and services including fisheries, biological diversity, nutrient retention, and clean water (Meyer et al. 1999). The quality and services offered by freshwater ecosystems could be significantly altered under a changing climate and changes in resource use by humans in response to climate change (Murdoch et al. 2000).

Climate change is predicted to have many effects on planet Earth (Meyer et al. 1999; Rahel and Olden 2008). Two of the leading and most studied aspects of climate change are increasing atmospheric temperature and carbon dioxide concentrations. Under a business-as-usual atmospheric emission scenario, pH in the Laurentian Great Lakes is projected to decrease by 0.29-0.49 units by the year 2100 (Phillips et al. 2015). Lake acidification could significantly impact calcifying bivalves such as native unionids and invasive dreissenids, zebra (*Dreissena polymorpha*) and quagga (*Dreissena rostriformis bugensis*) mussels whose shells are predominantly made of aragonite (Phillips et al. 2015). This could have large implications for the cycling of C, N, and P within the Great Lakes as dreissenid tissues have been shown to be a significant sink of nutrients (Ozersky et al. 2015).

Sterner (2010) states that a well-constrained organic carbon budget is foundational to understanding the dynamics and biogeochemistry of a given ecosystem. However, little work has outlined the inorganic carbon budget and cycling in Lake Superior. The relatively small number of studies and lack of wintertime sampling observations contribute to the inability to balance Lake Superior's carbon budget (Atilla et al. 2011). According to Bennington et al. (2012), inland waters have previously been neglected by inverse modelers because air-water CO_2 fluxes were unknown or assumed to be insignificant. Even if Lake Superior is shown to be overall net heterotrophic (source of CO_2 to the atmosphere), increasing atmospheric pCO_2 should promote acidification due to the reduced efflux from the lake during periods of mixing where the entire water column is equilibrated with the atmosphere (Phillips et al. 2015). Further studies are needed to balance the carbon budget by recognizing air-water CO_2 fluxes within the lake.

Alin and Johnson (2007) used published measurements of pH, total alkalinity, dissolved inorganic carbon, and temperature coupled with CO2SYS (Lewis and Wallace, 1998) to calculate CO_2 lake-atmosphere exchange with latitude for the world's large lakes. It was concluded that, on the basis of CO_2 concentrations alone, a gradient occurs ranging from net autotrophic in tropical latitudes to increasingly heterotrophic at higher latitudes (Alin and Johnson, 2007). Lake Superior, with an average latitude of about 47^0, falls in the middle of the latitude gradient studied (between the equator and about 67^0 N) by Alin and Johnson (2007). This brings into question where along the trophic gradient (i.e., net heterotrophic vs net autotrophic) Lake Superior generally resides as well as how this position may change seasonally throughout the year.

Few sampling efforts have outlined the inorganic carbon cycle throughout the lake. Urban et al. (2005) concluded net heterotrophy in Lake Superior based on small-scale, point measurements of photosynthesis, respiration, and bacterial growth taken along three transects extending from 0 to 21 km offshore of the Keweenaw Peninsula. McManus et al. (2003) determined the western arm of Lake Superior to be supersaturated everywhere during the summer 2001 stratified period, determining the lake to be a net source of CO_2 to the atmosphere with the highest pCO_2 levels at the surface. Based on U.S. EPA bi-yearly measurements (spring and summer), Atilla et al. (2011) concluded that the open waters of Lake Superior were a source of CO_2 to the atmosphere in spring and were approximately neutral in summer between 1996 and 2006. A modeling study by Bennington et al. (2012) attempted to further apply this data on an annual basis. It was concluded that the lake may act as a sink of CO_2 during the late winter/early spring before warming and the resultant flux of CO_2 to the atmosphere during spring (Bennington et al. 2012). The lake was determined to act as either a small sink or neutrally during the summer and to remain a sink until winter mixing returns (Bennington et al. 2012).

In contrast to the Atilla et al. (2011) and Urban et al. (2005) studies above, Kelly et al. (2001) concluded that there was net autotrophy (with a net CO_2 flux of 7.80 mMol m^{-2} d^{-1} into the lake) in Lake Superior based on samples from June to October 1989. This summertime CO_2 flux into the lake from the atmosphere is consistent with the results of the Bennington et al. (2012) modeling study. Kelly et al. (2001) also concluded that the

temporal variability in surface water pCO_2 in Lake Superior is lower than in smaller lakes due to lack of ice cover and winter CO_2 buildup.

The Environmental Protection Agency has been monitoring Lake Superior water quality since the early 1990s (Atilla et al. 2011). The bi-yearly water quality parameters that are measured at 19 open-lake stations are pH (electrode measurement), alkalinity, and temperature at four depths within the water column (Atilla et al. 2011; https://www.epa.gov/great-lakes-legacy-act/great-lakes-environmental-database-glenda). These data are useful in providing snapshots of the lake system but are restricted to April and August and to specific open-lake locations. The use of pH electrodes for these measurements poses a risk of erroneous data and electrode drift, leading to the need for more precise and accurate lake-wide pH measurements. According to French et al. (2002), freshwater electrode measured pH values are not sufficiently accurate or precise for modeling carbonate equilibria and long-term trends in aquatic ecosystems with little ionic strength. Spectrophotometric pH measurements, based on well-defined thermodynamic principles are more accurate and precise (French et al. 2002).

This study expands upon previous studies by applying improved pH measurement methods, measuring total inorganic carbon concentrations as well as alkalinity, and increasing the number of sampling locations and collection times in the western arm of Lake Superior. The main focus will be on organic and inorganic carbon cycling in the attempt to determine net heterotrophy or autotrophy and whether the lake is a net source or sink of atmospheric carbon. The main objective was to develop a western arm-wide survey of organic and inorganic carbon, pH (spectrophotometric measurement), and

alkalinity for the lake as well as to expand the assessment of seasonal changes in these parameters to spring, summer and fall and to perform preliminary winter assessments with limited under-ice sampling. The insight and benchmark water chemistry measurements gained through this study will inform future work to assess climate change effects in Earth's largest lake.

II. Methods

II.a Study Area

Lake Superior was sampled nine times from May to October and once in February over the years of 2014-15. The sampling locations, all located in the western arm of the lake, were visited as part of a coordinated sampling initiative to investigate lake biogeochemistry funded by the Legislative-Citizen Commission on Minnesota Resources (LCCMR). All cruises took place on the University of Minnesota Duluth's R/V *Blue Heron*. Rivers discharging to Lake Superior were also sampled to gain an insight as to the incoming water characteristics that may influence the carbon dynamics and buffering capacity of the lake. The rivers sampled were the St. Louis, Nemadji, and Amity Creek (all in the Superior, Wisconsin, Duluth, Minnesota area, see Appendix **Table VI-11**).

Table II-1. Lake Superior sampling dates over the years of 2014-15.

Cruise	**Blue Heron Cruise Number**	**Departure**	**Arrival**
LCCMR1	BH14-03	6/3/2014	6/6/2014
LCCMR2-3	BH14-09	7/22/2014	7/25/2014
LCCMR4	BH14-13	8/16/2014	8/19/2014
UNOLS Inspection		9/24/2014	9/24/2014
LCCMR5	BH14-19	9/30/2014	10/2/2014
Bayfield Ice Road		2/8/2015	2/8/2015
LCCMR6	BH15-02	5/19/2015	5/22/2015
LCCMR7	BH15-07	7/15/2015	7/17/2015
LCCMR8	BH15-12	9/8/2015	9/10/2015
LCCMR9	BH15-17	10/5/2015	10/7/2015

Figure II-1. Lake Superior western arm sampling locations.

II.b Sample Collection

Samples for determination of alkalinity, pH, total organic carbon (TOC), dissolved organic carbon (DOC), total inorganic carbon (TIC), and chlorophyll fluorescence were collected at each sampling location. Using careful sampling to prevent contamination, including the use of nitrile gloves for all carbon samples, all sample bottles were rinsed three times with sample prior to sample collection. River samples were collected in areas of active flow by submergence of the bottles under the water surface. Lake samples were collected using a SeaBird 32 Carousel outfitted with 12 8-liter capacity Niskin bottles deployed on CTD casts at depths to be determined at each sampling location. To minimize the effects of atmospheric exchange, lake samples for

TIC, alkalinity, and pH were allowed to overflow for the same duration as the bottle fill before sample collection. Alkalinity, pH, and DOC samples were collected in plastic Nalgene bottles, prior to filtering in the case of DOC, and analysis. TOC samples were collected directly without overflow in 40 mL amber sample vials, and TIC samples were collected in 500 mL amber glass bottles. All glass and plastic ware used in sampling had been leached with 10% hydrochloric acid (HCl) and thoroughly rinsed with deionized water prior to sampling date. All glassware was ashed at 450 °C for at least 4 hours prior to use.

II.c CTD Profiles

Conductivity, temperature, and depth (pressure) were measured using a SeaBird Model 911 lowered off the stern of the ship through the water column. This unit was attached below a carousel sampler fitted with 8-liter Niskin bottles and was also outfitted with sensors to measure dissolved oxygen, pH (electrode), oxidation reduction potential (ORP), chlorophyll fluorescence, colored dissolved particulate matter (CDOM), and photosynthetically active radiation (PAR).

II.d Atmospheric pCO_2

Atmospheric pCO_2 was obtained from the WLEF television tower located in Park Falls Wisconsin (45.9451° N, 90.2732° W); maintained by the National Oceanic and Atmospheric Administration (http://www.esrl.noaa.gov/gmd/dv/site/LEF.html).

Measurements of atmospheric pCO_2 were taken from the 396 m level and averaged for the duration of each cruise, representing what one would expect over Lake Superior (Ankur Desai; personal communication).

II.e Alkalinity

Alkalinity, also known as the acid neutralizing capacity of a whole-water sample, was analyzed by titration within 24 hours of sample collection by using the EPA GLNPO Total Alkalinity Titration protocol (http://www.epa.gov/greatlakes/lmmb/methods/alkali.pdf) and/or the USGS Gran titration protocol (http://water.usgs.gov/owq/FieldManual/Chapter6/section6.6). All alkalinity samples were stored in a refrigerator prior to analysis. A burette, and a HACH Manual Digital Titrator were used to titrate 0.234 M sulfuric acid (H_2SO_4) into a 100 mL aliquot of sample as measured by top-loading balance until a pH of 4.5 (EPA method), or a pH of 3 (USGS Gran method), determined by a Eutech Instruments pHTestr 20 pH meter previously calibrated with Fisher Scientific pH buffer standards. Analysis took place on both raw and filtered portions of sample. Filtration was through Millipore Type HNWP 0.45 µm filters using a manual vacuum pump and a glass filter apparatus. Moderate stirring action was used throughout the entire titration (USGS Gran method) and only increased near the endpoint (EPA method) to promote equilibration. Temperature was measured both before and after each titration. Known alkalinity control samples and MilliQ water blanks (including a filtration process blank) were titrated each day of sample analysis.

II.f pH

pH was analyzed spectrophotometrically on whole water within 24 hours of sample collection using a Genesis 6 UV-VIS Spectrophotometer. Prior to analysis, the samples, placed in a closed cuvette with minimal gas exchange, were warmed to a known temperature in a water bath. 2 mM Cresol red dye (70 µL for every 31 mL of sample) was added and each sample was measured for absorbance at the wavelengths of 740 nm (as a backscatter control) and 577 nm and 439 nm (the wavelengths of the base and acid forms of the dye) using a 10 cm cell. The resulting data was then used to calculate pH from the Henderson-Hasselbach equation, using the temperature-adjusted acid dissociation constant for cresol red (following French et al. 2002). An EDTA standard solution (pH 8.2) was used as an instrument and methods check standard.

II.g Organic Carbon

TOC and DOC were collected and analyzed following protocols in Zigah et al. 2011;2012; with samples preserved after collection in 40 mL amber vials using 6 M HCl (Certified American Chemical Society [ACS] Plus grade) to adjust the sample to a pH of 2.5. Dissolved organic carbon samples were processed by vacuum filtration using combusted Whatman GF/F filters. TOC and DOC samples were stored in the dark at 4 °C and were analyzed within 3 weeks of collection to minimize storage effects. A method blank was also processed as stated above on board the ship using MilliQ water and combusted GF/F filters. All samples were analyzed as non-purgeable organic carbon (NPOC) using a Shimadzu Total Organic Carbon-V_{CSH} Analyzer. Inorganic carbon was

removed by purging each sample for 3.5 minutes with high-grade CO_2-free air; before being injected (50 µL injection volume) and combusted at 720 °C. Evolved CO_2 gas was measured using a non-dispersive infrared (NDIR) detector. For each sample, a minimum of three injections were performed. If a standard deviation of 0.1 mg L^{-1} OC and coefficient of variation of 2% were not met, additional injections were performed up to a maximum of five and the closest three were averaged for sample concentration. Calibration and check standards were made using Acros Organics potassium hydrogen phthalate (KHP; ACS Reagent grade) and MilliQ water, and a deep-sea reference standard (Hansell lab, University of Miami) was included in every sample run.

II.h Inorganic Carbon

TIC was preserved after collection in 500 mL amber bottles (LCCMR1, 2-3, 4, 5, 6) and 40 mL amber vials (LCCMR7, 8, 9; each sample collected into replicate vials) using mercuric chloride ($HgCl_2$) and analyzed using a Shimadzu Total Organic Carbon-V_{CSH} Analyzer. Inorganic carbon in each sample was evolved to CO_2 gas with 25% by weight phosphoric acid (H_3PO_4), and measured using the NDIR detector. For each sample, a minimum of three injections (LCCMR1-6 manual sipper; LCCMR7-9 autosampler) were performed using a 50 µL injection volume for LCCMR1 and LCCMR5, and 100 µL volume for all other cruises and sample runs. If a standard deviation of 0.1 mg L^{-1} IC and coefficient of variation of 2% were not met, additional injections were performed up to a maximum of five and the closest three were averaged for sample concentration. Calibration and check standards were made using Ricca

Chemical Company Carbon Standard Inorganic (CAT NO 1845-16) and nitrogen-purged MilliQ water. Method blank samples were also included throughout the run using nitrogen-purged MilliQ water.

II.i Chlorophyll Fluorescence

Chlorophyll-*a* samples were first pre-filtered with an 80 µm Nitex screen to eliminate large zooplankton, and then recovered by filtration at low vacuum (≤6 inches or 150 mm Hg) of 100-400 mL of lake water through 0.2 µm cellulose nitrate filters. The samples were stored frozen and in the dark for a maximum of one month prior to analysis. Chlorophyll-*a* was extracted with 90% acetone (HPLC grade) and measured using a Turner Designs model 10-AU fluorometer previously calibrated with Turner Designs chlorophyll solutions of known concentration (EPA Method 445.0; Welschmeyer 1994).

II.j CO2SYS

pCO_2 values for river and lake samples were calculated using the program CO2SYS, which performs calculations relating parameters of the CO_2 system in seawater and freshwater (Lewis and Wallace, 1998). CO2SYS requires any two CO_2 system parameters (1. total alkalinity (TA), 2. total inorganic CO_2 (TCO_2), 3. fugacity (fCO_2) or partial pressure (pCO_2), and 4. pH) to serve as the inputs while the other two parameters are calculated at a given temperature and pressure (Lewis and Wallace, 1998). The program was run using freshwater dissociation constants and NBS scale pH (Millero,

1979). Surface water pCO_2 was calculated based on inputs of pH, TIC and both *in-situ* water temperature and laboratory determination temperature. The variability of calculated pCO_2 values by CO2SYS was most influenced by the pH input parameter, based on a sensitivity analysis conducted utilizing two of the following inputs (pH, TIC, alkalinity) and comparing the model-calculated output to the third measured parameter. The second input parameter, TIC, was selected based off of the limited amount of alkalinity measurements during the 2014 and 2015 sampling seasons. Model calculated alkalinity error percentages varied from -1.47% to -11.62% with an average error of -6.76% from measured alkalinity values in Lake Superior. The 153 spectrophotometric pH values obtained for the western arm of Lake Superior had an average standard deviation of 0.010 pH units. This level of precision in pH measurements far surpasses previous electrode measurements influenced by electrode drift. The 153 TIC samples obtained for Lake Superior had an average standard deviation of 0.11 mg L^{-1}.

II.k Statistical Analysis

In order to assess differences in the seasonality of lake surface pCO_2, paired two-sample t-tests for means were performed utilizing Microsoft Excel 2016 MSO (16.0.6828.1015). Because pairwise tests require the same number of observations for each input variable, stations not sampled at the same season in both years were removed, resulting in different degree of freedom numbers between each hypothesis test. Stations 6 and BP were not sampled during LCCMR1 and were therefore eliminated from LCCMR6 prior to input into the spring complete mixing significance test. Station BP which was not

sampled during LCCMR5 was eliminated from LCCMR9 prior to input into the early fall cooling significance test.

II.l U.S. EPA GLENDA pH and Alkalinity

To further assess the U.S. EPA GLENDA data, a yearly mean pH and alkalinity was calculated by averaging April and August surface water electrode pH and alkalinity measurements for the years 1996-2014. All routine field samples and quality control duplicates with the surface water depth code were utilized in the annual average with varying sampling depths all in the top 5 m of the water column. No samples were removed within each annual data set due to the already small amount of spatial data with only 19 spring and fall surface water stations per year. All electrode pH and alkalinity measurements included in annual averages were determined following the U.S. EPA LG500 method (Standard Operating Procedure for GLNPO Board Analyses [https://www3.epa.gov/greatlakes/monitoring/sop/chapter_5/LG500.pdf]) utilizing a Fisher Accumet Model 15 pH meter and strong acid titration (EPA GLNPO Total Alkalinity Titration protocol discussed previously). Surface water CTD electrode pH measurements taken following the U.S. EPA LG301 method (https://www3.epa.gov/greatlakes/monitoring/sop/chapter_3/LG301.pdf) from 2006-2012 were not included in annual averages due to extensive sample deviation likely outside the range of actual surface lake pH.

III. Results

III.a Temperature

In-situ CTD surface water (5 m) temperature measurements for the western arm of Lake Superior are shown below for 2014 (**Figure III-1** through **III-4)** and for 2015 (**Figure III-5** through **III-8)**. All CTD temperature measurements correspond to the depth of carousel sampling for both organic and inorganic carbon species. Near-shore (St. 11) and off-shore (St. 3, WM) temperature profiles are also included in each figure to show differences in lake stratification.

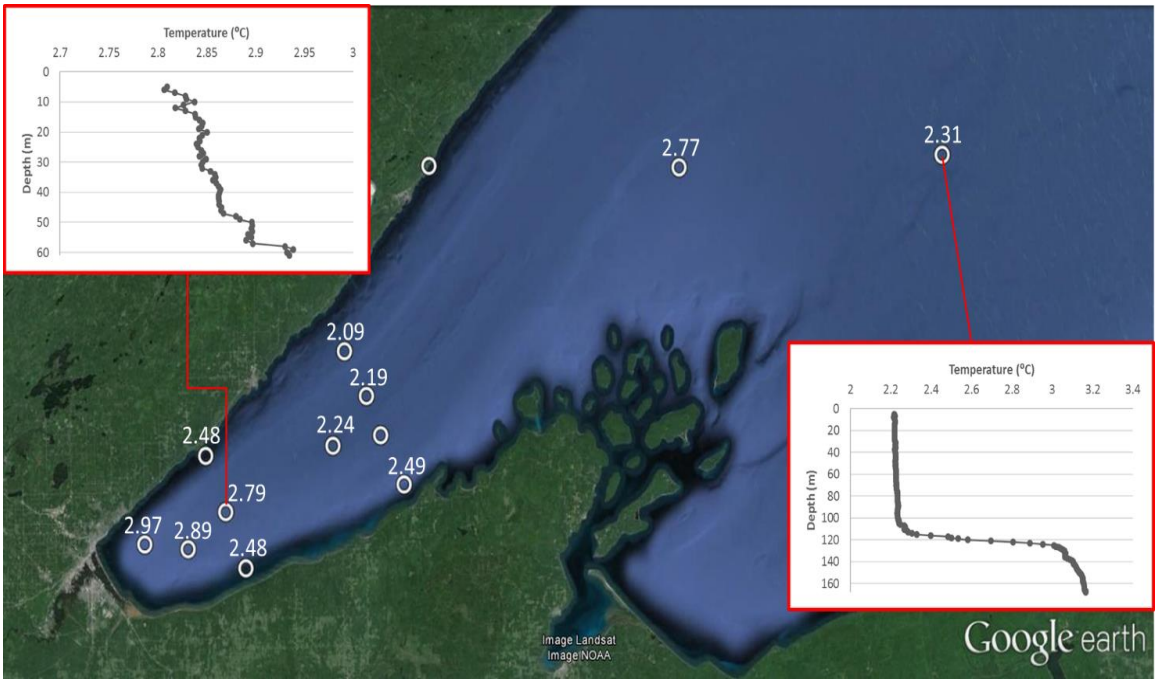

Figure III-1. *In-situ* CTD temperature measurements for western arm sampling stations corresponding to the sampling depth during LCCMR1 (June 2014). All surface water temperature measurements and samples taken at 5 m depth. Insets show water-column temperature profiles for Stations 11 (top left) and 3 (bottom right).

Figure III-1 shows relatively little variation in lake surface temperature throughout the entire western arm coming out of the harsh 2013-14 winter, in which over 90 percent of the lake was covered in ice from the beginning of February to early April (NOAA, Great Lakes Environmental Research Laboratory). Station 11 shows a relatively isothermal water column while Station 3 (WM) shows inverse stratification with bottom water approximately 1 ^{o}C warmer than surface water. As short-wave solar radiation is absorbed within the surface of the lake coupled with wind driven mixing, it begins to transmit further into the water column. **Figure III-2** shows the extent of solar warming in early summer, with the highest surface water temperature increases occurring in the near-shore stations as opposed to the off-shore station. The shallower south shore of the lake also warms faster than the deeper north shore. Station 11 is beginning to show thermal stratification in the top meters of the water column while the depth profile at Station 3 (WM) shows little temperature change.

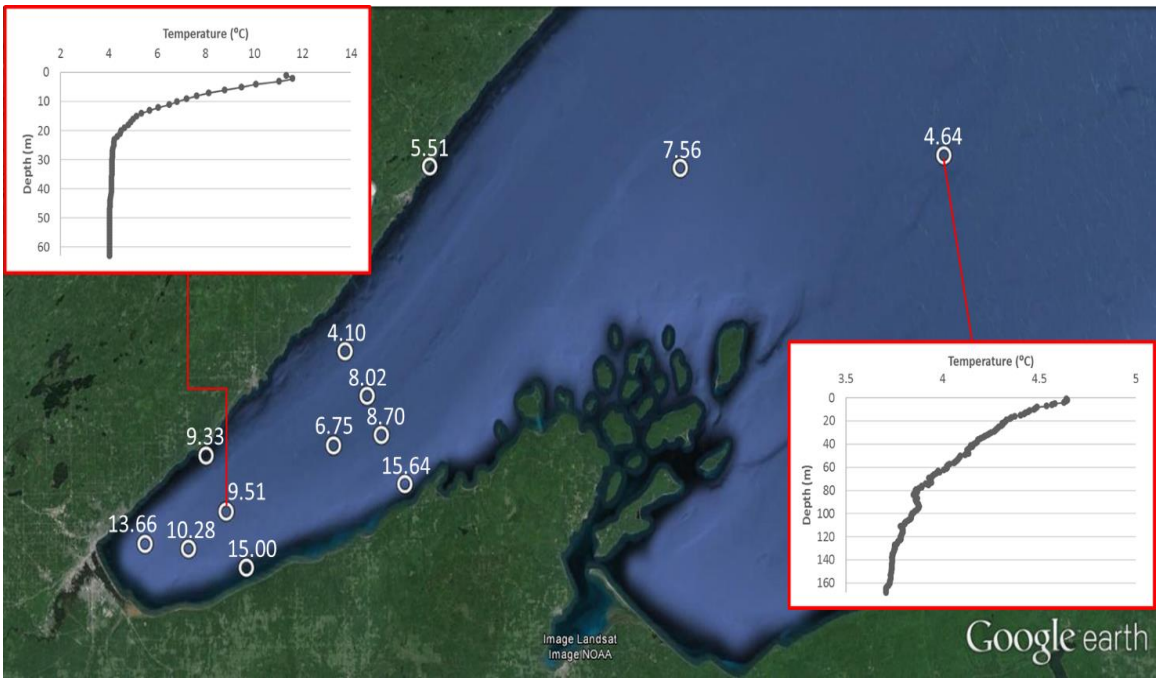

Figure III-2. *In-situ* CTD temperature measurements for western arm sampling stations corresponding to the sampling depth during LCCMR2-3 (July 2014). All surface water temperature measurements and samples taken at 5 m depth except St. 7 (15.64 °C) and 12 (15.00 °C) which were taken at 2 m. Insets show water-column temperature profiles for Stations 11 (top left) and 3 (bottom right).

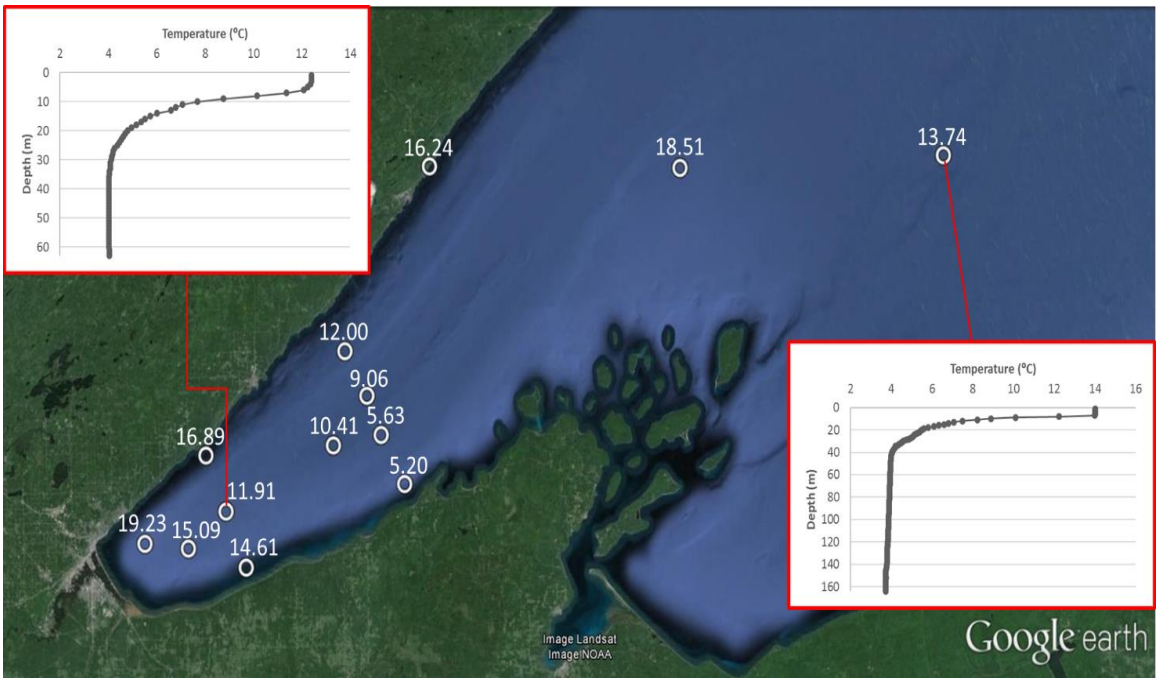

Figure III-3. *In-situ* CTD temperature measurements for western arm sampling stations corresponding to the sampling depth during LCCMR4 (August 2014). All surface water temperature measurements and samples taken at 5 m depth. Insets show water-column temperature profiles for Stations 11 (top left) and 3 (bottom right).

Figure III-3 shows the western arm of the lake continuing to warm with all stations showing thermal stratification in mid-August. Although Stations 6 and 7 (with temperatures of 5.63 and 5.20 °C respectively) show cooler water temperatures than the surrounding stations, their 5 m sampling depth corresponds to the depth of the thermocline. Further warming by solar radiation and wind driven mixing show increases in both the strength and depth of the thermocline in **Figure III-4**, coupled with slight surface water cooling throughout the western arm.

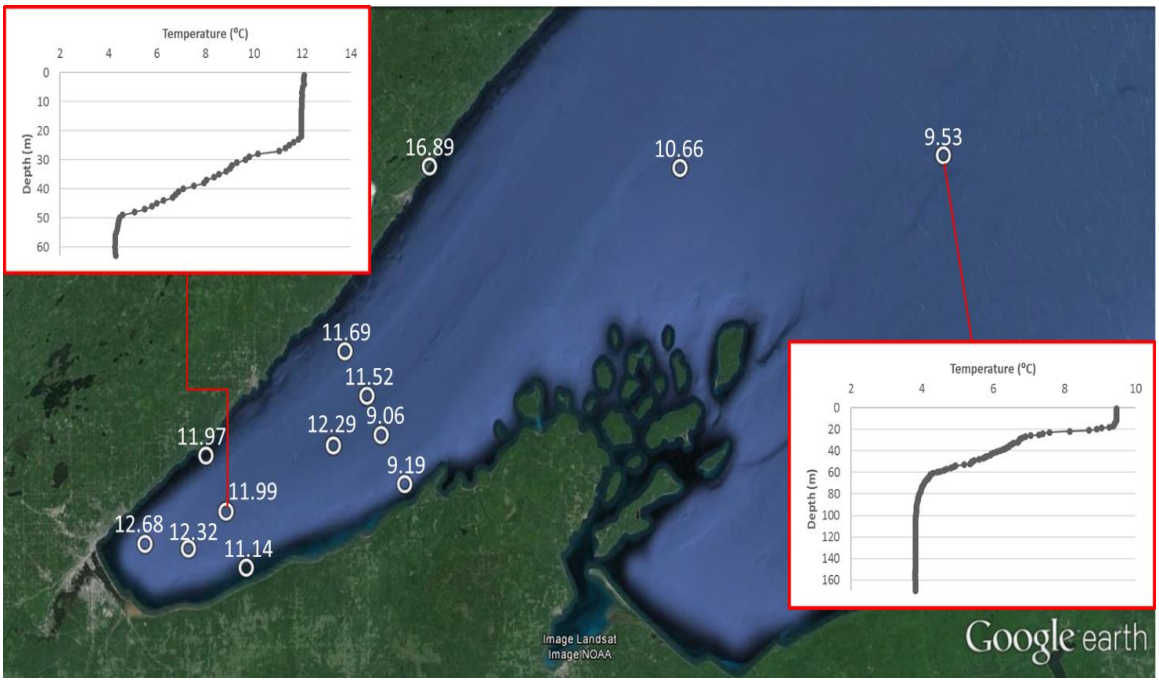

Figure III-4. *In-situ* CTD temperature measurements for western arm sampling stations corresponding to the sampling depth during LCCMR5 (Sept.-Oct. 2014). All surface water temperature measurements and samples taken at 5 m depth. Insets show water-column temperature profiles for Stations 11 (top left) and 3 (bottom right).

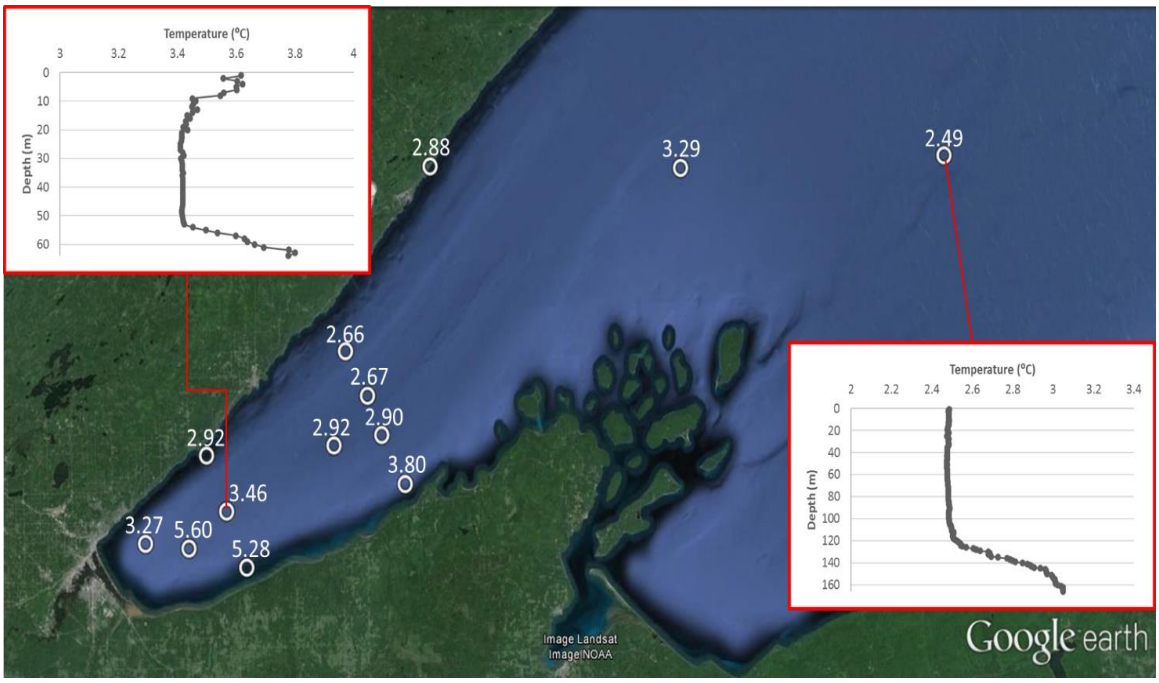

Figure III-5. *In-situ* CTD temperature measurements for western arm sampling stations corresponding to the sampling depth during LCCMR6 (May 2015). All surface water temperature measurements and samples taken at 5 m depth. Insets show water-column temperature profiles for Stations 11 (top left) and 3 (bottom right).

Figure III-5 shows little variation in surface water temperature after the 2014-15 winter in which over 90 percent of the lake was frozen from the middle of February to early March (NOAA, Great Lakes Environmental Research Laboratory). The 2015 ice-out date is one month earlier than the previous year, in which ice-out occurred in early April. Surface water temperatures at the near-shore stations were slightly higher in May, 2015 than they were in June, 2014. Station 11 shows a relatively isothermal water column while Station 3 (WM) shows inverse stratification with bottom water approximately 0.5 ^{o}C warmer than surface water. **Figure III-6** shows surface water warming more quickly

than the previous summer with lake-wide stratification occurring in mid-July (as opposed to mid-August in 2014).

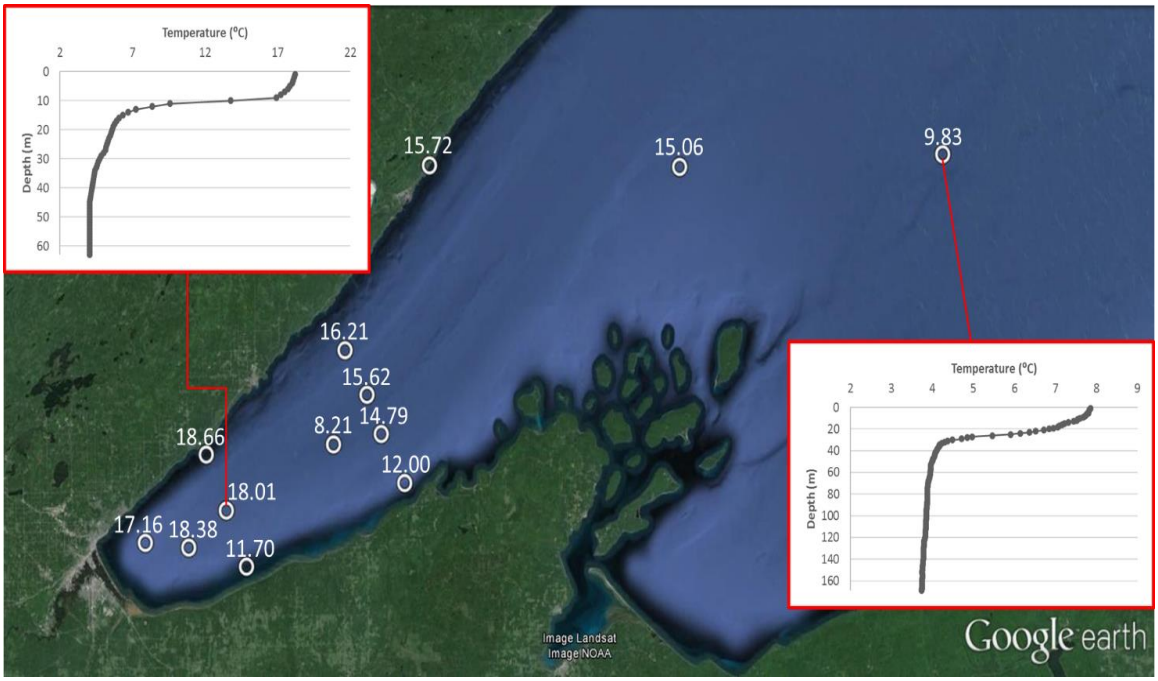

Figure III-6. *In-situ* CTD temperature measurements for western arm sampling stations corresponding to the sampling depth during LCCMR7 (July 2015). All surface water temperature measurements and samples taken at 5 m depth. Surface water temperature for Station 3 (WM) higher than depth profile due to different CTD casts for multiple sampling depths. Insets show water-column temperature profiles for Stations 11 (top left) and 3 (bottom right).

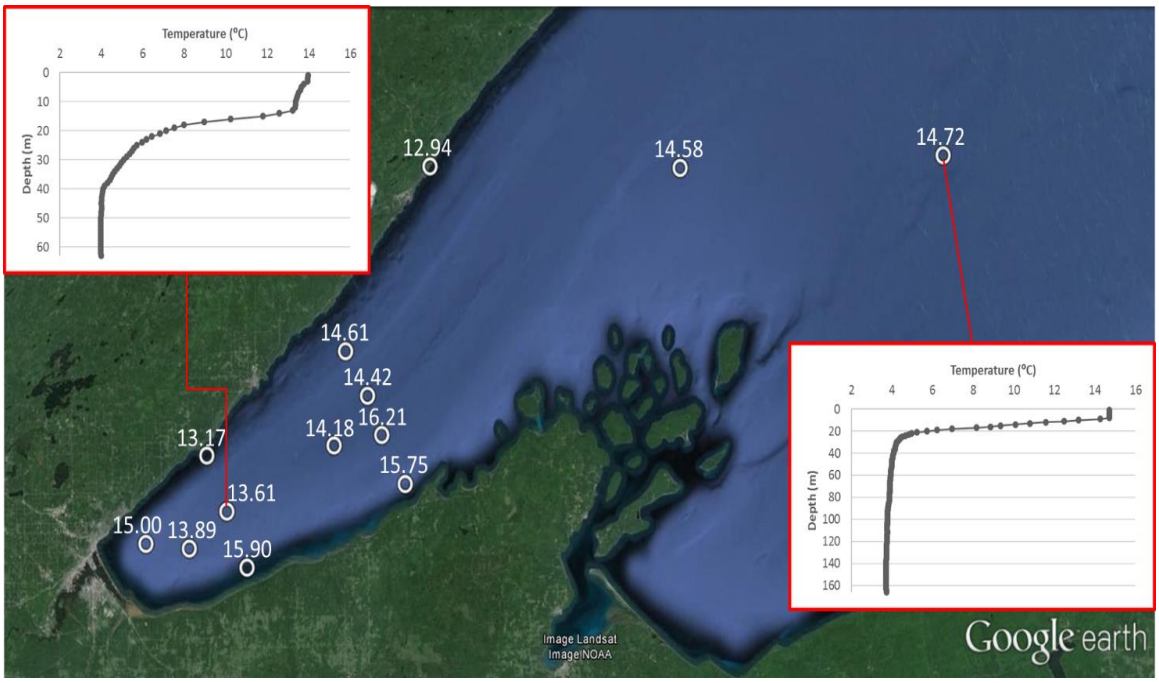

Figure III-7. *In-situ* CTD temperature measurements for western arm sampling stations corresponding to the sampling depth during LCCMR8 (September 2015). All surface water temperature measurements and samples taken at 5 m depth. Insets show water-column temperature profiles for Stations 11 (top left) and 3 (bottom right).

While the near-shore stations remain relatively constant in surface water temperature, the surface water of the open-lake (St. 3, WM) continues to warm in **Figure III-7** while thermocline remains at a constant depth. The depth profile inset for Station 11 shows a deepening of the thermocline corresponding with slight surface water cooling as compared to **Figure III-6**. This pattern continues in **Figure III-8** with further deepening of the thermocline at Station 11 while the surface waters of the western arm cooled overall. The depth of the thermocline in the open water remained relatively constant at 20 m depth (Station 3, WM; **Figure III-8**).

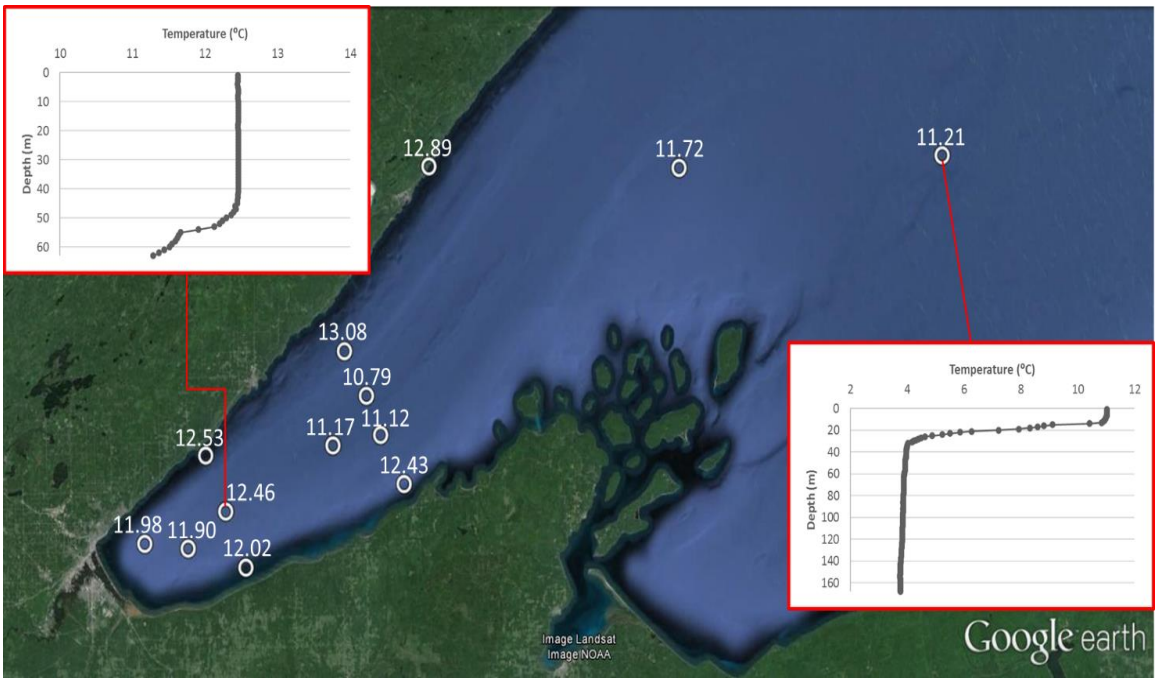

Figure III-8. *In-situ* CTD temperature measurements for western arm sampling stations corresponding to the sampling depth during LCCMR9 (October 2015). All surface water temperature measurements and samples taken at 5 m depth. Insets show water-column temperature profiles for Stations 11 (top left) and 3 (bottom right).

III.b pH

Spectrophotometric pH measurements for the western arm of Lake Superior are shown below for 2014 (**Figure III-9** through **III-12)** and for 2015 (**Figure III-13** through **III-16)**. A near-shore (St. 11) and off-shore (St. 3, WM) pH profile is included in each figure to show differences with depth during isothermal and stratified conditions. All pH depth profile insets included in **Figure III-9** though **III-16** are plotted using the same scale to show seasonal and spatial variations in pH.

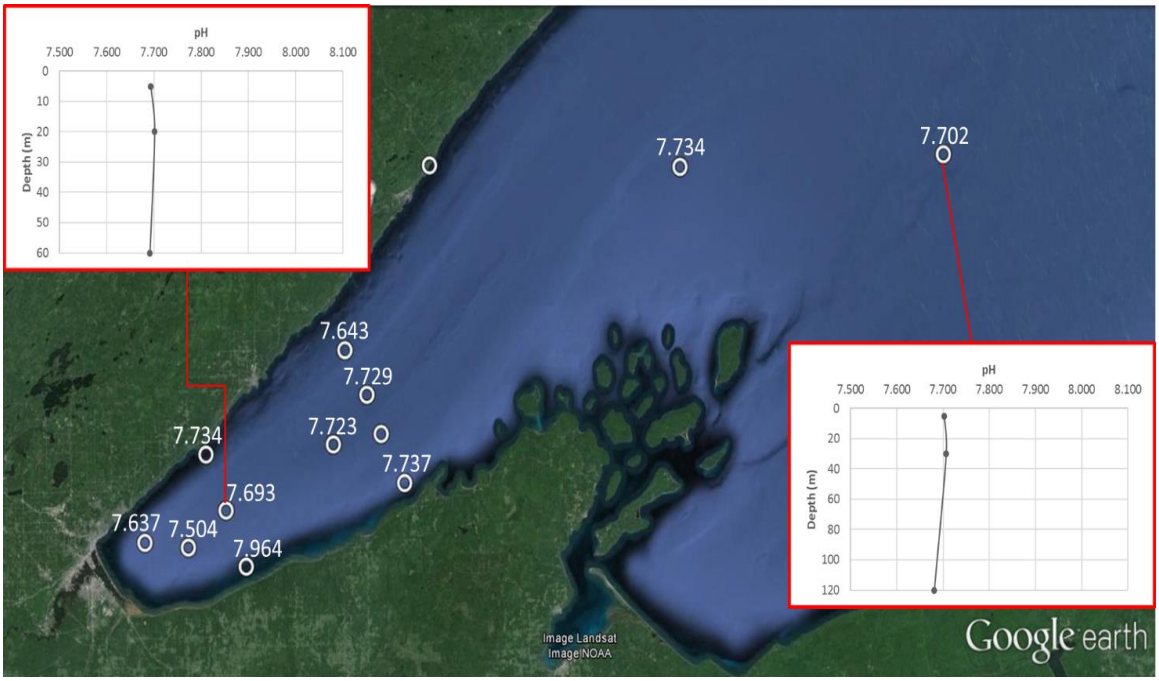

Figure III-9. Spectrophotometric pH measurements for western arm sampling stations during LCCMR1 (June 2014). All surface water pH measurements taken at 5 m depth.

Figure III-9 shows the lowest pH values collected for the western arm of Lake Superior coming out of the 2013-14 winter during June, 2014. The lowest pH values were determined to be in the far western side of the lake at Station 4 (OS; pH 7.637; near the Duluth harbor entrance) and Station 1 (pH 7.504; near the Superior harbor shipping entrance). These two stations correspond to major riverine inputs of organic material and nutrients to the lake during spring runoff with the St. Louis River discharging through the Duluth entry point and the Nemadji River discharging through the Superior entry point. The pH depth profiles at the near-shore Station 11 and off-shore Station 3 (WM) show little variation in pH with depth in the water column.

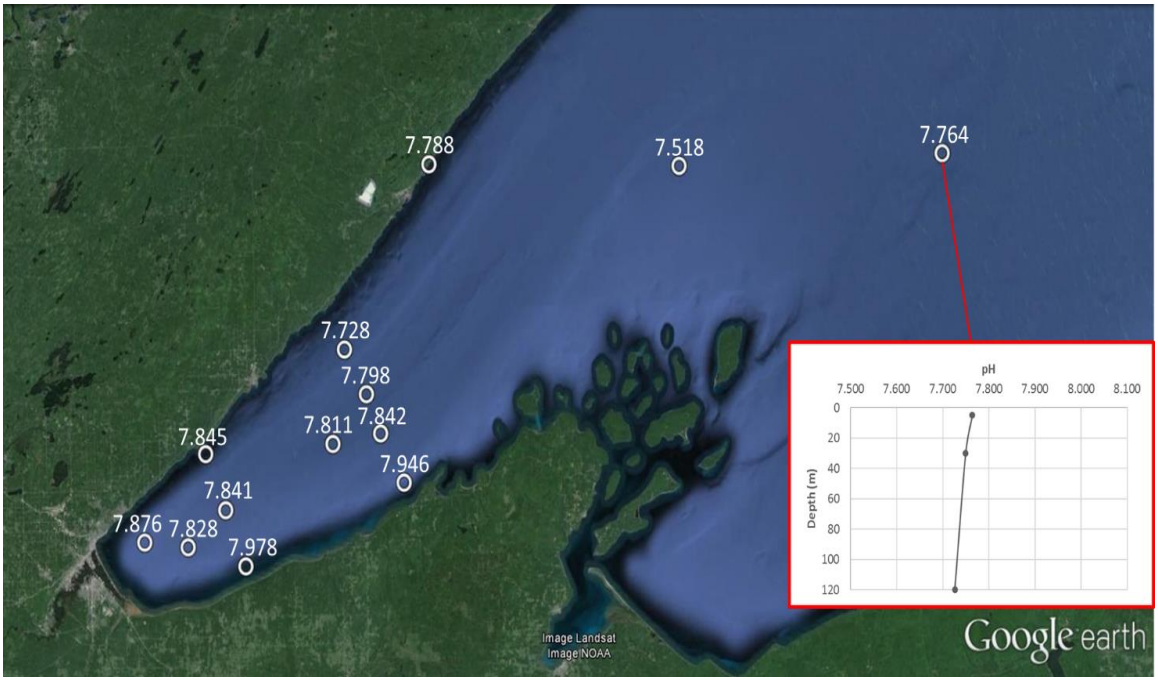

Figure III-10. Spectrophotometric pH measurements for western arm sampling stations during LCCMR2-3 (July 2014). All surface water pH measurements taken at 5 m depth except St. 7 (7.946) and 12 (7.978) which were taken at 2 m. No pH depth profile inset was included for St. 11 due to only two sampling depths.

Figure III-10 shows increases in pH values for all stations within the lake in July, 2014 from June, 2014 (**Figure III-9**) with the exception of Station 8 (pH 7.518). The highest pH values within the western arm correspond the near-shore stations (St. 10 [pH 7.845], 4 [OS; pH 7.876], 1 [pH 7.828], 12 [pH 7.978], 7 [pH 7.946]). Station 3 (WM) shows little variation in pH with depth. As the surface waters of the lake continue to warm and lake-wide thermal stratification occurs in August, 2014 (**Figure III-3)**, surface-water pH values continue to rise for the entire western arm (**Figure III-11**). Station 11 and Station 3 (WM) both show decreasing pH values with depth with the highest pH in the epilimnion above the thermocline and lowest pH below the thermocline in the hypolimnion.

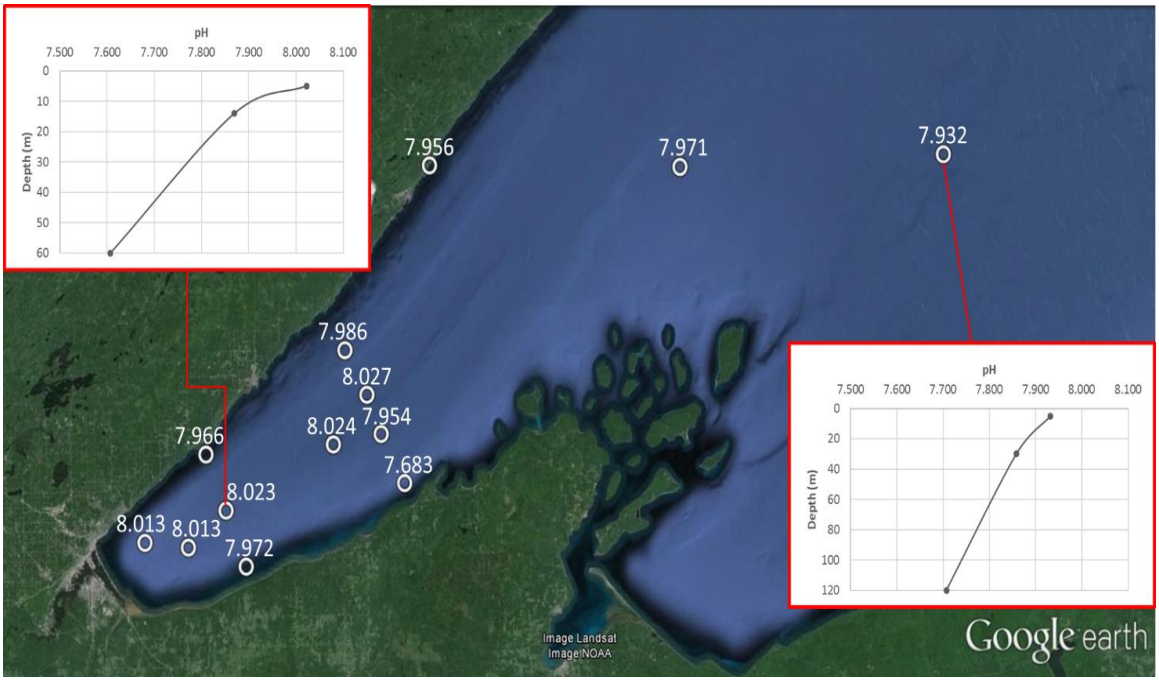

Figure III-11. Spectrophotometric pH measurements for western arm sampling stations during LCCMR4 (August 2014). All surface water pH measurements taken at 5 m depth.

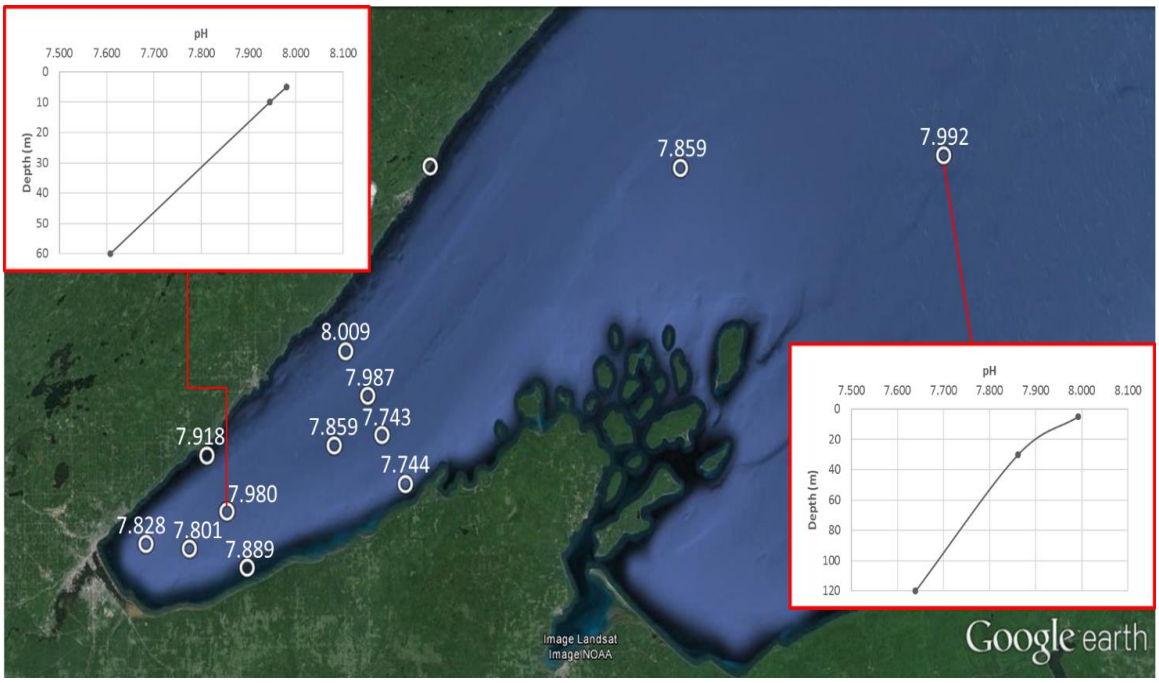

Figure III-12. Spectrophotometric pH measurements for western arm sampling stations during LCCMR5 (Sept.-Oct. 2014). All surface water pH measurements taken at 5 m depth.

Figure III-12 shows an overall decrease in surface-water pH for the near-shore stations (St. 10 [pH 7.918], 11 [pH 7.980], 4 [OS; pH 7.828], 1 [pH 7.801], 12 [pH 7.889]) and an increase in pH offshore at Station 3 (WM) during September-October, 2014. Stations 11 and 3 (WM) both continue to show decreasing pH values with depth, consistent with lake-wide thermal stratification (**Figure III-4**).

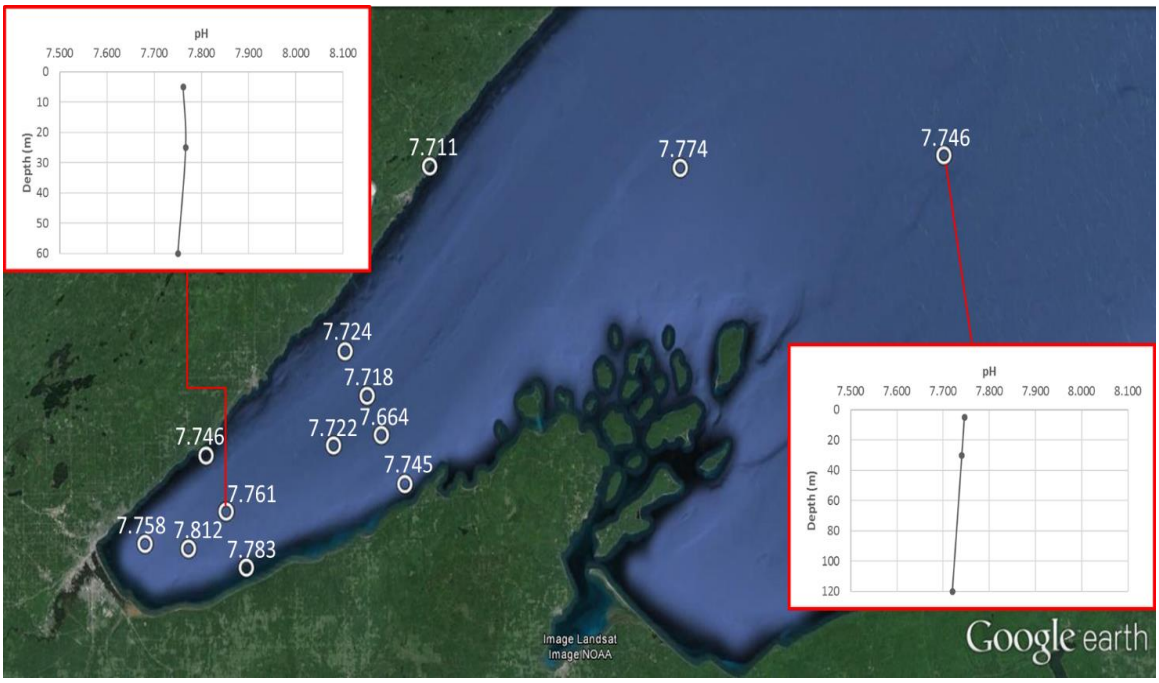

Figure III-13. Spectrophotometric pH measurements for western arm sampling stations during LCCMR6 (May 2015). All surface water pH measurements taken at 5 m depth.

Figure III-13 shows relatively homogenous and lower surface-water pH values for the western arm of Lake Superior coming out of the 2014-15 winter during May 2015, consistent with June 2014 (**Figure III-9**). Station 11 and Station 3 (WM) show little variation in pH values with depth in the water column. As the surface waters warm and lake-wide thermal stratification takes hold in July 2015 (**Figure III-6**), pH values begin to rise in **Figure III-14**. The most pronounced surface-water pH increases occurred at the far western arm near-shore stations (St. 2 [CD1; pH 8.067], 10 [pH 8.033], 4 [OS; pH 8.043], 1 [pH 8.079], 11 [pH 8.030], 7 [pH 8.077]) while the open lake (St. 3, WM) showed only a slight increase in pH. Both Station 11 and Station 3 (WM) show decreases

in pH values with depth in the water column, consistent with the beginning of lake-wide thermal stratification in August, 2014 (**Figure III-3**).

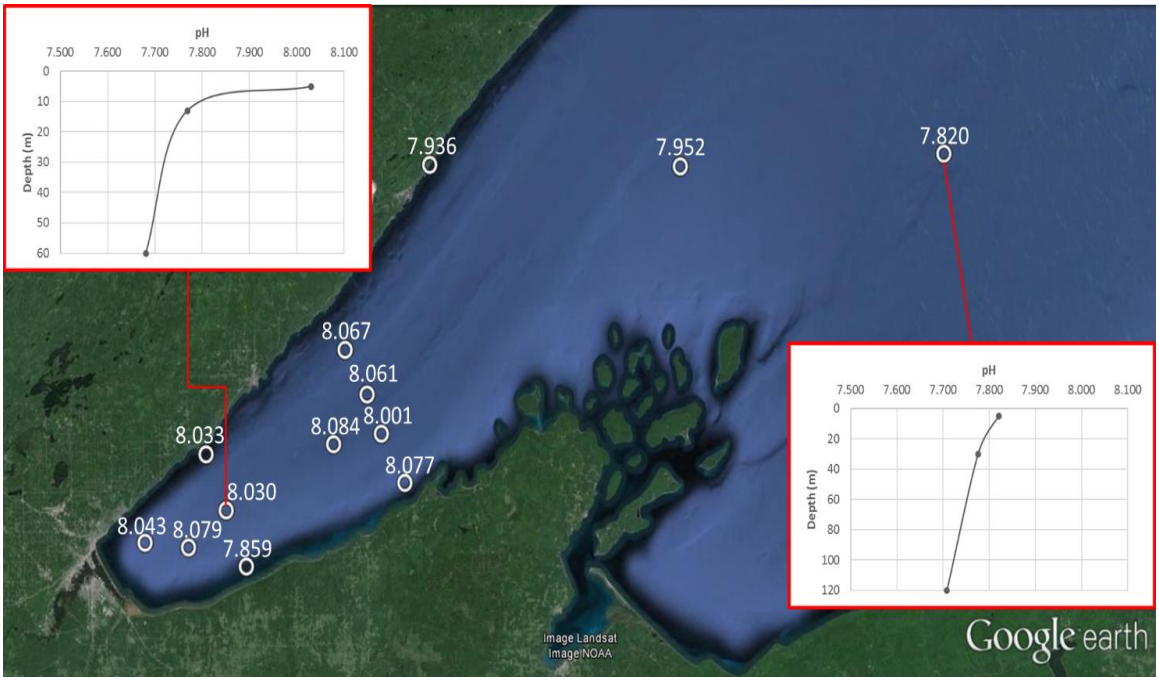

Figure III-14. Spectrophotometric pH measurements for western arm sampling stations during LCCMR7 (July 2015). All surface water pH measurements taken at 5 m depth.

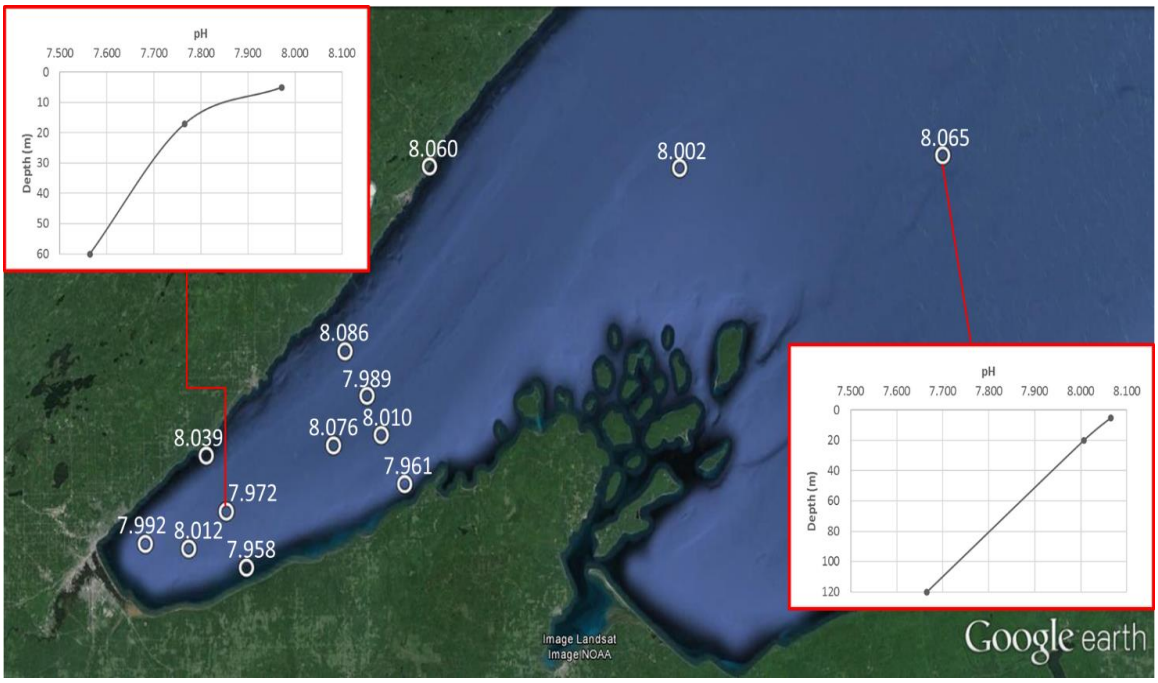

Figure III-15. Spectrophotometric pH measurements for western arm sampling stations during LCCMR8 (September 2015). All surface water pH measurements taken at 5 m depth.

Figure III-15 shows little variation in surface-water pH values in the near-shore stations in the far western arm of the lake from July 2015 (**Figure III-**14) to September 2015 while the open lake (St. 3, WM) pH increased substantially; consistent with the 2014 sampling (September-October, 2014; **Figure III-12**). This corresponds to an increasing temperature in the epilimnion of the open lake (St. 3, WM) and a decreasing temperature in the near-shore (St. 11) shown in **Figure III-7**. Stations 11 and 3 (WM) both continue to show decreasing pH values with depth, consistent with lake-wide thermal stratification (**Figure III-7**).

Figure III-16 shows an overall decrease for the western arm of the lake for both the near-shore and open lake stations. This is consistent with lower surface water temperatures for all stations within the lake (**Figure III-8**). Station 11 shows little variation in pH values with depth while the open lake (St. 3, WM) continues to show a decrease in pH with depth in the water column.

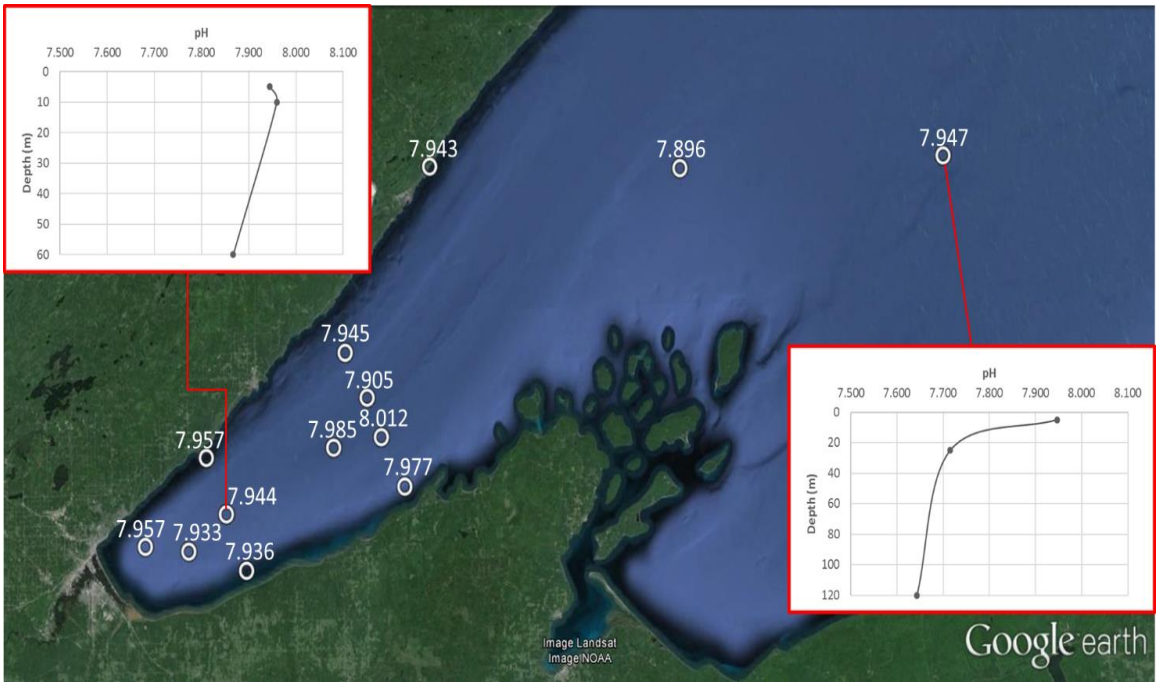

Figure III-16. Spectrophotometric pH measurements for western arm sampling stations during LCCMR9 (October 2015). All surface water pH measurements taken at 5 m depth.

III.c Lake Surface pCO_2

Surface water pCO_2 values for the western arm of Lake Superior are shown below for 2014 (**Figure III-17** through **III-20)** and for 2015 (**Figure III-21** through **III-24)** plotted as the percent difference from atmospheric pCO_2 (ΔpCO_2). Stations with positive red values represent net heterotrophic outgassing conditions and negative green values represent net autotrophic CO_2 dissolution conditions relative to the atmosphere. Black circles represent stations where water samples were not taken.

Figure III-17 shows the western arm of the lake to be predominantly heterotrophic coming out of the 2013-14 winter season with the exception of Station 12 (-31%). The lake continues to stay uniformly heterotrophic through mid-July, 2014, as shown in **Figure III-18**. This is consistent with slow surface water temperature warming and the lack of lake-wide thermal stratification (**Figure III-1** and **III-2**).

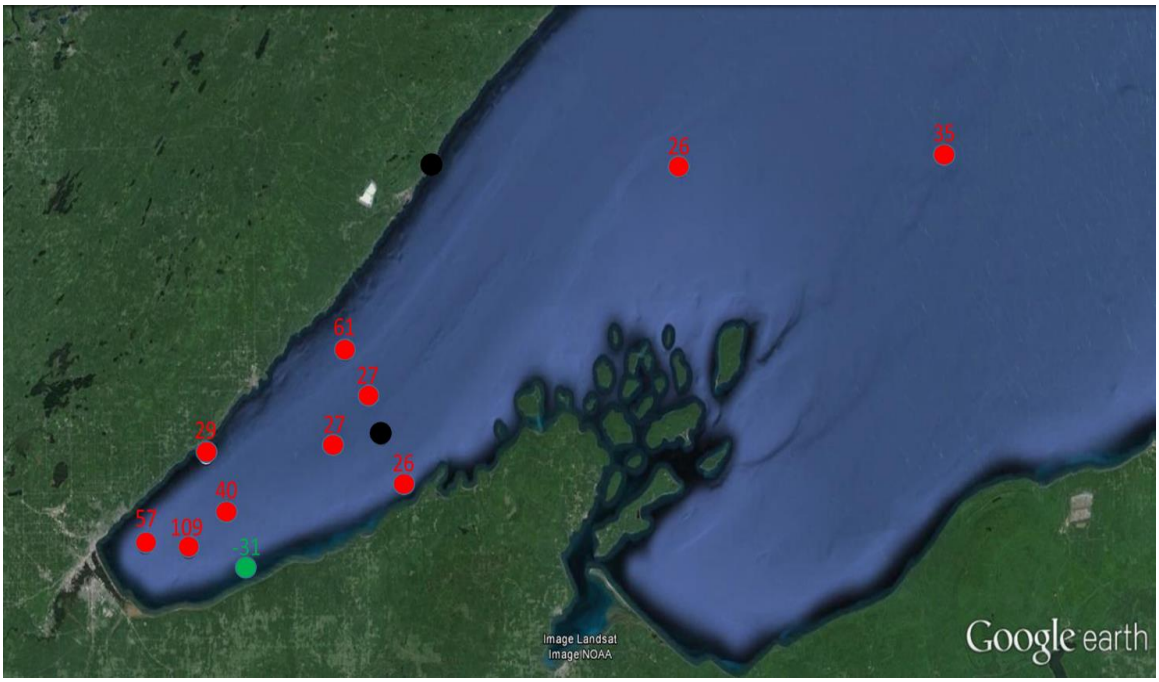

Figure III-17. Percent lake surface-atmosphere pCO_2 difference ($\Delta pCO2$) for western arm sampling stations during LCCMR1 (June 2014). All surface water samples taken at 5 m depth. In **Figures III-17** through **III-24**, red symbols and labels indicate outgassing values; green indicates transfer of CO_2 into lake waters; black indicates a station location that is missing data for this cruise.

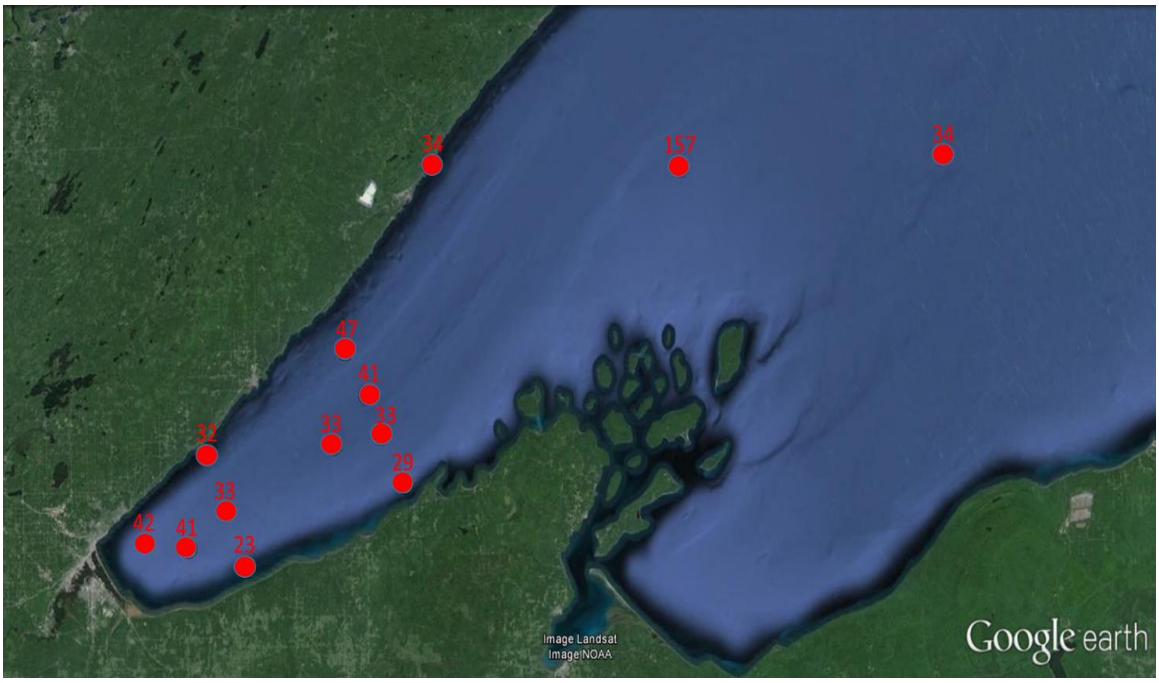

Figure III-18. Percent lake surface-atmosphere pCO_2 difference ($\Delta pCO2$) for western arm sampling stations during LCCMR2-3 (July 2014). All surface water samples taken at 5 m depth except St. 7 (29%) and 12 (23%) which were taken at 2 m.

As the surface water of the western arm continues to warm and lake-wide thermal stratification takes hold (**Figure III-3**), Stations 11 (-8%), 9 (-14%), 2 (CD1; -1%), 5 (-18%), and 6 (-14%) become net autotrophic (**Figure III-19**). **Figure III-19** also shows the near-shore stations (St. BP [23%], 10 [23%], 4 [OS; 19%], 1 [3%], 12 [14%], 7 [61%]) as well as the open lake (St. 3, WM) remaining net heterotrophic in mid-August, 2014.

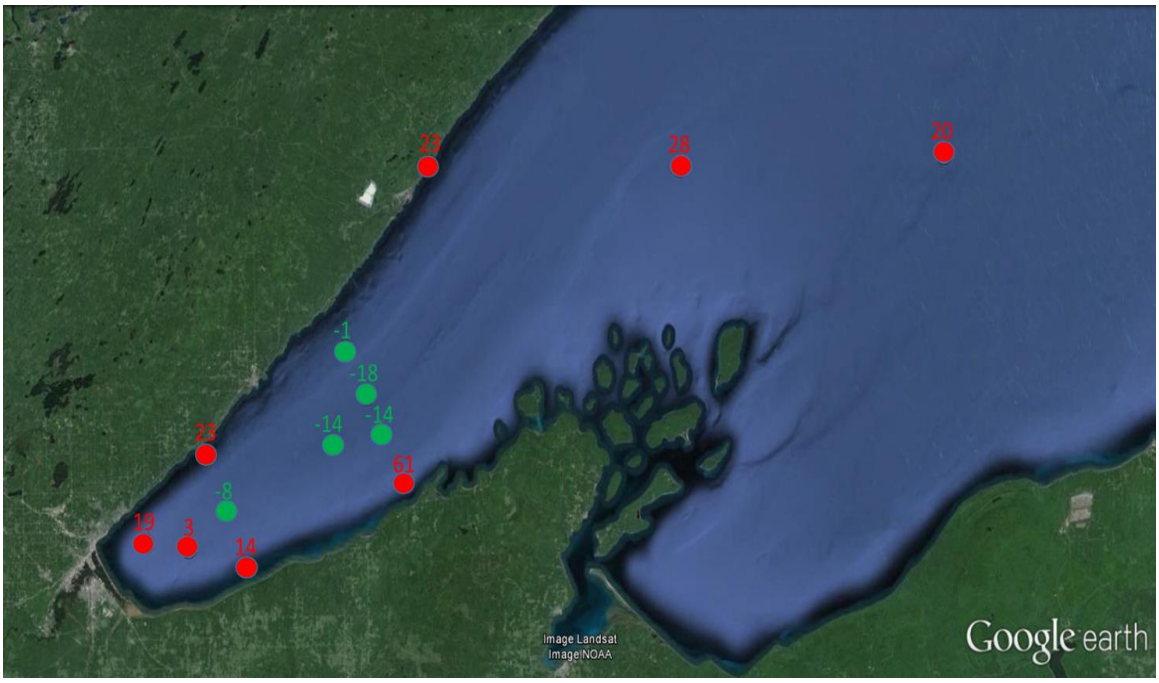

Figure III-19. Percent lake surface-atmosphere pCO_2 difference ($\Delta pCO2$) for western arm sampling stations during LCCMR4 (August 2014). All surface water samples taken at 5 m depth.

The open lake (St. 3, WM) eventually becomes net autotrophic in early October, 2014, with the near-shore (St. 10 [15%], 4 [OS; 45%], 1 [54%], 12 [19%], 7 [57%]) remaining net heterotrophic overall (**Figure III-20**).

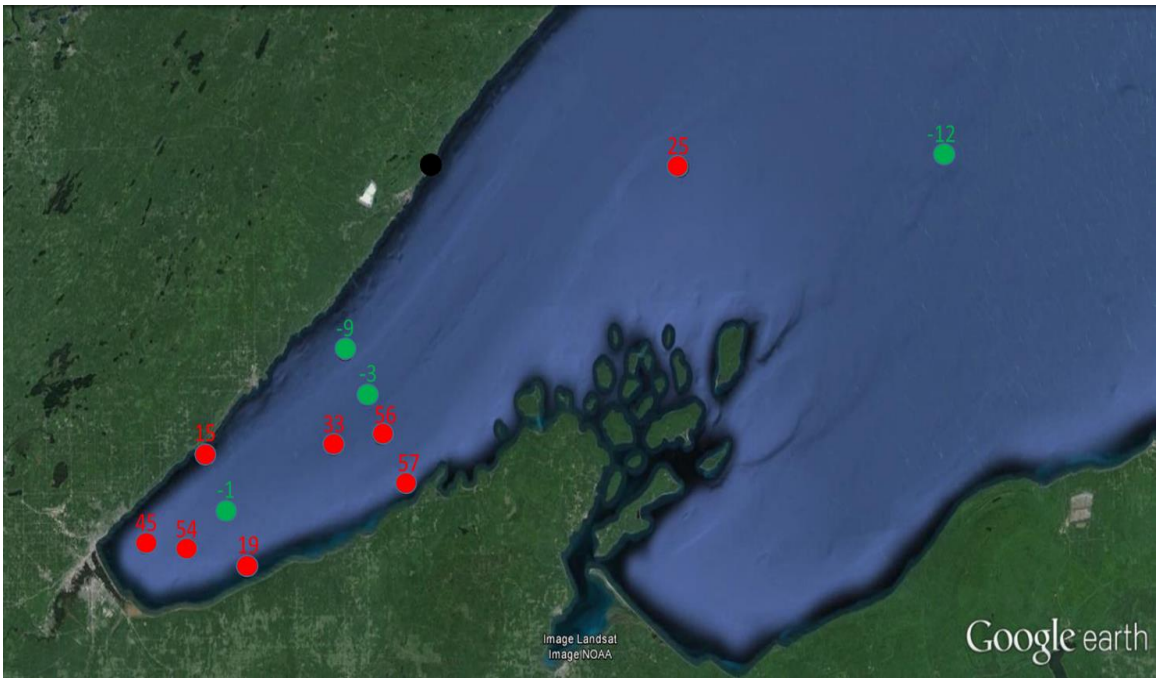

Figure III-20. Percent lake surface-atmosphere pCO_2 difference ($\Delta pCO2$) for western arm sampling stations during LCCMR5 (Sept.-Oct. 2014). All surface water samples taken at 5 m depth.

Figures III-21 through **III-24** show a similar but accelerated cycle for surface lake pCO_2 in the western arm. The lake starts out net heterotrophic throughout the entire western arm in mid-May, 2015 coming out of the 2014-15 winter season (**Figure III-21**). As solar radiation heats the surface waters and lake-wide thermal stratification takes hold by mid-July 2015 (**Figure III-6**), the western arm (St. 4 [OS; -2%], 1 [-5%], 9 [-34%], 2 [CD1; -11%], 5 [-9%], 7 [-23%]) begins to shift to net autotrophic (**Figure III-22**). The open lake (St. 3, WM) remains heterotrophic (**Figure III-22**) until early September, 2015 when autotrophy eventually reaches the open water of the lake (**Figure III-23**). **Figure III-23** also shows the north shore stations (St. 10 [-14%], 2 [CD1; -20%], BP [-20%]) of

the lake to be net autotrophic with the south shore stations showing overall heterotrophy (St. 12 [14%], 7 [11%]).

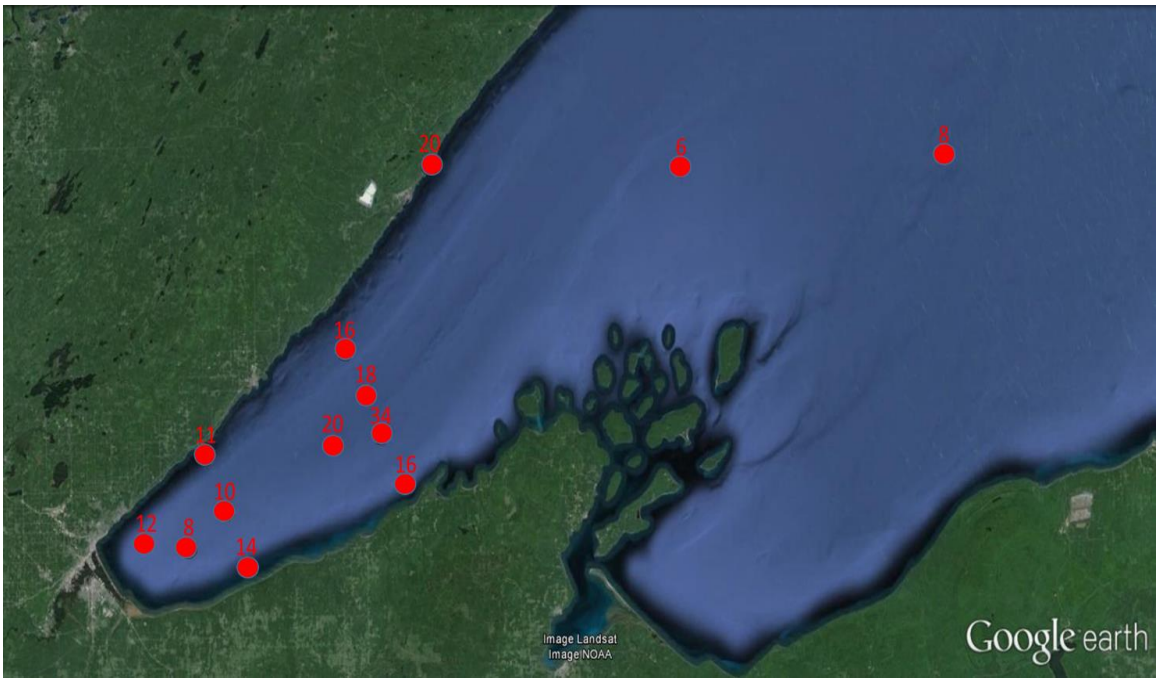

Figure III-21. Percent lake surface-atmosphere pCO_2 difference ($\Delta pCO2$) for western arm sampling stations during LCCMR6 (May 2015). All surface water samples taken at 5 m depth.

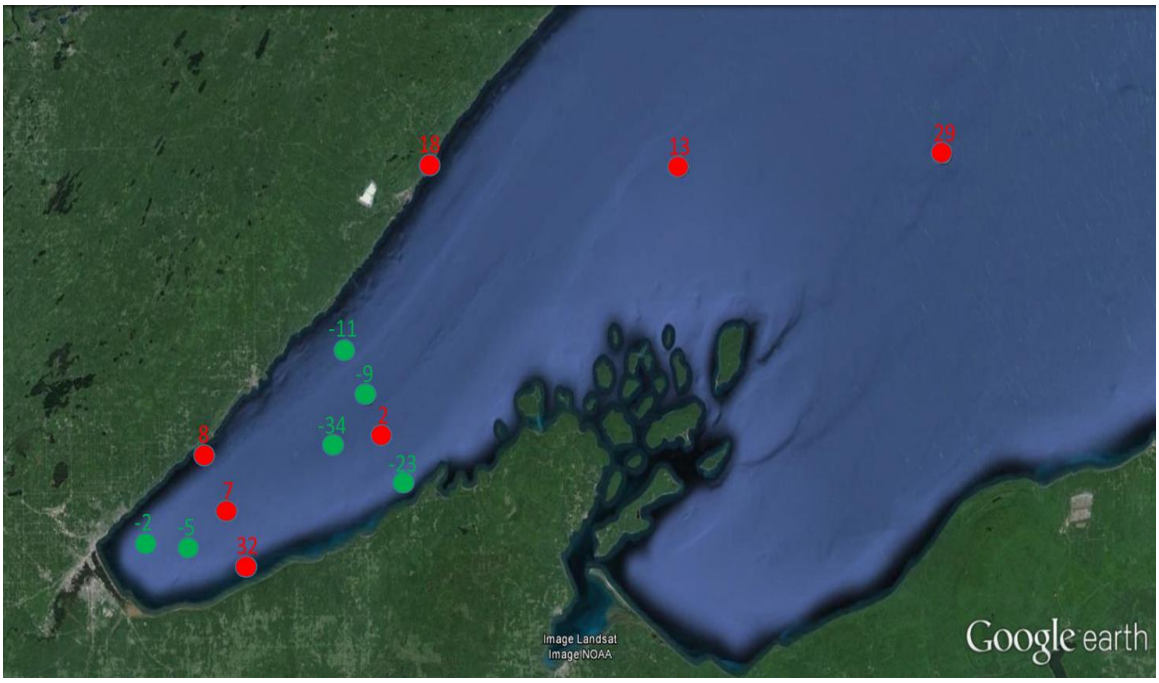

Figure III-22. Percent lake surface-atmosphere pCO_2 difference ($\Delta pCO2$) for western arm sampling stations during LCCMR7 (July 2015). All surface water samples taken at 5 m depth.

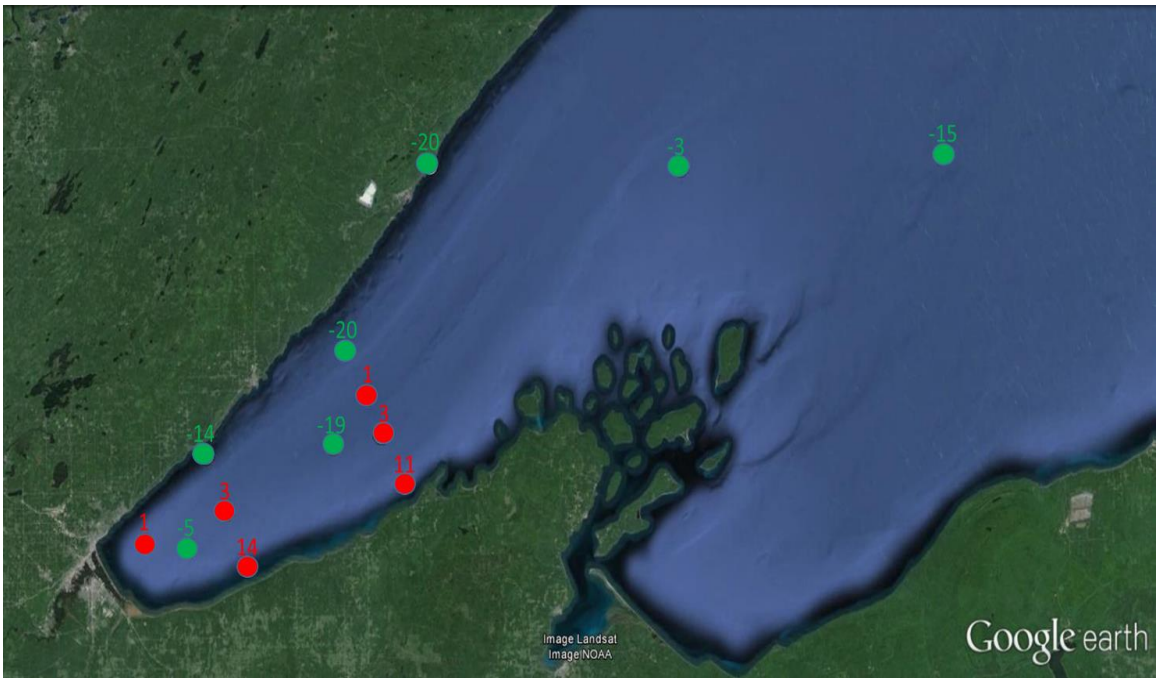

Figure III-23. Percent lake surface-atmosphere pCO_2 difference ($\Delta pCO2$) for western arm sampling stations during LCCMR8 (September 2015). All surface water samples taken at 5 m depth.

As the surface water of the western arm begins to cool, the north shore stations (St. 10 [1%], 2 [CD1; 6%], BP [6%]) of the lake cycle back to net heterotrophy while the open lake (St. 3, WM) remains autotrophic in early October, 2015 (**Figure III-24**). A pocket of overall autotrophy can be seen along the south shore at stations 9 (-11%), 6 (-16%), and 7 (-5%) (**Figure III-24**).

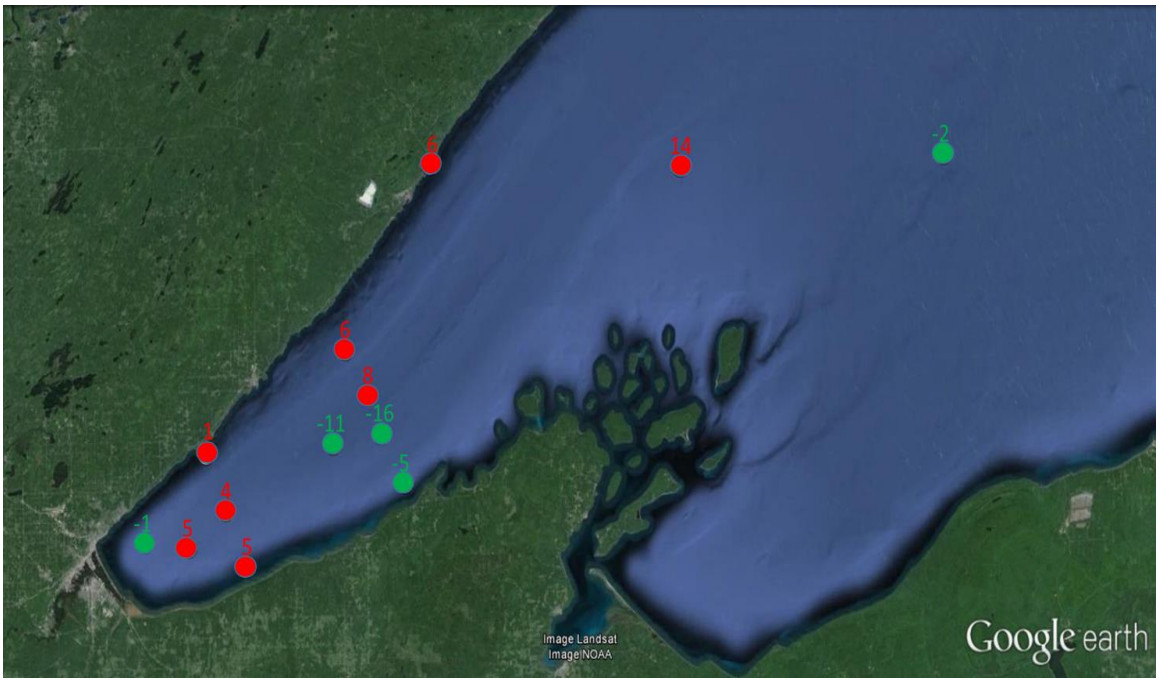

Figure III-24. Percent lake surface-atmosphere pCO_2 difference ($\Delta pCO2$) for western arm sampling stations during LCCMR9 (October 2015). All surface water samples taken at 5 m depth.

Plots of overall lake surface pCO_2 (µatm) for all LCCMR cruises within the western arm of Lake Superior are shown below in **Figure III-25** and **III-26**. Both plots show the same yearly cycle for surface lake pCO_2 with the most supersaturated CO_2 conditions occurring after winter, before decreasing and approaching equilibrium with atmospheric pCO_2 in late summer, and finally increasing during fall. **Figure III-25** and **III-26** both show that pCO_2 variability amongst all stations sampled in the western arm is greater coming out of the harsh 2013-14 winter in which a later ice-out date was observed than in 2014-15.

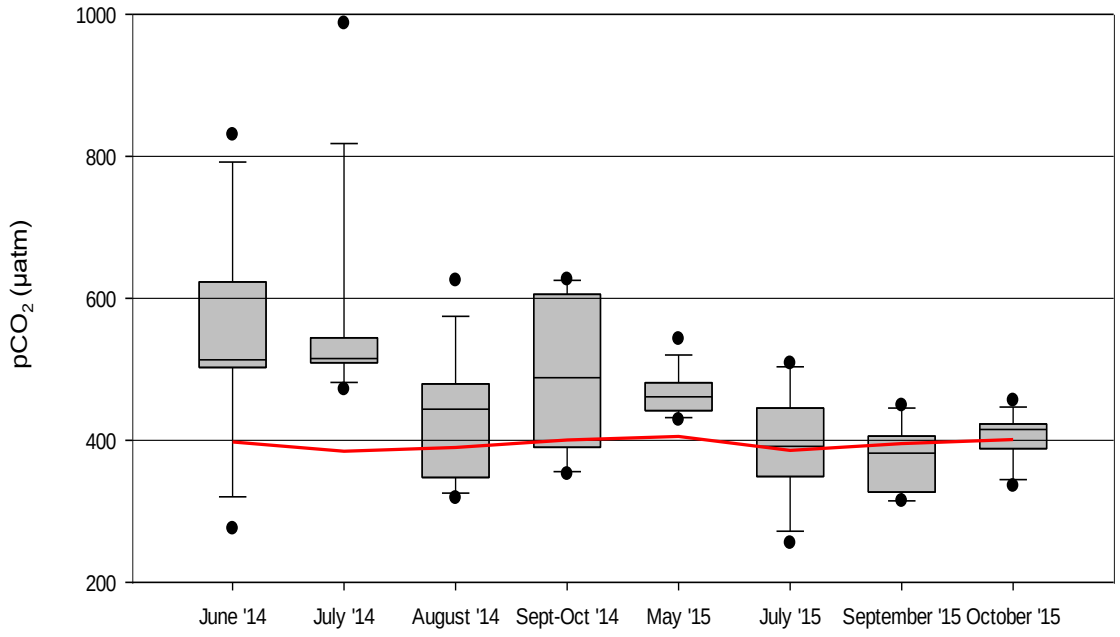

Figure III-25. Boxplot of lake surface pCO_2 (µatm) for all LCCMR cruises. Plotted are the median, 10th, 25th, 75th, 90th percentiles and maximum/ minimum values. Atmospheric pCO_2 is plotted in red (WLEF Tower, Park Falls, WI).

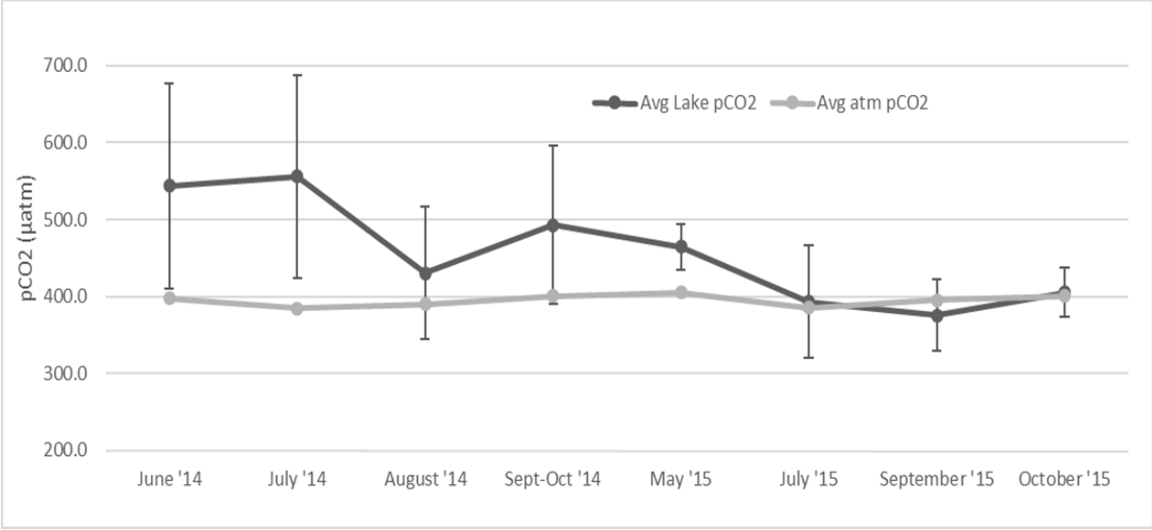

Figure III-26. Standard plot of mean lake surface pCO_2 (µatm) for all LCCMR cruises within the western arm of Lake Superior. Atmospheric pCO_2 (grey) is plotted for reference (WLEF Tower, Park Falls, WI). Error bars represent ± 1 standard deviation from the mean pCO_2 value for all lake stations during each trip.

III.d pCO_2 and Chlorophyll Fluorescence

Figures III-27 through **III-33** below show lake surface pCO_2 and chlorophyll fluorescence for each station over time. The chlorophyll fluorescence axis has been inverted to better show the anti-phase relationship of lake surface pCO_2 and chlorophyll fluorescence. LCCMR7 (Appendix **Figure VI-1**) was not included here due to instrument difficulties when these chlorophyll samples were processed (Sandra Brovold; personal communication). **Figures III-27** through **III-33** show a corresponding chlorophyll fluorescence decrease with increasing pCO_2. Elevated chlorophyll fluorescence would be expected to drive down lake surface pCO_2 due to the fixation of inorganic CO_2 to organic carbon within the water column by phytoplankton primary production. The inherent variability between lake surface pCO_2 and chlorophyll fluorescence for each station may be explained by differences in water column respiration perhaps due to riverine terrestrial DOC and TOC input, as well as cruise timing with some stations visited during daylight (production dominated) and others during night (respiration dominated). Lake surface pCO_2 plotted with chlorophyll fluorescence for all cruises at the open lake St. 3 (WM) and near-shore St. 11 are included in **Figures VI-2** and **VI-3**, with the near-shore showing a greater variability between pCO_2 and chlorophyll fluorescence (**Figure VI-3**).

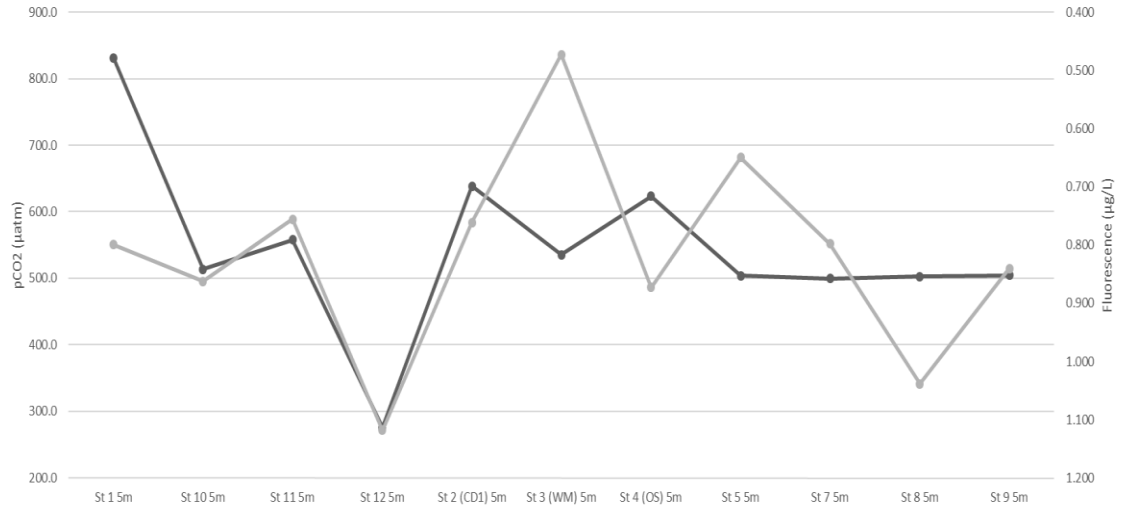

Figure III-27. Standard plot of mean lake surface pCO_2 (µatm; black) and chlorophyll fluorescence (µg L^{-1}; grey) at all western arm sampling stations during LCCMR1 (June 2014). All surface water samples taken at 5 m depth.

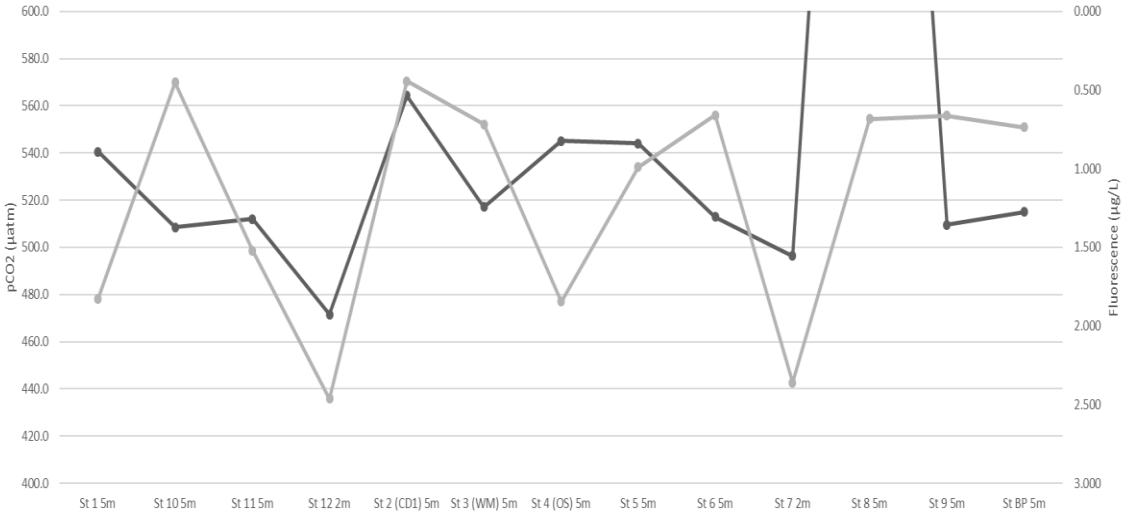

Figure III-28. Standard plot of mean lake surface pCO_2 (µatm; black) and chlorophyll fluorescence (µg L^{-1}; grey) at all western arm sampling stations during LCCMR2-3 (July 2014). All surface water samples taken at 5 m depth except St. 7 and 12 (2 m). St. 8 pCO_2 axis has been trimmed to improve visual relationship.

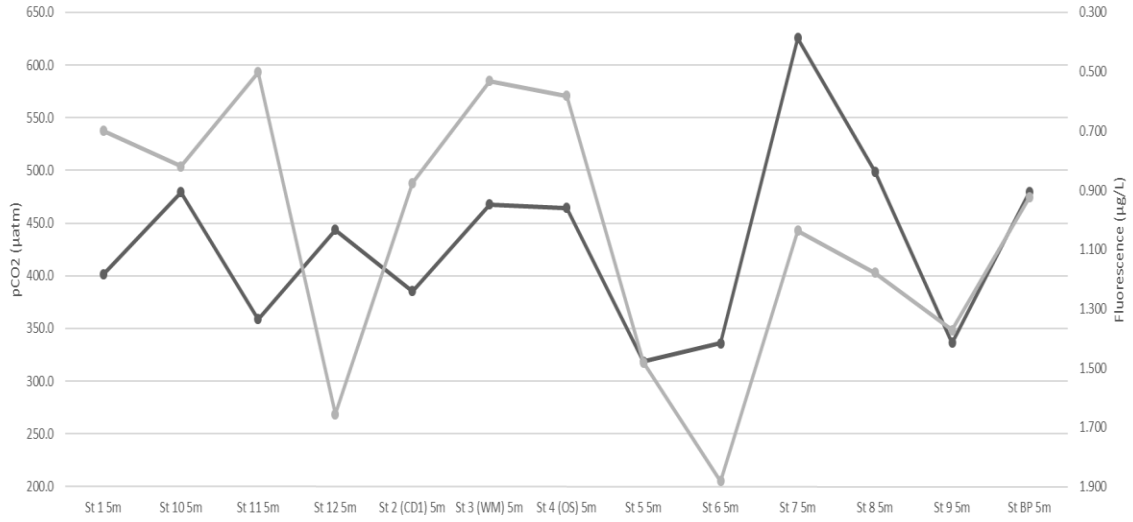

Figure III-29. Standard plot of mean lake surface pCO_2 (µatm; black) and chlorophyll fluorescence (µg L^{-1}; grey) at all western arm sampling stations during LCCMR4 (August 2014). All surface water samples taken at 5 m depth.

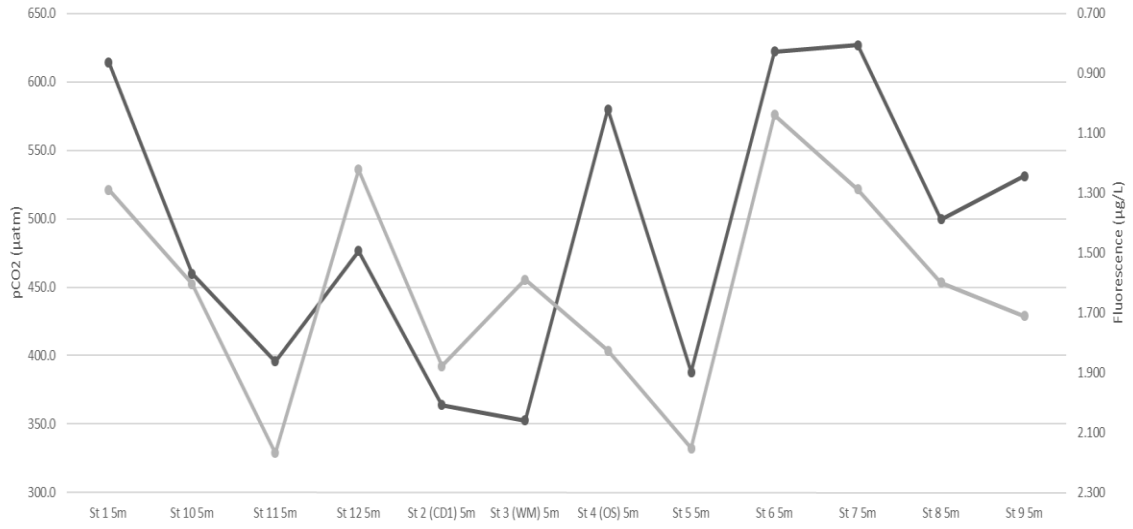

Figure III-30. Standard plot of mean lake surface pCO_2 (µatm; black) and chlorophyll fluorescence (µg L^{-1}; grey) at all western arm sampling stations during LCCMR5 (Sept.-Oct. 2014). All surface water samples taken at 5 m depth.

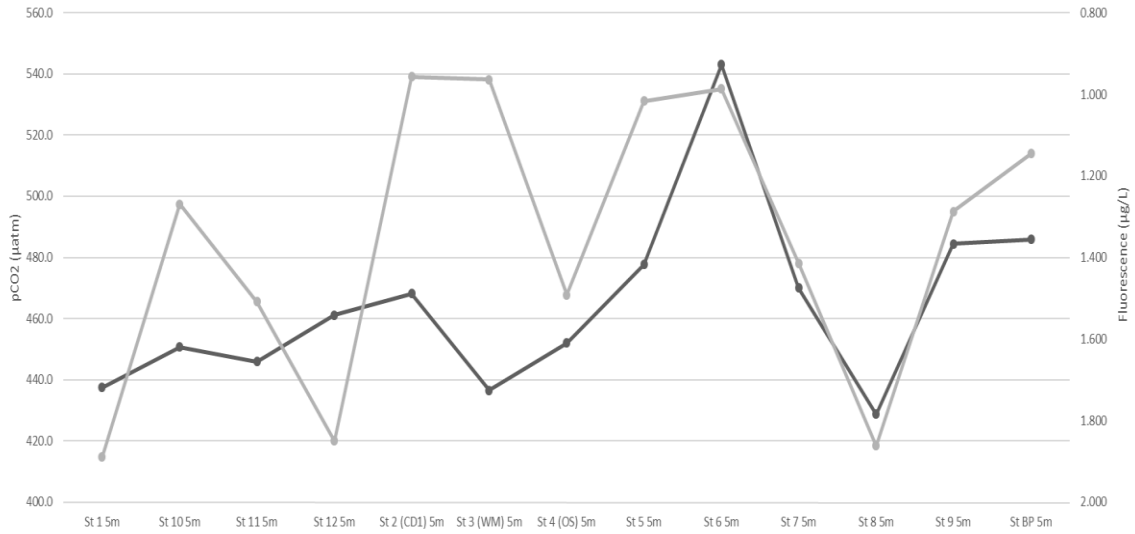

Figure III-31. Standard plot of mean lake surface pCO_2 (µatm; black) and chlorophyll fluorescence (µg L^{-1}; grey) at all western arm sampling stations during LCCMR6 (May 2015). All surface water samples taken at 5 m depth.

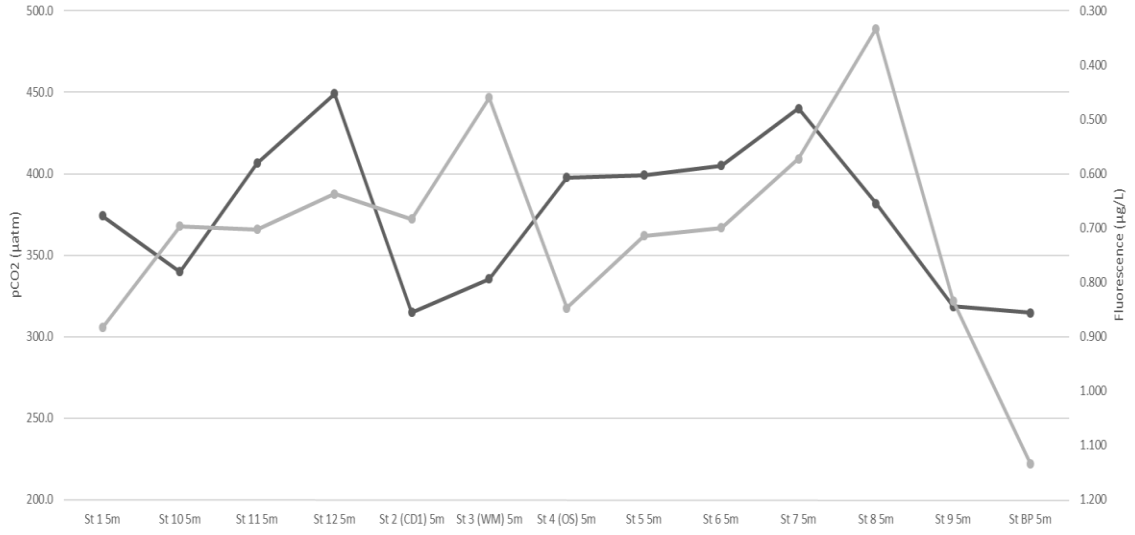

Figure III-32. Standard plot of mean lake surface pCO_2 (µatm; black) and chlorophyll fluorescence (µg L^{-1}; grey) at all western arm sampling stations during LCCMR8 (September 2015). All surface water samples taken at 5 m depth.

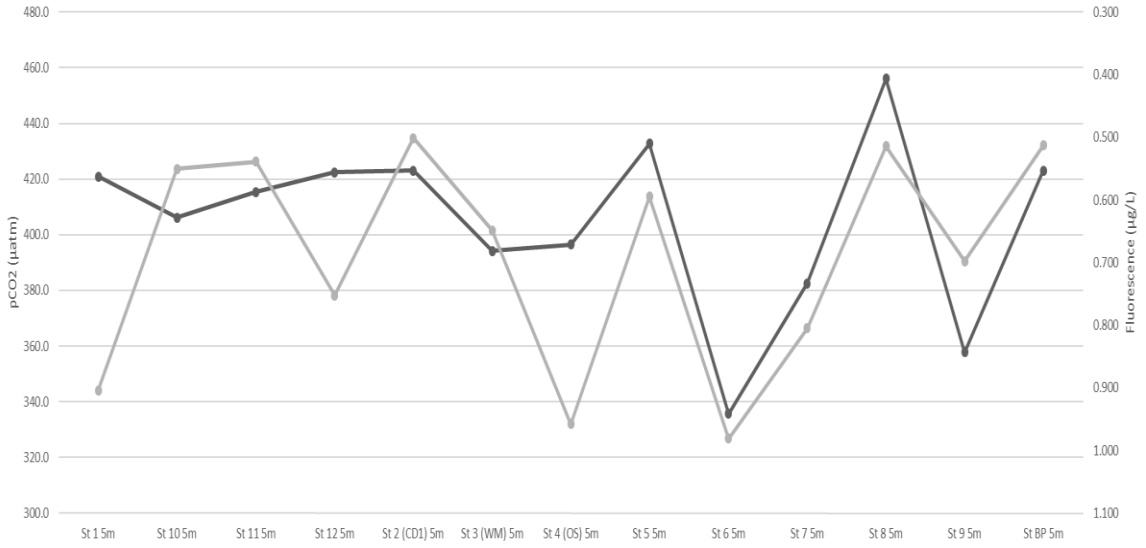

Figure III-33. Standard plot of mean lake surface pCO_2 (µatm; black) and chlorophyll fluorescence (µg L^{-1}; grey) at all western arm sampling stations during LCCMR9 (October 2015). All surface water samples taken at 5 m depth.

IV. Discussion

IV.a Seasonality of Lake Surface pCO_2

The western arm of Lake Superior was determined to be net heterotrophic in spring (a source of CO_2 to the atmosphere), approximately neutral in summer, before again turning net heterotrophic in the fall (**Figure III-25** and **III-26**). Surface-water pCO_2 was found to be higher and more variable overall in the 2014 sampling season coming out of the harsher 2013-14 winter. The variability between sampling stations in the western arm can be seen in the boxplots contained in **Figure III-25**. Austin and Colman (2007) have shown that ice coverage in large northern lakes during the previous winter is a strong predictor for the date of the beginning of thermal stratification. The 2013-14 winter produced over 90 percent ice cover on Lake Superior from the beginning of February to early April delaying lake-wide thermal stratification until August 2014; as opposed to July in the 2015 sampling season (NOAA, Great Lakes Environmental Research Laboratory; **Figure III-3**). An isothermal, well-mixed water column would help distribute more inorganic carbon from respiration and more OC that could fuel respiration to the surface for extended periods into the summer, while inhibiting *in-situ* primary production, allowing respiration to dominate and the lake to become a net source of CO_2 to the atmosphere (Austin and Colman, 2007; Bennington et al. 2012).

Wintertime ice cover may also serve to increase pCO_2 within the surface waters of the western arm of the lake by diminishing the water-atmosphere flux boundary (Austin and Colman, 2007; Bennington et al. 2012; Huttunen et al. 2003; Striegl et al. 2001). CO_2 has been shown to accumulate in the water column during ice covered winter conditions in Finnish lakes and reservoirs (Huttunen et al. 2003), and in Minnesota and

Wisconsin lakes (Striegl et al. 2001) indicating the potential for release at ice melt. This under ice buildup of CO_2 coupled with a delay in the increase of summertime water temperatures is likely responsible for the higher and more variable pCO_2 observations seen during the 2014 sampling season in the western arm of Lake Superior (**Figure III-25**).

Although inland water ecosystems represent a small fraction of the Earth's surface area, their importance to the processing of terrestrial organic carbon cannot be overlooked (Cole et al. 2007). Cole et al. (2007) estimate that inland waters (lakes, rivers, and reservoirs) process over half of the total 1.9 Pg C y^{-1} that enters from the terrestrial landscape, with at least 0.8 Pg C y^{-1} returning to the atmosphere through gas exchange and 0.2 Pg C y^{-1} being buried in aquatic sediments. Although the watershed to water surface area for Lake Superior is small and hence there are lower nutrient and organic carbon inputs from the landscape (Cotner et al. 2004), the heterotrophic predominance during much of the year could supply large amounts of inorganic carbon to the overlying atmosphere. Lake Superior appears to act as a negative feedback loop buffering changes in local climate. This is due to the strong dominance of heterotrophy that is observed after cold winters which delay the start of thermal stratification, ultimately outgassing more CO_2 (**Figure IV-1**). It is expected that during warmer winters (consistent with a warming climate), the lake would outgas less CO_2 serving to buffer the surrounding atmosphere.

The yearly pCO_2 cycle that was determined for Lake Superior in this study is consistent with previous findings utilizing U.S. EPA bi-yearly cruise data (Atilla et al. 2011; Bennington et al. 2012). Atilla et al. (2011) concluded that the open waters of Lake

Superior were a source of CO_2 to the atmosphere in spring and were approximately neutral in summer between 1996 and 2006. This is consistent with **Figures III-25** and **III-26** in the results section above. Bennington et al. (2012) concluded the lake to be a sink of CO_2 during the late winter/early spring before warming and the outgassing of CO_2 to the atmosphere during spring, then acting as either a small sink or neutral during the summer and remaining a sink until the return of winter mixing. Although the lake was determined to be on average a net source of CO_2 over the entire 2014 season, **Figures III-4** and **III-26** show that heterotrophy increases during LCCMR5 (Sept-Oct, 2014) when the entire western arm is still thermally stratified; earlier than previous modeled predictions by Bennington et al. (2012).

Alin and Johnson (2007) concluded, on the basis of CO_2 concentrations alone, that a gradient occurs ranging from net autotrophic in tropical latitudes to increasingly heterotrophic at higher latitudes. Lake Superior, with an average latitude of about 47^0, falls in the middle of the latitude gradient studied (between the equator and about 67^0 N) by Alin and Johnson (2007). Based on the results of this study, it can be concluded that Lake Superior resides in the middle of the trophic gradient being net heterotrophic (a source of CO_2) in the spring and fall, and approximately neutral during the summer. Because of this yearly overall equilibrium in pCO_2 between the lake surface and overlying atmosphere, it is hypothesized that Lake Superior and other lakes residing in the middle of the trophic gradient will be most susceptible to a warming climate. Austin and Colman (2007) have shown that Lake Superior surface water temperatures increased about twice as fast as regional atmospheric temperatures (0.1 and 0.05 ^{o}C yr^{-1}

respectively) from 1979-2006. Increasing water temperatures coupled with increased atmospheric pCO_2 could lead to enhanced algal growth in these oligotrophic mid-gradient systems where temperature limits production; ultimately shifting the trophic gradient northward.

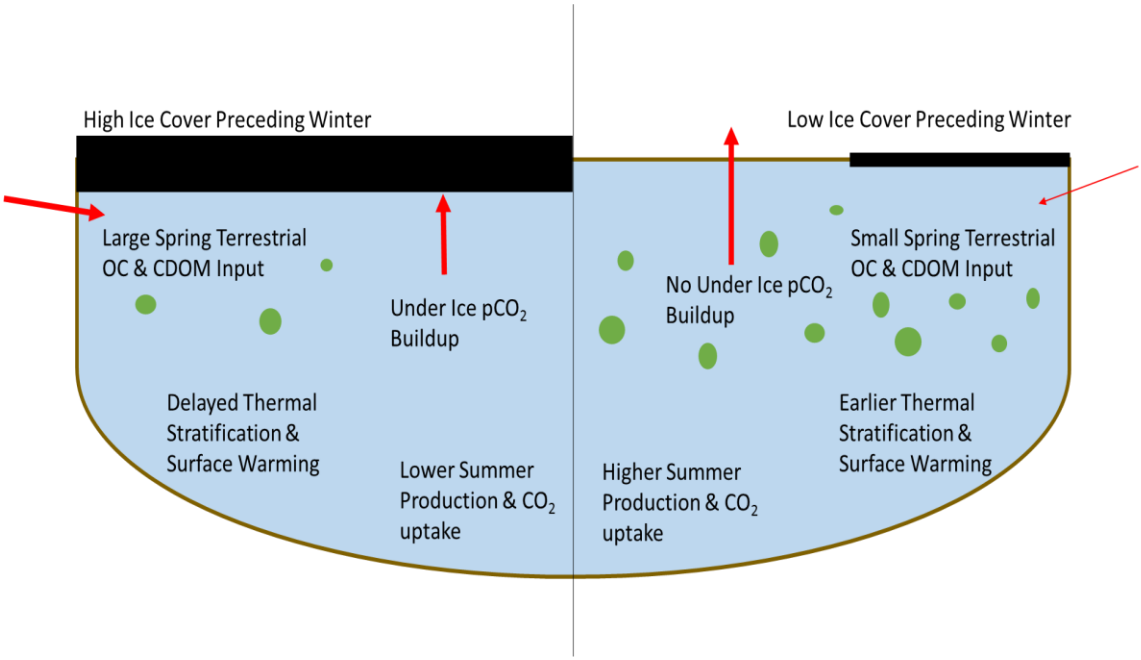

Figure IV-1. Conceptual model of Lake Superior negative feedback loop based on the preceding winter.

IV.b Comparison to *in-situ* SAMI pCO_2 Data

Little data exists measuring pCO_2 via *in-situ* moored instruments in Lake Superior. In addition to the low-frequency U.S. EPA data analyzed and discussed above, Atilla et al. (2011) also used direct high-frequency pCO_2 measurements taken in 2001 utilizing a Submersible Autonomous Moored Instrument in the western arm of Lake

Superior near Duluth capable of measuring CO_2 (SAMI-CO_2; Described in DeGrandpre et al. 1995; 1997). Based on a partial seasonal cycle (June-September), SAMI pCO_2 was determined to be highest for the 24 days of June and lowest for the month of August (**Figure IV-2**; Atilla et al. 2011). The instrument also showed the surface waters to be net heterotrophic until mid-July, before cycling to net autotrophic through August, and finally switching back to net heterotrophic in early September (**Figure IV-2**; Atilla et al. 2011). This partial seasonal cycle of *in-situ* surface water pCO_2 is consistent with the low-frequency sampling based results concluded in this study. **Figure IV-2** also shows the diurnal range of pCO_2 to be lowest in the month of June and to increase through September. Atilla et al. (2011) determined the daily timing of the maxima and minima pCO_2 to occur on a timescale of approximately 17 h, with no tendency for the maxima to occur during the night and the minima to occur during the day, indicating that daily biological activity was not responsible for the high-frequency daily pCO_2 variations. However, lower frequency weekly timescale changes in SAMI pCO_2 were driven primarily by changes in dissolved inorganic carbon and pH with phytoplankton consuming CO_2 during photosynthesis and bacteria releasing CO_2 during respiration (Atilla et al. 2011).

Baehr and DeGrandpre (2002) used SAMI-CO_2 to measure the under ice buildup of pCO_2 in Placid Lake; a mesotrophic, dimictic lake in Montana. Based on an *in-situ* time series from 1997 and 1998, under ice pCO_2 ranged from 1020 to 1700 µatm, roughly 3 to 5 times higher than atmospheric pCO_2 levels (Baehr and DeGrandpre, 2002). It was concluded that respiration of accumulated organic matter dominated the overall trend in

elevated lake pCO_2 (Baehr and DeGrandpre, 2002), consistent with the elevated spring surface water pCO_2 observed in this study.

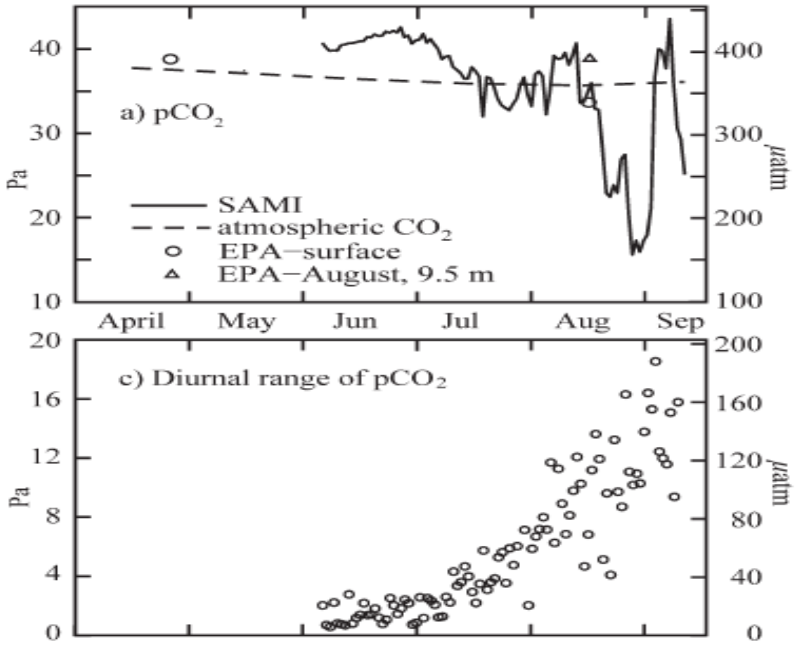

Figure IV-2. Directly measured pCO_2 and diurnal range of pCO_2 (Pa and µatm) by the SAMI in the western arm of Lake Superior near Duluth from June-September 2001 with atmospheric pCO_2 observed at WLEF tower in Park Falls, WI represented by dashed line (Atilla et al. 2011).

IV.c Statistical Comparison of 2014-15 pCO_2 Data

In order to assess differences in the seasonality of lake surface pCO_2, paired two-sample t-tests for means were performed for spring complete mixing, summer lake-wide thermal stratification, and early fall cooling conditions utilizing the ΔpCO_2 values for both the 2014 and 2015 sampling season (summarized in **Figure IV-3**).

During spring complete mixing conditions, it was determined that there was a statistically significant difference ($\alpha = 0.05$) between the 2014 (LCCMR1- June 2014) and 2015 (LCCMR6- May 2015) ΔpCO_2 ($t = 2.31$, $df = 10$, $p = 0.044$). The results of this test indicate that previous-winter ice cover duration and the diminished water-atmosphere flux boundary on Lake Superior affects pCO_2 levels within the water column; consistent with previous studies (Austin and Colman, 2007; Bennington et al. 2012; Huttunen et al. 2003; Striegl et al. 2001). The ΔpCO_2 during summer lake-wide thermal stratification between the 2014 (LCCMR4- August 2014) and 2015 (LCCMR7- July 2015) sampling season was determined to be statistically insignificant ($t = 1.15$, $df = 12$, $p = 0.27$) at the $\alpha = 0.05$ significance level. Note that thermal stratification seasonality in Lake Superior is also influenced by the relative strength of the previous winter, and the resulting ice cover percentage and duration delayed lake-wide thermal stratification by approximately one month in 2014 vs. 2015. Even though the LCCMR6 cruise (May 2015) occurred 15 days earlier than the LCCMR1 cruise (June 2014), there was a significant difference in the ΔpCO_2 with LCCMR1 having a higher overall ΔpCO_2. This delay can also be seen in the statistically insignificant results of the summer lake-wide thermal stratification test, in which ΔpCO_2 measurements were equal (at both the $\alpha = 0.05$ and $\alpha = 0.10$ significance level) despite the 32-day difference in ship departure dates between LCCMR4 (August 2014) and LCCMR7 (July 2015).

During early fall cooling conditions, the ΔpCO_2 between the 2014 (LCCMR5- October 2014) and 2015 (LCCMR9- October 2015) sampling season was determined to be statistically significant ($t = 2.55$, $df = 11$, $p = 0.027$) at the $\alpha = 0.05$ significance level. The

results of this test show that the surface waters of Lake Superior were more supersaturated with respect to CO_2 in October, 2014 than one year later in October, 2015. These two cruises also occurred at nearly the same calendar date in October between the two sampling seasons, with a difference of only 5 days between ship departure dates, further confirming the merit of this statistical difference in ΔpCO_2 values.

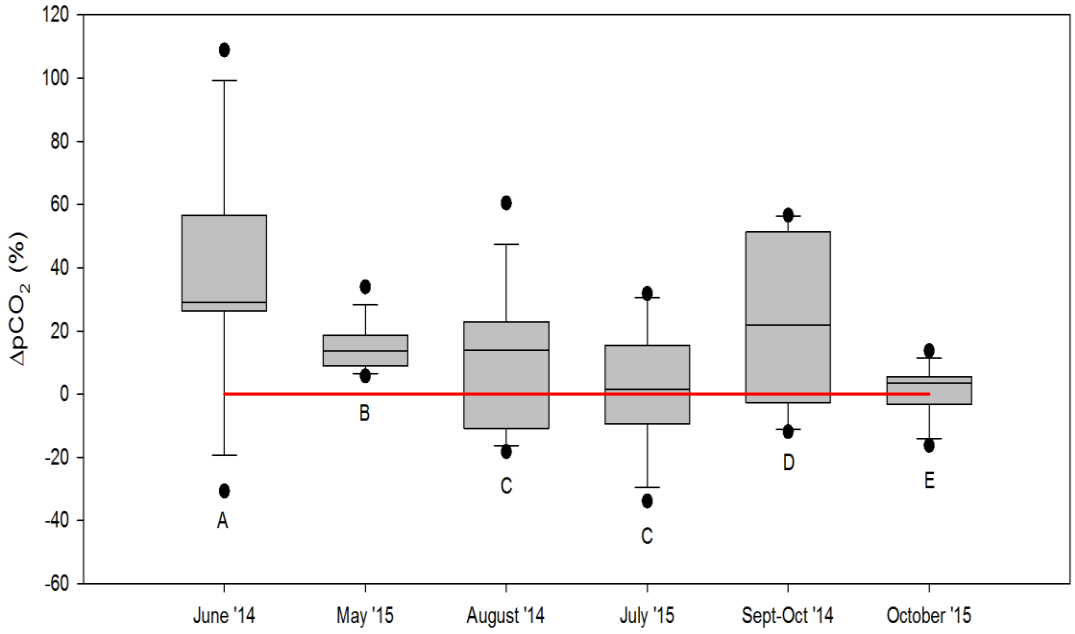

Figure IV-3. Boxplot of lake surface ΔpCO_2 (%) values utilized as inputs in paired two-sample t-tests for spring complete mixing (June ’14 and May ’15), summer lake-wide thermal stratification (August ’14 and July ’15), and early fall cooling conditions (Sept-Oct ’14 and October ’15). Plotted are the median, 10^{th}, 25^{th}, 75^{th}, 90^{th} percentiles and maximum/ minimum values with atmospheric equilibrium included in red. Boxplots with different letters are significantly different (α=0.05).

IV.d MODIS Satellite Images

In order to better assess the effects of river discharge and sediment plumes within Lake Superior, Moderate Resolution Imaging Spectroradiometer (MODIS) images were gathered from the National Oceanic and Atmospheric Administration Great Lakes Environmental Research Laboratory and are included in appendix **Figure VI-4** through **VI-11** (NOAA-GLERL). MODIS images were compared and selected based on sampling cruise date overlap and amount of overlying cloud cover. **Figure VI-4** (taken on 6/4/2014) shows a sediment plume in the far western arm on the south shore near the Superior entry point; this image was taken during the LCCMR1 cruise dates (6/3/2014 – 6/6/2014). The high organic carbon and nutrient outflow likely associated with this sediment plume from the Nemadji River may explain the variability in surface water pCO_2 that was observed between Station 1 and 12, where the ΔpCO_2 was 109 and -31 respectively (**Figure III-17**). The Nemadji River has also been shown to be supersaturated with respect to CO_2 (about 3.5-5 times atmospheric CO_2 levels) based on six independent samples over the years 2014-2015 (**Table VI-11**). **Figures VI-4** through **VI-11** also show the progression in surface water algal blooms throughout the summer and the overall variability in the surface water of the western arm of Lake Superior.

IV.e Under Ice pCO_2

Under ice sampling has rarely been done on the open waters of Lake Superior due to the difficulty of winter sampling in a partially ice-covered lake (Titze and Austin, 2014). Based on two samples taken at 10 and 20 m within the under-ice water column at

46.7737° N, 90.8130° W and analyzed in the same manner as described here for pH, and TIC, it was determined that the lake off the Wisconsin shore near the Apostle Islands was supersaturated with respect to pCO_2 (441 and 453 µatm respectively; not included here). Although supersaturated, these under-ice pCO_2 values were well within the range of ice-free sampled pCO_2 leading to further questions about the behavior of inorganic carbon cycling and the extent of under-ice heterotrophy during winter ice cover in this oligotrophic lake.

Contrary to the nearshore lake sampling described above, extensive under-ice CO_2 buildup was exhibited in the Lake Superior watershed in the Nemadji and St. Louis River where ice conditions also allowed under-ice water column sampling to be conducted. **Table VI-11** shows that pCO_2 values ranged from 1280 to 2021 µatm under ice (sampled on 1/28/2015 and 1/29/2015), about 3 to 5 times atmospheric pCO_2 levels respectively.

IV.f pH Variability and CO2SYS

On a seasonal basis, measured pH values followed an antiphase relationship to pCO_2 with the lowest values occurring in the spring and increasing throughout the summer (**Figure IV-4**). According to Kratz et al. (1987), winter pH depressions can be caused by changes in total alkalinity caused by strong acid input in meltwater, pCO_2 build up under ice, and accumulation of weakly ionizable organic acids. Based on Lake Superior's extremely low ratio of watershed drainage area to lake surface area of 1.55 (Cotner et al. 2004), it can be concluded that under-ice pCO_2 build up likely causes the

low spring pH measurements observed offshore in this study after ice out. Alternatively, nearshore inputs of sediment and colored dissolved organic matter (CDOM) may reduce phytoplankton growth due to light limitation and enhance microbial respiration due to the increased warming of colored waters coupled with organic carbon and nutrient inputs (Minor et al. 2014). The seasonal pH trends shown in **Figure IV-4** below provide further evidence that inorganic carbon cycling in Lake Superior may act as a negative feedback loop to buffer changes in local climate. Based on these results, under a future climate warming scenario, the lake would be expected to stratify sooner leading to increases in both surface water temperature and pH by primary production.

Increasing lake-wide pH has previously been shown by Phillips et al. (2015) utilizing U.S. EPA biannual survey data averaging April and August pH measurements from 1996-2011. Although there are large uncertainties in the biannual electrode pH measurements collected by the U.S. EPA, the results are consistent with the increasing spectrophotometric pH measurements collected in this study suggesting that air-water equilibration is not the dominant process controlling the long-term trend in annual mean pH (Phillips et al. 2015). It is hypothesized that increased algal growth due to increasing temperatures under a changing climate is overriding the effects of CO_2-induced acidification (Phillips et al. 2015). Lake Superior's already predominant heterotrophic (outgassing of CO_2) conditions throughout much of the season would also minimize the effects of increasing atmospheric CO_2 levels, until the atmospheric CO_2 reaches concentrations that overwhelm the effects of the changes in water temperature on carbon

dioxide solubility, and the effects of stratification and resultant biological processes (**Figure III-25** and **III-26**; **Table VI-1**).

The U.S. EPA GLENDA yearly average pH and alkalinity for the years 1996-2014 are shown in **Figure IV-5** and **IV-6**. Also included in **Figure IV-5** and **IV-6** are annually averaged top 5 m surface water spectrophotometric pH and alkalinity measurements collected in 2005 at a mooring location offshore of Grand Marais, MN and in 2006 at a mooring offshore of Two Harbors, MN (Strom, 2007); as well as the LCCMR western arm surface water measurements discussed previously. The precision of the 2006 spectrophotometric pH data was affected by damage to the spectrophotometer's wavelength detector but is included here for reference (Strom, 2007). The LCCMR alkalinity measurements included in **Figure IV-6** contain one cruise (LCCMR5) of data measured by the EPA method in 2014 and three cruises (LCCMR6, 7, 8) of data by both EPA and USGS Gran method including duplicates for both years. It is important to note the methodological, spatial, and time differences in sampling when comparing the U.S. EPA, Strom, and LCCMR data sets.

Figure IV-5 shows surface water electrode pH in Lake Superior to be weakly correlated from 1996-2014, with a slight average increase of 0.01 pH units yr^{-1}. Although this data set shows little definite proof of a significant pH increase, this is consistent with the Lake Superior negative feedback loop conclusion discussed previously. The range in surface water electrode pH measurements represented by the error bars in **Figure IV-5** further certifies the susceptibility of electrode drift in low ionic constituent waters like Lake Superior, and the continuing necessity of spectrophotometric pH measurements.

Figure IV-6 shows that surface water alkalinity in Lake Superior has increased about 6% from 1996-2014 with an average rate of 3.1 µeq L^{-1} yr^{-1} as $CaCO_3$. Increasing alkalinity (and hence a greater concentration of [HCO_3^-] and [CO_3^{2-}]) could in-turn lead to increasing pH, as shown in **Figure IV-5**. This increase in alkalinity coupled with the hydrologic budget and long residence time (~ 200 years) for Lake Superior suggests that large changes in riverine alkalinity are occurring. Alkalinity concentrations described here are within a similar range of previous studies by Weiler (1978) and Chapra et al. (2012) using both Canadian (Canada Centre for Inland Waters [CCIW] and Environment Canada [EC]) and U.S. data (U.S. EPA GLNPO) over the years of 1968-2009. Although no significant trend in alkalinity was determined from 1970-2009 by Chapra et al. (2012) using both EC and U.S. EPA data, yearly averages only contained spring open-lake stations (at least 150 m depth) excluding near-shore biological and riverine influence.

In order to assess the temperature effect on pH, a small-scale pH bottle experiment was conducted using sterile-filtered Lake Superior water and incubations at both room temperature (~20 °C) and ~5 °C; temperatures roughly equivalent to summer stratification and spring mixing surface water temperatures in Lake Superior. All samples were allowed to equilibrate to temperature in a 1-L beaker and then transferred into 500 mL amber bottles to reduce available headspace and allow closure of one "cold" bottle by a greased stopper. The amber bottles were then equilibrated to room temperature and measured using the spectrophotometric pH methods discussed above. **Figure IV-7** shows that the stoppered 5 °C bottle had the lowest pH at 7.845, followed by the open 5 °C bottle pH at 7.862, and lastly the open 20 °C had the highest pH at 7.996. The

intermediate pH observed in the open 5 ºC bottle is more reminiscent of the stoppered 5 ºC bottle because of the reduced flux boundary between the 500 mL amber bottles and the 1-L beakers during the final room temperature equilibration. Higher temperatures and hence a lower solubility of CO_2 gas increases observed pH.

Increasing surface water temperatures (Austin and Colman, 2007) and alkalinity (U.S. EPA GLENDA) coupled with increases in primary production would all work together to increase pH in Lake Superior where temperature limits production. Such a scenario may be occurring in other mid to high latitude large lakes around the world (Lake Baikal, Lake Nipigon, Great Slave Lake, Great Bear Lake) as the climate warms.

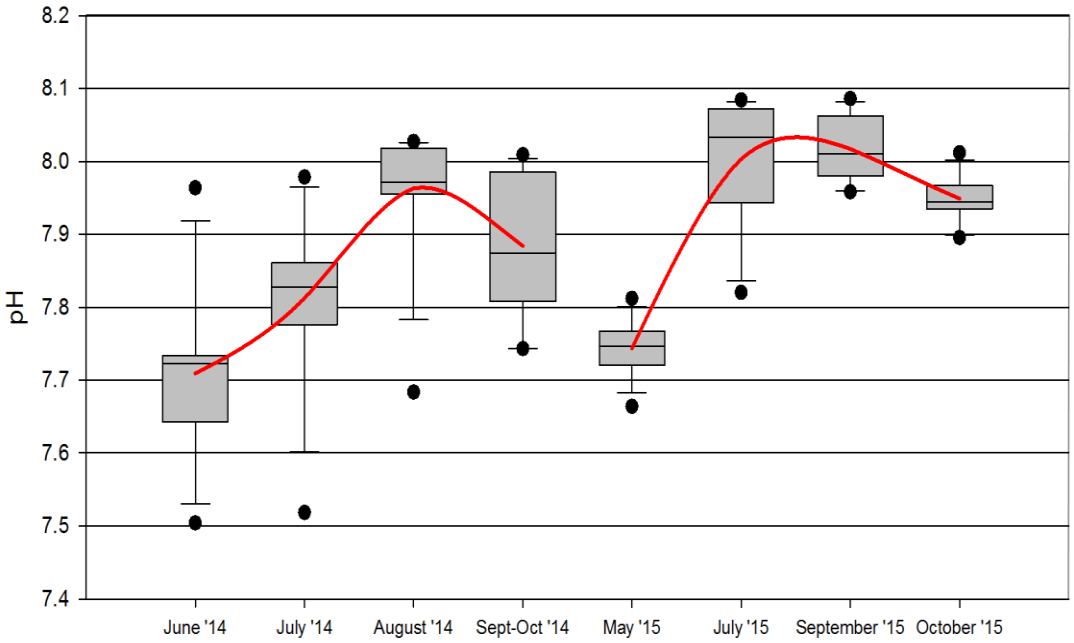

Figure IV-4. Boxplot of lake surface pH for all LCCMR cruises. Plotted are the median, 10th, 25th, 75th, 90th percentiles and maximum/ minimum values. Western arm average pH values are included to show seasonal variation (red line).

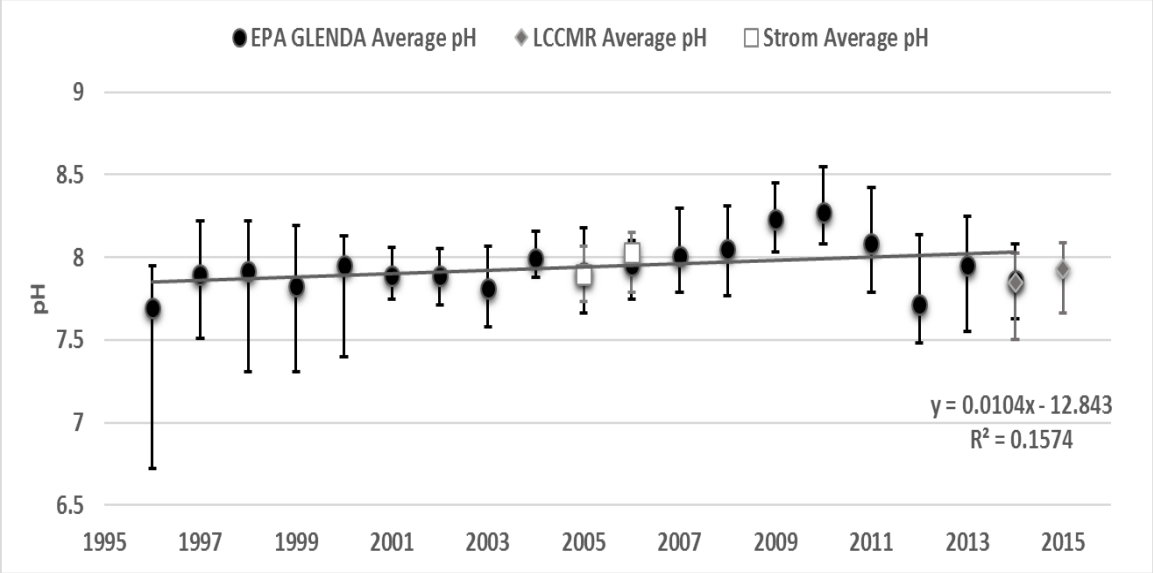

Figure IV-5. Standard plot of mean annual (April and August) surface water electrode pH (LG500 method) for Lake Superior calculated from U.S. EPA GLENDA data over the years of 1996-2014. Plotted in white are annual surface water spectrophotometric pH measurements for two stations in the western arm over 2005-2006 (Strom, 2007) and in grey are the LCCMR annual surface water spectrophotometric pH measurements for the western arm over 2014-2015 (this study). Error bars for all three data sets represent maximum and minimum annual surface water pH measurements.

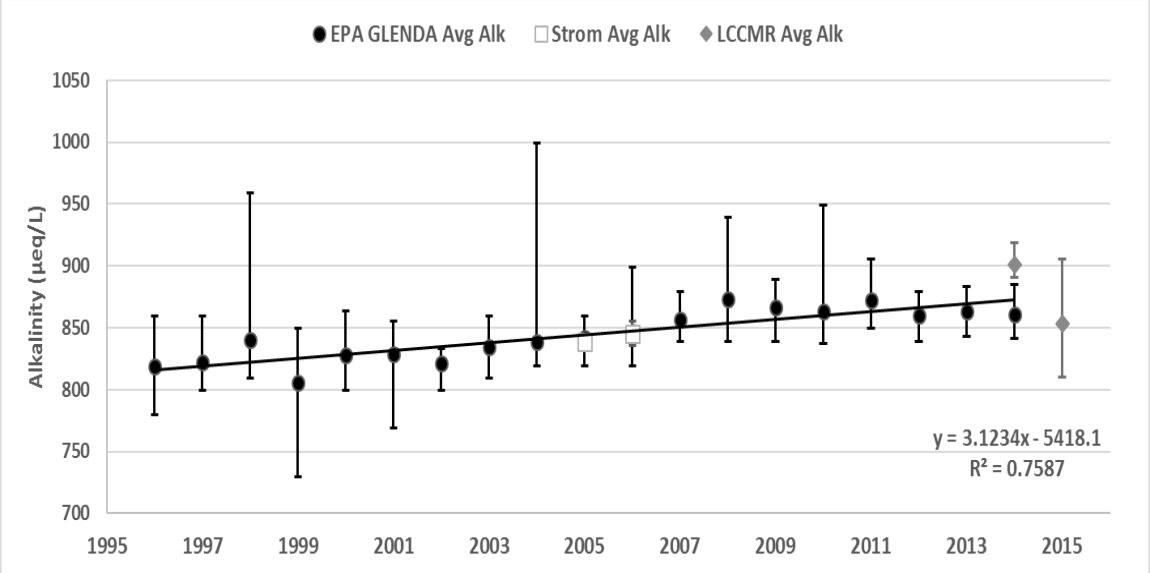

Figure IV-6. Standard plot of mean annual (April and August) surface water alkalinity for Lake Superior calculated from U.S. EPA GLENDA data over the years of 1996-2014. Plotted in white are annual surface water alkalinity measurements for two stations in the western arm over 2005-2006 (Strom, 2007) and in grey are the LCCMR annual surface water alkalinity measurements (this study) for the western arm over 2014-2015. The alkalinity samples are not blank-corrected; error bars represent the maximum and minimum annual surface water alkalinity measurements.

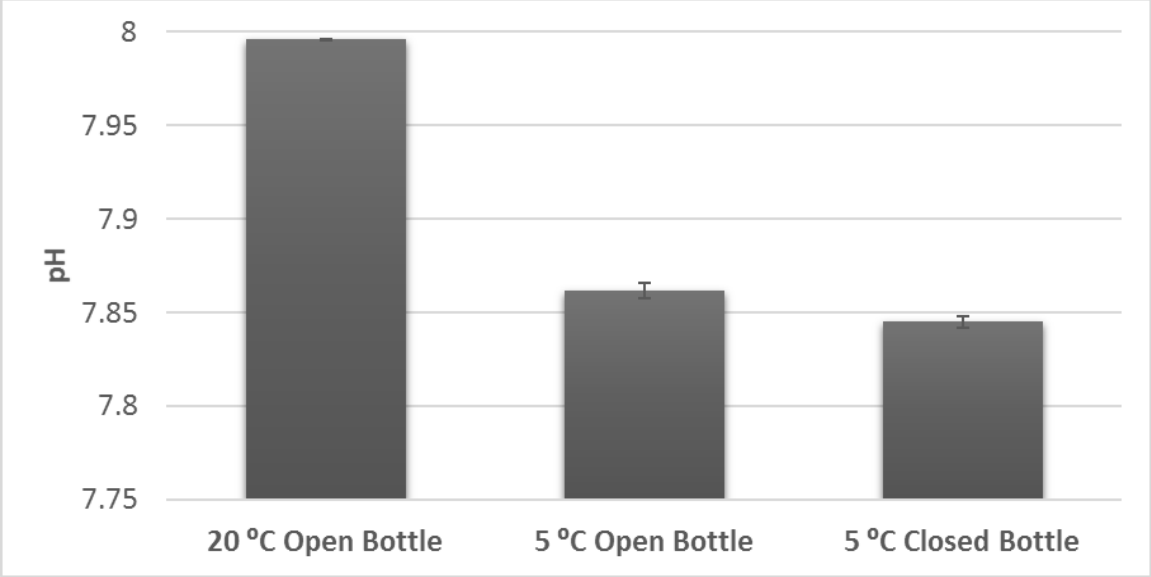

Figure IV-7. Spectrophotometric pH bottle experiment results for sterile filtered Lake Superior water incubated at both room and refrigerator temperature conditions. Error bars represent ±1 standard deviation for each sample.

IV.g Directions for Future Research

In order to further characterize the seasonality and yearly trends in surface water pH throughout Lake Superior, continued spectrophotometric determination of pH is needed. Future studies should increase both the sampling area and yearly repetition to better assess seasonal changes in surface water pH throughout the entire lake. Improved spectrophotometric pH sampling will also provide better insight as to the pCO_2 flux boundary between the atmosphere and lake surface. It will also help to determine whether atmospherically induced acidification is currently occurring in Lake Superior or likely to occur in the near future.

Future sampling efforts should also continue to monitor alkalinity concentrations within the both the lake and incoming rivers to assess whether changes in water chemistry are sourced primarily from the watershed through riverine input or from other sources (i.e., atmosphere or internal primary production). Incoming riverine water chemistry sampling will also provide insight as to whether increased physical and chemical weathering or other stressors such as anthropogenic influences are occurring within the Lake Superior watershed.

V. Bibliography

Alin, S.R., Johnson, T.C., 2007. Carbon cycling in large lakes of the world: A synthesis of production, burial, and lake-atmosphere exchange estimates. Global Biogeochem. Cycles 21, GB3002.

Atilla, N., McKinley, G.A., Bennington, V., Baehr, M., Urban, N., DeGrandpre, M., Desai, A.R., Wu, C., 2011. Observed variability of Lake Superior pCO_2. Limnol. Oceanogr. 56 (3), 775-786.

Austin, J.A., Colman, S.M., 2007. Lake Superior summer water temperatures are increasing more rapidly than regional air temperatures: A positive ice-albedo feedback. Geophysical Research Letters 34, L06604.

Baehr, M.M., DeGrandpre, M.D., 2002. Under-ice CO_2 and O_2 variability in a freshwater lake. Biogeochemistry 61 (1), 95-113.

Bennington, V., McKinley, G.A., Urban, N.R., McDonald, C.P., 2012. Can special heterogeneity explain the perceived imbalance in Lake Superior's carbon budget? A model study. J. Geophys. Res. 117, G03020.

Chapra, S.C., Dove, A., Warren, G.J., 2012. Long-term trends of Great Lakes major ion chemistry. J. Great Lakes Res. 38, 550-560.

Cole, J.J., Prairie, Y.T., Caraco, N.F., McDowell, W.H., Tranvik, L.J., Striegl, R.G., Duarte, C.M., Kortelainen, P., Downing, J.A., Middelburg, J.J., Melack, J., 2007. Plumbing the global carbon cycle: integrating inland waters into the terrestrial carbon budget. Ecosystems 10, 171-184.

Cotner, J.B., Biddanda, B.A., Makino, W., Stets, E., 2004. Organic carbon biogeochemistry of Lake Superior. Aquatic Ecosystem Health & Management 7 (4), 451-464.

DeGrandpre, M.D., Hammar, T.R., Smith, S.P., Sayles, F.L., 1995. In situ measurements of seawater pCO_2. Limnol. Oceanogr. 40 (5), 969-975.

DeGrandpre, M.D., Hammar, T.R., Wallace, D.W.R., Wirick, C.D., 1997. Simultaneous mooring-based measurements of seawater CO_2 and O_2 off Cape Hatteras, North Carolina. Limnol. Oceanogr. 42 (1), 21-28.

French, C.R., Carr, J.J., Dougherty, E.M., Eidson, L.A.K., Reynolds, J.C., DeGrandpre, M.D., 2002. Spectrophotometric pH measurements of freshwater. Analytica Chimica Acta 453, 13-20.

Huttunen, J.T., J. Alm, A. Liikanen, S. Juutinen, T. Larmola, T. Hammar, J. Silvola, and P.J. Martikainen. 2003. Fluxes of methane, carbon dioxide and nitrous oxide in boreal lakes and potential anthropogenic effects on the aquatic greenhouse gas emissions. Chemosphere 52, 609-621.

Kelly, C.A., Fee, E., Ramlal, P.S., Rudd, J.W.M., Hesslein, R.H., Anema, C., Schindler, E.U., 2001. Natural variability of carbon dioxide and net epilimnetic production in the surface waters of boreal lakes of different sizes. Limnol. Oceanogr. 46 (5), 1054-1064.

Kratz T.K., Cook, R.B., Bowser, C.J., Brezonik, P.L., 1987. Winter and spring pH depressions in northern Wisconsin lakes caused by increases in pCO_2. Can. J. Fish. Aquat. Sci. 44, 1082-1088.

Lewis, E., Wallace, D., 1998. Program developed for CO_2 system calculations, report, Carbon Dioxide Inf. Anal. Cent., Oak Ridge Natl. Lab., Oak Ridge, Tenn.

McManus, J., Heinen, E.A., Baehr, M.M., 2003. Hypolimnetic oxidation rates in Lake Superior: Role of dissolved organic material on the lake's carbon budget. Limnol. Oceanogr. 48 (4), 1624-1632.

Meyer, J.L., Sale, M.J., Mulholland, P.J., LeRoy Poff, N., 1999. Impacts of climate change on aquatic ecosystem functioning and health. Journal of the American Water Resources Association 35 (6), 1373-1386.

Millero, F.J., 1979. The thermodynamics of the carbonate system in seawater. Geochimica et Cosmochemica Acta 43, 1651-1661.

Minor, E.C., Forsman, B., Guildford, S.J., 2014. The effect of a flood pulse on the water column of western Lake Superior, USA. J. Great Lakes Res. 40, 455-462.

Murdoch, P.S., Baron, J.S., Miller, T.L., 2000. Potential effects of climate change on surface-water quality in North America. Journal of the American Water Resources Association 36 (2), 347-366.

Ozersky, T., Evans, D.O., Ginn, B.K., 2015. Invasive mussels modify the cycling, storage and distribution of nutrients and carbon in a large lake. Freshwater Biology 60, 827-843.

Phillips, J.C., McKinley, G.A., Bennington, V., Bootsma, H.A., Pilcher, D.J., Sterner, R.W., Urban, N.R., 2015. The potential for CO_2-induced acidification in freshwater: A Great Lakes case study. Oceanography 28 (2), 136-145.

Rahel, F.J., Olden, J.D., 2008. Assessing the effects of climate change on aquatic invasive species. Conservation Biology 22, 521-533.

Sterner, R.W., 2010. *In situ*-measured primary production in Lake Superior. J. Great Lakes Res. 36 (1), 139-149.

Striegl, R.G., Kortelainen, P., Chanton, J.P., Wickland, K.P., Bugna, G.C., Rantakari, M., 2001. Carbon dioxide partial pressure and ^{13}C content of north temperate and boreal lakes at spring ice melt. Limnol. Oceanogr. 46 (4), 941-945.

Strom, J.D., 2007. Seasonal evolution of dissolved gas concentrations in western Lake Superior: Implications for respiration, primary production and carbon cycling. M.S. Thesis, Univ. of Minnesota, 102 pages.

Titze, D.J., Austin, J.A., 2014. Winter thermal structure of Lake Superior. Limnol. Oceanogr. 59 (4), 1336-1348.

Urban, N.R., Auer, M.T., Green, S.A., Lu, X., Apul, D.S., Powell, K.D., Bub, L., 2005. Carbon cycling in Lake Superior. J. Geophys. Res. 110, C06S90.

Weiler, R.R., 1978. Chemistry of Lake Superior. Internat. Assoc. Great Lakes Res. 4 (3-4), 370-385.

Welschmeyer, N.A. 1994. Fluorometric analysis of chlorophyll *a* in the presence of chlorophyll *b* and pheopigments. Limnol. Oceanogr. 39 (8), 1985-1992.

Zigah, P.K., Minor, E.C., Werne, J.P., McCallister, S.L., 2011. Radiocarbon and stable carbon isotopic insights into provenance and cycling of carbon in Lake Superior. Limnol. Oceanogr. 56 (3), 867-886.

Zigah, P.K., Minor, E.C., Werne, J.P., McCallister, S.L., 2012. An isotopic (Δ14C, δ13C, and δ15N) investigation of particulate organic matter and zooplankton biomass in Lake Superior and across a size-gradient of aquatic systems. Biogeosciences 9, 3663-3678.

VI. Appendix

Table VI-1. Percent lake surface-atmosphere pCO_2 difference ($\Delta pCO2$) for Lake Superior western arm sampling stations during all LCCMR cruises. Negative values represent net autotrophic conditions within the lake. * represents stations where water sampling was at 2 m depth.

Station	June '14	July '14	August '14	Sept-Oct '14	May '15	July '15	September '15	October '15
St 1 5m	109	41	3	54	8	-5	-5	5
St 10 5m	29	32	23	15	11	8	-14	1
St 11 5m	40	33	-8	-1	10	7	3	4
St 12 5m	-31	23*	14	19	14	32	14	5
St 2 (CD1) 5m	61	47	-1	-9	15	-11	-20	6
St 3 (WM) 5m	35	34	20	-12	8	29	-15	-2
St 4 (OS) 5m	57	42	19	45	12	-1	1	-1
St 5 5m	27	41	-18	-3	18	-8	1	8
St 6 5m		33	-14	55	34	1	2	-16
St 7 5m	26	29*	60	57	16	-23	11	-5
St 8 5m	26	157	28	25	6	13	-3	14
St 9 5m	27	32	-14	33	19	-34	-19	-11
St BP 5m		34	23		20	18	-20	5

Table VI-2. Chlorophyll fluorescence ($\mu g\ L^{-1}$) for Lake Superior western arm sampling stations during all LCCMR cruises. * represents stations where water sampling was at 2 m depth.

Station	June '14	July '14	August '14	Sept-Oct '14	May '15	July '15	September '15	October '15
St 1 5m	0.799	1.827	0.700	1.288	1.889	0.217	0.884	0.904
St 10 5m	0.863	0.452	0.820	1.603	1.270	1.804	0.697	0.551
St 11 5m	0.756	1.521	0.502	2.169	1.509	1.040	0.703	0.539
St 12 5m	1.118	2.462*	1.655	1.221	1.850	0.261	0.637	0.752
St 2 (CD1) 5m	0.761	0.444	0.875	1.877	0.956	0.147	0.684	0.501
St 3 (WM) 5m	0.473	0.718	0.531	1.589	0.964	0.102	0.460	0.649
St 4 (OS) 5m	0.873	1.844	0.581	1.826	1.491	0.206	0.847	0.958
St 5 5m	0.650	0.990	1.482	2.153	1.016	1.439	0.714	0.595
St 6 5m		0.661	1.882	1.039	0.986	0.231	0.700	0.981
St 7 5m	0.798	2.360*	1.036	1.288	1.414	0.212	0.573	0.805
St 8 5m	1.038	0.683	1.178	1.598	1.862	0.084	0.333	0.514
St 9 5m	0.840	0.664	1.372	1.711	1.287	0.231	0.834	0.698
St BP 5m		0.737	0.924		1.146	1.115	1.135	0.513

Table VI-3. Spectrophotometric pH values for Lake Superior western arm sampling stations for all depths sampled during LCCMR 2014 cruises.

Date	Cruise	Station	pH	St. Dev.	Date	Cruise	Station	pH	St. Dev.
6/3/2014	LCCMR1	St 4 (OS) 5m	7.637	0.024	8/16/2014	LCCMR4	St 1 5m	8.013	0.012
6/3/2014	LCCMR1	St 1 5m	7.504	0.176	8/16/2014	LCCMR4	St 2 (CD1) 18m	7.868	0.011
6/3/2014	LCCMR1	St 2 (CD1) 210m	7.618	0.001	8/16/2014	LCCMR4	St 2 (CD1) 210m	7.696	0.006
6/3/2014	LCCMR1	St 2 (CD1) 35m	7.673	0.004	8/16/2014	LCCMR4	St 2 (CD1) 5m	7.986	0.023
6/3/2014	LCCMR1	St 2 (CD1) 5m	7.643	0.034	8/16/2014	LCCMR4	St 4 (OS) 5m	8.013	0.015
6/4/2014	LCCMR1	St 3 (WM) 5m	7.702	0.013	8/17/2014	LCCMR4	St 3 (WM) 120m	7.707	0.007
6/4/2014	LCCMR1	St 3 (WM) 120m	7.681	0.011	8/17/2014	LCCMR4	St 3 (WM) 30m	7.858	0.004
6/4/2014	LCCMR1	St 3 (WM) 30m	7.706	0.008	8/17/2014	LCCMR4	St 3 (WM) 5m	7.932	0.002
6/5/2014	LCCMR1	St 8 5m	7.734	0.022	8/18/2014	LCCMR4	St 10 5m	7.966	0.005
6/5/2014	LCCMR1	St 10 5m	7.734	0.002	8/18/2014	LCCMR4	St 11 14m	7.870	0.011
6/5/2014	LCCMR1	St 11 20m	7.701	0.013	8/18/2014	LCCMR4	St 11 5m	8.023	0.001
6/5/2014	LCCMR1	St 11 60m	7.691	0.008	8/18/2014	LCCMR4	St 11 60m	7.607	0.011
6/5/2014	LCCMR1	St 11 5m	7.693	0.012	8/18/2014	LCCMR4	St 12 5m	7.972	0.012
6/5/2014	LCCMR1	St 12 5m	7.964	0.080	8/18/2014	LCCMR4	St 8 5m	7.971	0.006
6/5/2014	LCCMR1	St 9 5m	7.723	0.010	8/18/2014	LCCMR4	St 9 5m	8.024	0.010
6/6/2014	LCCMR1	St 5 5m	7.729	0.003	8/19/2014	LCCMR4	St BP 5m	7.956	0.005
6/6/2014	LCCMR1	St 7 5m	7.737	0.002	8/19/2014	LCCMR4	St 5 5m	8.027	0.004
6/4/2014	LCCMR1	EDTA (pH 8.0)	8.241	0.001	8/19/2014	LCCMR4	St 6 5m	7.954	0.000
7/22/2014	LCCMR2-3	St 4 (OS) 5m	7.876	0.001	8/19/2014	LCCMR4	St 7 5m	7.683	0.015
7/22/2014	LCCMR2-3	St 1 5m	7.828	0.002	8/16/2014	LCCMR4	EDTA (pH 8.0)	8.202	0.019
7/22/2014	LCCMR2-3	St 2 (CD1) 5m	7.728	0.002	9/24/2014	UNOLS Inspection	St 4 (OS) 25m	7.769	0.005
7/22/2014	LCCMR2-3	St 2 (CD1) 35m	7.724	0.001	9/24/2014	UNOLS Inspection	St 4 (OS) 5m	7.833	0.013
7/22/2014	LCCMR2-3	St 2 (CD1) 210m	7.723	0.014	9/24/2014	UNOLS Inspection	EDTA (pH 8.0)	8.190	0.000
7/23/2014	LCCMR2-3	St 3 (WM) 5m	7.764	0.001	9/30/2014	LCCMR5	St 2 (CD1) 5m	8.009	0.001
7/23/2014	LCCMR2-3	St 3 (WM) 120m	7.726	0.002	9/30/2014	LCCMR5	St 2 (CD1) 20m	7.920	0.026
7/23/2014	LCCMR2-3	St 3 (WM) 30m	7.749	0.002	9/30/2014	LCCMR5	St 2 (CD1) 210m	7.599	0.018
7/24/2014	LCCMR2-3	St 8 5m	7.518	0.134	9/30/2014	LCCMR5	St 4 (OS) 5m	7.828	0.021
7/24/2014	LCCMR2-3	St 10 5m	7.845	0.000	9/30/2014	LCCMR5	St 1 5m	7.801	0.020
7/24/2014	LCCMR2-3	St 11 5m	7.841	0.040	10/1/2014	LCCMR5	St 3 (WM) 5m	7.992	0.011
7/24/2014	LCCMR2-3	St 11 12m	7.713	0.039	10/1/2014	LCCMR5	St 3 (WM) 30m	7.861	0.013
7/24/2014	LCCMR2-3	St 12 2m	7.978	0.003	10/1/2014	LCCMR5	St 3 (WM) 120m	7.639	0.007
7/24/2014	LCCMR2-3	St 9 5m	7.811	0.005	10/1/2014	LCCMR5	St 8 5m	7.859	0.005
7/25/2014	LCCMR2-3	St BP 5m	7.788	0.001	10/2/2014	LCCMR5	St 12 5m	7.889	0.013
7/25/2014	LCCMR2-3	St 5 5m	7.798	0.004	10/2/2014	LCCMR5	St 11 60m	7.607	0.001
7/25/2014	LCCMR2-3	St 7 2m	7.946	0.026	10/2/2014	LCCMR5	St 11 10m	7.945	0.007
7/25/2014	LCCMR2-3	St 6 5m	7.842	0.004	10/2/2014	LCCMR5	St 11 5m	7.980	0.000
7/25/2014	LCCMR2-3	EDTA (pH 8.0)	8.225	0.004	10/2/2014	LCCMR5	St 9 5m	7.859	0.013
					10/2/2014	LCCMR5	St 10 5m	7.918	0.000
					10/2/2014	LCCMR5	St 7 5m	7.744	0.001
					10/2/2014	LCCMR5	St 6 5m	7.743	0.012
					10/2/2014	LCCMR5	St 5 5m	7.987	0.004
					10/1/2014	LCCMR5	EDTA (pH 8.0)	8.266	0.004

Table VI-4. Spectrophotometric pH values for Lake Superior western arm sampling stations for all depths sampled during LCCMR 2015 cruises.

Date	Cruise	Station	pH	St. Dev.	Date	Cruise	Station	pH	St. Dev.
2/8/2015	Bayfield Ice Road	Bayfield 10m	7.756	0.002	9/8/2015	LCCMR8	St 4 (OS) 5m	7.992	0.022
2/8/2015	Bayfield Ice Road	Bayfield 20m	7.745	0.012	9/8/2015	LCCMR8	St 1 5m	8.012	0.003
2/8/2015	Bayfield Ice Road	EDTA (pH 8.0)	8.277	0.002	9/8/2015	LCCMR8	St 12 5m	7.958	0.004
5/19/2015	LCCMR6	St 4 (OS) 5m	7.758	0.005	9/8/2015	LCCMR8	St 7 5m	7.961	0.006
5/20/2015	LCCMR6	St 1 5m	7.812	0.007	9/8/2015	LCCMR8	St 6 5m	8.010	0.008
5/20/2015	LCCMR6	St 12 5m	7.783	0.010	9/8/2015	LCCMR8	St 8 5m	8.002	0.008
5/20/2015	LCCMR6	St 9 5m	7.722	0.011	9/9/2015	LCCMR8	St 3 (WM) 5m	8.065	0.002
5/20/2015	LCCMR6	St 7 5m	7.745	0.019	9/9/2015	LCCMR8	St 3 (WM) 20m	8.006	0.016
5/20/2015	LCCMR6	St 6 5m	7.664	0.007	9/9/2015	LCCMR8	St 3 (WM) 120m	7.665	0.000
5/21/2015	LCCMR6	St 3 (WM) 5m	7.746	0.005	9/9/2015	LCCMR8	St 2 (CD1) 5m	8.086	0.002
5/21/2015	LCCMR6	St 3 (WM) 120m	7.720	0.010	9/9/2015	LCCMR8	St 2 (CD1) 22m	7.798	0.009
5/21/2015	LCCMR6	St 3 (WM) 30m	7.741	0.014	9/9/2015	LCCMR8	St 2 (CD1) 210m	7.651	0.004
5/21/2015	LCCMR6	St 8 5m	7.774	0.003	9/9/2015	LCCMR8	St BP 5m	8.060	0.000
5/21/2015	LCCMR6	St 2 (CD1) 210m	7.670	0.000	9/10/2015	LCCMR8	St 9 5m	8.076	0.006
5/21/2015	LCCMR6	St 2 (CD1) 20m	7.720	0.006	9/10/2015	LCCMR8	St 5 5m	7.989	0.001
5/21/2015	LCCMR6	St 2 (CD1) 5m	7.724	0.002	9/10/2015	LCCMR8	St 10 5m	8.039	0.002
5/21/2015	LCCMR6	St BP 5m	7.711	0.014	9/10/2015	LCCMR8	St 11 5m	7.972	0.002
5/22/2015	LCCMR6	St 5 5m	7.718	0.007	9/10/2015	LCCMR8	St 11 17m	7.765	0.001
5/22/2015	LCCMR6	St 10 5m	7.746	0.002	9/10/2015	LCCMR8	St 11 60m	7.564	0.007
5/22/2015	LCCMR6	St 11 60m	7.750	0.000	9/9/2015	LCCMR8	EDTA (pH 8.0)	8.194	0.001
5/22/2015	LCCMR6	St 11 25m	7.766	0.010	10/5/2015	LCCMR9	St 4 (OS) 5m	7.957	0.002
5/22/2015	LCCMR6	St 11 5m	7.761	0.010	10/5/2015	LCCMR9	St 1 5m	7.933	0.014
5/21/2015	LCCMR6	EDTA (pH 8.0)	8.280	0.001	10/5/2015	LCCMR9	St 12 5m	7.936	0.010
7/15/2015	LCCMR7	St 4 (OS) 5m	8.043	0.004	10/5/2015	LCCMR9	St 7 5m	7.977	0.002
7/15/2015	LCCMR7	St 1 5m	8.079	0.001	10/5/2015	LCCMR9	St 8 5m	7.896	0.003
7/15/2015	LCCMR7	St 12 5m	7.859	0.011	10/6/2015	LCCMR9	St 3 (WM) 120m	7.643	0.012
7/15/2015	LCCMR7	St 7 5m	8.077	0.008	10/6/2015	LCCMR9	St 3 (WM) 25m	7.715	0.001
7/15/2015	LCCMR7	St 8 5m	7.952	0.005	10/6/2015	LCCMR9	St 3 (WM) 5m	7.947	0.004
7/16/2015	LCCMR7	St 3 (WM) 5m	7.820	0.014	10/6/2015	LCCMR9	St 5 5m	7.905	0.005
7/16/2015	LCCMR7	St 3 (WM) 30m	7.776	0.002	10/6/2015	LCCMR9	St 2 (CD1) 210m	7.642	0.001
7/16/2015	LCCMR7	St 3 (WM) 120m	7.708	0.001	10/6/2015	LCCMR9	St 2 (CD1) 45m	7.774	0.007
7/16/2015	LCCMR7	St 5 5m	8.061	0.003	10/6/2015	LCCMR9	St 2 (CD1) 5m	7.945	0.008
7/16/2015	LCCMR7	St 2 (CD1) 5m	8.067	0.005	10/6/2015	LCCMR9	St BP 5m	7.943	0.001
7/16/2015	LCCMR7	St 2 (CD1) 30m	7.855	0.006	10/7/2015	LCCMR9	St 9 5m	7.985	0.001
7/16/2015	LCCMR7	St 2 (CD1) 120m	7.712	0.000	10/7/2015	LCCMR9	St 6 5m	8.012	0.009
7/16/2015	LCCMR7	St BP 5m	7.936	0.006	10/7/2015	LCCMR9	St 10 5m	7.957	0.000
7/17/2015	LCCMR7	St 9 5m	8.084	0.002	10/7/2015	LCCMR9	St 11 60m	7.867	0.000
7/17/2015	LCCMR7	St 6 5m	8.001	0.005	10/7/2015	LCCMR9	St 11 10m	7.959	0.000
7/17/2015	LCCMR7	St 10 5m	8.033	0.007	10/7/2015	LCCMR9	St 11 5m	7.944	0.000
7/17/2015	LCCMR7	St 11 5m	8.030	0.003	10/7/2015	LCCMR9	EDTA (pH 8.0)	8.229	0.002
7/17/2015	LCCMR7	St 11 13m	7.768	0.003					
7/17/2015	LCCMR7	St 11 60m	7.681	0.003					
7/15/2015	LCCMR7	EDTA (pH 8.0)	8.209	0.004					

Table VI-5. Dissolved, total, and particulate organic carbon concentrations (mg L^{-1}) for Lake Superior western arm sampling stations for all depths sampled during LCCMR 2014 cruises.

Date	Cruise	Station	DOC (mg/L C)	DOC St. Dev. (mg/L C)	TOC (mg/L C)	TOC St. Dev. (mg/L C)	POC (mg/L C)
6/3/2014	LCCMR1	St 4 (OS) 5m	1.81	0.03	1.88	0.02	0.07
6/3/2014	LCCMR1	St 1 5m	1.73	0.04	1.86	0.02	0.13
6/3/2014	LCCMR1	St 2 (CD1) 210m	0.98	0.02	1.17	0.02	0.19
6/3/2014	LCCMR1	St 2 (CD1) 35m	1.02	0.02	1.30	0.02	0.28
6/3/2014	LCCMR1	St 2 (CD1) 5m	0.99	0.01	1.32	0.02	0.33
6/4/2014	LCCMR1	St 3 (WM) 5m	1.13	0.02	1.09	0.02	-0.03
6/4/2014	LCCMR1	St 3 (WM) 120m	1.02	0.02	1.17	0.02	0.15
6/4/2014	LCCMR1	St 3 (WM) 30m	0.99	0.02	1.15	0.02	0.15
6/5/2014	LCCMR1	St 8 5m	0.89	0.01	1.17	0.02	0.29
6/5/2014	LCCMR1	St 10 5m	1.07	0.01	1.27	0.02	0.20
6/5/2014	LCCMR1	St 11 20m	1.26	0.02	1.63	0.02	0.37
6/5/2014	LCCMR1	St 11 60m	1.67	0.02	1.73	0.03	0.06
6/5/2014	LCCMR1	St 11 5m	1.24	0.02	1.43	0.02	0.20
6/5/2014	LCCMR1	St 12 5m					
6/5/2014	LCCMR1	St 9 5m	1.09	0.02	1.12	0.01	0.03
6/6/2014	LCCMR1	St 5 5m	0.95	0.01	1.24	0.02	0.30
6/6/2014	LCCMR1	St 7 5m	0.98	0.01	1.06	0.02	0.08
8/6/2014	LCCMR1	Check Std 1.49 mg/L C			1.56	0.02	
7/22/2014	LCCMR2-3	St 4 (OS) 5m	2.94	0.06	3.08	0.04	0.14
7/22/2014	LCCMR2-3	St 1 5m	2.22	0.04	2.11	0.04	-0.11
7/22/2014	LCCMR2-3	St 2 (CD1) 5m	1.02	0.01	1.06	0.02	0.04
7/22/2014	LCCMR2-3	St 2 (CD1) 35m	1.16	0.02	1.13	0.02	-0.02
7/22/2014	LCCMR2-3	St 2 (CD1) 210m	1.15	0.01	1.08	0.01	-0.07
7/23/2014	LCCMR2-3	St 3 (WM) 5m	1.06	0.03	0.98	0.02	-0.07
7/23/2014	LCCMR2-3	St 3 (WM) 120m	0.98	0.02	1.10	0.02	0.12
7/23/2014	LCCMR2-3	St 3 (WM) 30m	1.11	0.02	1.06	0.02	-0.05
7/24/2014	LCCMR2-3	St 8 5m	1.01	0.02	1.14	0.02	0.13
7/24/2014	LCCMR2-3	St 10 5m	1.08	0.03	1.11	0.02	0.02
7/24/2014	LCCMR2-3	St 11 5m	1.44	0.02	1.62	0.03	0.18
7/24/2014	LCCMR2-3	St 11 12m	1.55	0.02	1.55	0.03	0.01
7/24/2014	LCCMR2-3	St 12 2m	3.38	0.07	3.62	0.08	0.24
7/24/2014	LCCMR2-3	St 9 5m	1.13	0.02	1.05	0.01	-0.08
7/25/2014	LCCMR2-3	St BP 5m	1.21	0.01	1.24	0.02	0.03
7/25/2014	LCCMR2-3	St 5 5m	1.07	0.02	1.12	0.03	0.06
7/25/2014	LCCMR2-3	St 7 2m	2.35	0.04	2.81	0.03	0.47
7/25/2014	LCCMR2-3	St 6 5m	1.23	0.02	1.18	0.01	-0.06
8/7/2014	LCCMR2-3	Check Std 1.04 mg/L C			0.95	0.02	
8/16/2014	LCCMR4	St 1 5m	1.79	0.05	1.83	0.03	0.04
8/16/2014	LCCMR4	St 2 (CD1) 18m	1.40	0.02	1.40	0.02	-0.01
8/16/2014	LCCMR4	St 2 (CD1) 210m	1.44	0.03	1.42	0.02	-0.02
8/16/2014	LCCMR4	St 2 (CD1) 5m	1.46	0.05	1.66	0.01	0.19
8/16/2014	LCCMR4	St 4 (OS) 5m	2.07	0.04	2.11	0.05	0.03
8/17/2014	LCCMR4	St 3 (WM) 120m	1.49	0.02	1.43	0.06	-0.06
8/17/2014	LCCMR4	St 3 (WM) 30m	1.37	0.03	1.43	0.02	0.07
8/17/2014	LCCMR4	St 3 (WM) 5m	1.44	0.03	1.58	0.03	0.13
8/18/2014	LCCMR4	St 10 5m	1.60	0.02	1.80	0.04	0.20
8/18/2014	LCCMR4	St 11 14m	1.65	0.03	1.55	0.02	-0.10
8/18/2014	LCCMR4	St 11 5m	2.13	0.04	2.15	0.03	0.02
8/18/2014	LCCMR4	St 11 60m	1.66	0.04	1.69	0.02	0.03
8/18/2014	LCCMR4	St 12 5m	1.95	0.02	2.19	0.05	0.24
8/18/2014	LCCMR4	St 8 5m	2.25	0.03	2.50	0.05	0.25
8/18/2014	LCCMR4	St 9 5m	1.81	0.04	2.43	0.06	0.63
8/19/2014	LCCMR4	St BP 5m	1.67	0.02	1.84	0.04	0.18
8/19/2014	LCCMR4	St 5 5m	1.87	0.03	1.72	0.03	-0.15
8/19/2014	LCCMR4	St 6 5m	1.85	0.03	1.72	0.03	-0.14
8/19/2014	LCCMR4	St 7 5m	1.72	0.04	2.01	0.03	0.29
8/26/2014	LCCMR4	Check Std 1.55 mg/L C			1.54	0.01	
9/30/2014	LCCMR5	St 2 (CD1) 5m	1.9	0.04	1.9	0.02	0.0
9/30/2014	LCCMR5	St 2 (CD1) 20m	1.8	0.02	2.0	0.02	0.1
9/30/2014	LCCMR5	St 2 (CD1) 210m	1.6	0.04	1.7	0.05	0.1
9/30/2014	LCCMR5	St 4 (OS) 5m	2.0	0.02	2.0	0.04	0.0
9/30/2014	LCCMR5	St 1 5m	2.0	0.05	2.0	0.01	0.0
10/1/2014	LCCMR5	St 3 (WM) 5m	1.7	0.03	1.7	0.03	0.0
10/1/2014	LCCMR5	St 3 (WM) 30m	1.7	0.03	1.7	0.04	0.0
10/1/2014	LCCMR5	St 3 (WM) 120m	1.7	0.04	1.6	0.02	-0.1
10/1/2014	LCCMR5	St 8 5m	1.9	0.04	1.8	0.04	-0.1
10/2/2014	LCCMR5	St 12 5m	1.9	0.02	1.8	0.05	-0.1
10/2/2014	LCCMR5	St 11 60m	1.7	0.01	1.6	0.00	-0.1
10/2/2014	LCCMR5	St 11 10m	1.9	0.03	1.9	0.03	0.1
10/2/2014	LCCMR5	St 11 5m	1.8	0.04	1.9	0.05	0.1
10/2/2014	LCCMR5	St 9 5m	1.8	0.02	1.9	0.05	0.1
10/2/2014	LCCMR5	St 10 5m	1.9	0.02	1.9	0.04	0.0
10/2/2014	LCCMR5	St 7 5m	1.9	0.05	1.9	0.03	0.0
10/2/2014	LCCMR5	St 6 5m	1.8	0.03	1.9	0.03	0.1
10/2/2014	LCCMR5	St 5 5m	1.9	0.03	1.9	0.01	0.0
10/8/2014	LCCMR5	Check Std 2.66 mg/L C			2.8	0.03	

Table VI-6. Dissolved, total, and particulate organic carbon concentrations (mg L^{-1}) for Lake Superior western arm sampling stations for all depths sampled during LCCMR 2015 cruises.

Date	Cruise	Station	DOC (mg/L C)	DOC St. Dev. (mg/L C)	TOC (mg/L C)	TOC St. Dev. (mg/L C)	POC (mg/L C)
2/8/2015	Bayfield Ice Road	Bayfield 10m	1.26	0.01	1.30	0.02	0.04
2/8/2015	Bayfield Ice Road	Bayfield 20m	1.30	0.02	1.30	0.03	0.00
2/10/2015	Bayfield Ice Road	Check Std 2.43 mg/L C			2.39	0.05	
5/19/2015	LCCMR6	St 4 (OS) 5m	1.16	0.02	1.26	0.01	0.10
5/20/2015	LCCMR6	St 1 5m	1.28	0.02	1.36	0.03	0.08
5/20/2015	LCCMR6	St 12 5m	1.14	0.01	1.17	0.02	0.03
5/20/2015	LCCMR6	St 9 5m	1.07	0.02	1.18	0.02	0.11
5/20/2015	LCCMR6	St 7 5m	1.10	0.02	1.17	0.01	0.07
5/20/2015	LCCMR6	St 6 5m	1.09	0.02	1.14	0.02	0.05
5/21/2015	LCCMR6	St 3 (WM) 5m	1.04	0.02	1.11	0.02	0.07
5/21/2015	LCCMR6	St 3 (WM) 120m	1.08	0.02	1.08	0.02	0.00
5/21/2015	LCCMR6	St 3 (WM) 30m	1.00	0.01	1.12	0.02	0.12
5/21/2015	LCCMR6	St 8 5m	1.00	0.02	1.15	0.02	0.15
5/21/2015	LCCMR6	St 2 (CD1) 210m	1.07	0.02	1.11	0.01	0.04
5/21/2015	LCCMR6	St 2 (CD1) 20m	1.12	0.01	1.12	0.02	0.00
5/21/2015	LCCMR6	St 2 (CD1) 5m	1.05	0.02	1.13	0.01	0.08
5/21/2015	LCCMR6	St BP 5m	1.09	0.01	1.09	0.01	-0.01
5/22/2015	LCCMR6	St 5 5m	1.07	0.01	1.08	0.02	0.01
5/22/2015	LCCMR6	St 10 5m	1.10	0.01	1.18	0.02	0.09
5/22/2015	LCCMR6	St 11 60m	1.12	0.02	1.17	0.02	0.05
5/22/2015	LCCMR6	St 11 25m	1.09	0.02	1.23	0.04	0.14
5/22/2015	LCCMR6	St 11 5m	1.03	0.01	1.14	0.02	0.11
5/26/2015	LCCMR6	Check Std 1.31 mg/L C			1.26	0.01	
7/15/2015	LCCMR7	St 4 (OS) 5m	1.56	0.03	1.72	0.04	0.16
7/15/2015	LCCMR7	St 1 5m	1.99	0.04	2.05	0.04	0.06
7/15/2015	LCCMR7	St 12 5m	1.88	0.03	2.02	0.04	0.14
7/15/2015	LCCMR7	St 7 5m	1.60	0.03	1.66	0.04	0.06
7/15/2015	LCCMR7	St 8 5m	1.15	0.02	1.17	0.01	0.02
7/16/2015	LCCMR7	St 3 (WM) 5m	1.09	0.01	1.13	0.02	0.04
7/16/2015	LCCMR7	St 3 (WM) 30m	1.08	0.01	1.12	0.03	0.04
7/16/2015	LCCMR7	St 3 (WM) 120m	1.08	0.01	1.13	0.02	0.05
7/16/2015	LCCMR7	St 5 5m	1.69	0.02	1.72	0.03	0.04
7/16/2015	LCCMR7	St 2 (CD1) 5m	1.36	0.01	1.45	0.03	0.09
7/16/2015	LCCMR7	St 2 (CD1) 30m	1.18	0.00	1.14	0.02	-0.04
7/16/2015	LCCMR7	St 2 (CD1) 120m	1.11	0.02	1.13	0.02	0.02
7/16/2015	LCCMR7	St BP 5m	1.56	0.03	1.52	0.02	-0.04
7/17/2015	LCCMR7	St 9 5m	1.44	0.03	1.53	0.03	0.08
7/17/2015	LCCMR7	St 6 5m	1.48	0.03	1.38	0.03	-0.10
7/17/2015	LCCMR7	St 10 5m	1.85	0.03	1.86	0.03	0.01
7/17/2015	LCCMR7	St 11 5m	1.57	0.02	1.56	0.02	-0.01
7/17/2015	LCCMR7	St 11 13m	1.31	0.01	1.31	0.02	0.00
7/17/2015	LCCMR7	St 11 60m	1.13	0.02	1.17	0.03	0.05
7/23/2015	LCCMR7	Check Std 1.98 mg/L C			1.91	0.04	
9/8/2015	LCCMR8	St 4 (OS) 5m	1.08	0.01	1.16	0.03	0.08
9/8/2015	LCCMR8	St 1 5m	1.03	0.02	1.14	0.05	0.11
9/8/2015	LCCMR8	St 12 5m	1.13	0.00	1.21	0.02	0.08
9/8/2015	LCCMR8	St 7 5m	1.12	0.01	1.25	0.01	0.13
9/8/2015	LCCMR8	St 6 5m	1.14	0.02	1.18	0.01	0.04
9/8/2015	LCCMR8	St 8 5m	1.02	0.02	1.11	0.02	0.09
9/9/2015	LCCMR8	St 3 (WM) 5m	0.95	0.00	1.06	0.02	0.12
9/9/2015	LCCMR8	St 3 (WM) 20m	0.88	0.06	1.01	0.01	0.12
9/9/2015	LCCMR8	St 3 (WM) 120m	0.84	0.01	1.08	0.02	0.25
9/9/2015	LCCMR8	St 2 (CD1) 5m	1.03	0.00	1.11	0.01	0.07
9/9/2015	LCCMR8	St 2 (CD1) 22m	0.89	0.04	1.01	0.02	0.12
9/9/2015	LCCMR8	St 2 (CD1) 210m	0.87	0.01	0.99	0.02	0.12
9/9/2015	LCCMR8	St BP 5m	1.76	0.04	1.87	0.03	0.11
9/10/2015	LCCMR8	St 9 5m	0.96	0.02	1.04	0.02	0.08
9/10/2015	LCCMR8	St 5 5m	1.00	0.02	1.04	0.02	0.04
9/10/2015	LCCMR8	St 10 5m	1.03	0.01	1.11	0.02	0.09
9/10/2015	LCCMR8	St 11 5m	0.98	0.03	1.09	0.02	0.11
9/10/2015	LCCMR8	St 11 17m	0.99	0.02	1.05	0.03	0.05
9/10/2015	LCCMR8	St 11 60m	0.89	0.03	1.03	0.00	0.14
9/16/2015	LCCMR8	Check Std 1.30 mg/L C			1.16	0.04	
10/5/2015	LCCMR9	St 4 (OS) 5m	1.09	0.07	1.27	0.02	0.19
10/5/2015	LCCMR9	St 1 5m	0.96	0.02	1.30	0.01	0.34
10/5/2015	LCCMR9	St 12 5m	1.25	0.08	1.44	0.03	0.19
10/5/2015	LCCMR9	St 7 5m	1.24	0.03	1.24	0.03	0.00
10/5/2015	LCCMR9	St 8 5m	1.16	0.03	1.29	0.03	0.13
10/6/2015	LCCMR9	St 3 (WM) 120m	1.01	0.05	1.28	0.03	0.27
10/6/2015	LCCMR9	St 3 (WM) 25m	0.76	0.01	1.20	0.02	0.44
10/6/2015	LCCMR9	St 3 (WM) 5m	1.16	0.09	1.43	0.02	0.27
10/6/2015	LCCMR9	St 5 5m	0.96	0.03	1.44	0.11	0.49
10/6/2015	LCCMR9	St 2 (CD1) 210m	1.14	0.04	1.26	0.06	0.12
10/6/2015	LCCMR9	St 2 (CD1) 45m	1.07	0.03	1.08	0.02	0.01
10/6/2015	LCCMR9	St 2 (CD1) 5m	1.08	0.04	1.16	0.03	0.08
10/6/2015	LCCMR9	St BP 5m	0.94	0.03	1.55	0.04	0.61
10/7/2015	LCCMR9	St 9 5m	0.98	0.03	1.51	0.02	0.53
10/7/2015	LCCMR9	St 6 5m	0.93	0.02	1.60	0.04	0.67
10/7/2015	LCCMR9	St 10 5m	1.15	0.04	1.20	0.01	0.05
10/7/2015	LCCMR9	St 11 60m	0.99	0.02	1.58	0.02	0.59
10/7/2015	LCCMR9	St 11 10m	0.92	0.02	1.24	0.19	0.32
10/7/2015	LCCMR9	St 11 5m	1.10	0.05	1.26	0.01	0.16
10/20/2015	LCCMR9	Check Std 1.21 mg/L C			1.32	0.04	

Table VI-7. Blank corrected acid neutralizing capacity concentrations (unfiltered; mg L^{-1} & µeq L^{-1} as $CaCO_3$) for Lake Superior western arm sampling stations for all depths sampled during LCCMR 2014 cruises.

Date	Cruise	Station	ANC (mg/L CaCO3)	ANC (ueq/L) CaCO3
9/24/2014	UNOLS Inspection	St 4 (OS) 25m	42.6	851
9/24/2014	UNOLS Inspection	St 4 (OS) 5m	43.8	874
9/24/2014	UNOLS Inspection	Check Std 80.0 mg/L CaCO3	79.0	1578
10/2/2014	LCCMR5	St 12 5m	42.9	858
10/2/2014	LCCMR5	St 11 60m	43.8	874
10/2/2014	LCCMR5	St 11 10m	43.3	865
10/2/2014	LCCMR5	St 11 5m	42.8	856
10/2/2014	LCCMR5	St 9 5m	43.5	870
10/2/2014	LCCMR5	St 10 5m	42.9	858
10/2/2014	LCCMR5	St 7 5m	42.4	846
10/2/2014	LCCMR5	St 6 5m	42.4	846
10/2/2014	LCCMR5	St 5 5m	42.4	846
10/2/2014	LCCMR5	Check Std 80.0 mg/L CaCO3	83.0	1658

Table VI-8. Blank-corrected acid neutralizing capacity concentrations (unfiltered; mg L^{-1} & µeq L^{-1} as $CaCO_3$) for Lake Superior western arm sampling stations for all depths sampled during LCCMR 2015 cruises. Samples with * determined by USGS Gran titration method.

Date	Cruise	Station	ANC (mg/L CaCO3)	ANC (ueq/L) CaCO3
2/8/2015	Bayfield Ice Road	Bayfield 10m	43.3	865
2/8/2015	Bayfield Ice Road	Bayfield 20m	43.9	877
2/8/2015	Bayfield Ice Road	Check Std 40.0 mg/L CaCO3	40.1	801
5/19/2015	LCCMR6	St 4 (OS) 5m	41.7	833
5/20/2015	LCCMR6	St 1 5m	42.3	845
5/20/2015	LCCMR6	St 12 5m	40.8	815
5/20/2015	LCCMR6	St 9 5m	41.1	821
5/20/2015	LCCMR6	St 7 5m	40.2	804
5/20/2015	LCCMR6	St 6 5m	40.8	815
5/21/2015	LCCMR6	St 3 (WM) 5m	40.2	804
5/21/2015	LCCMR6	St 3 (WM) 120m	40.5	809
5/21/2015	LCCMR6	St 3 (WM) 30m	40.8	815
5/21/2015	LCCMR6	St 8 5m	40.5	809
5/21/2015	LCCMR6	St 2 (CD1) 210m	40.8	815
5/21/2015	LCCMR6	St 2 (CD1) 20m	41.1	821
5/21/2015	LCCMR6	St 2 (CD1) 5m	40.8	815
5/21/2015	LCCMR6	St BP 5m	41.4	827
5/22/2015	LCCMR6	St 5 5m	41.4	827
5/22/2015	LCCMR6	St 10 5m	40.8	815
5/22/2015	LCCMR6	St 11 60m	40.8	815
5/22/2015	LCCMR6	St 11 5m	41.7	833
5/21/2015	LCCMR6	Check Std 40.0 mg/L CaCO3	39.3	786
7/15/2015	LCCMR7	St 4 (OS) 5m	41.1	822
7/15/2015	LCCMR7	St 1 5m	42.6	851
7/15/2015	LCCMR7	St 12 5m	43.6	872
7/15/2015	LCCMR7	St 7 5m	41.7	834
7/15/2015	LCCMR7	St 8 5m	40.6	810
7/16/2015	LCCMR7	St 3 (WM) 5m	41.4	828
7/16/2015	LCCMR7	St 3 (WM) 30m	41.1	822
7/16/2015	LCCMR7	St 3 (WM) 120m	40.6	810
7/16/2015	LCCMR7	St 5 5m	42.3	846
7/16/2015	LCCMR7	St 2 (CD1) 5m	41.7	834
7/16/2015	LCCMR7	St 2 (CD1) 30m	41.7	834
7/16/2015	LCCMR7	St 2 (CD1) 120m	42.0	840
7/16/2015	LCCMR7	St BP 5m	40.6	810
7/17/2015	LCCMR7	St 9 5m	42.3	846
7/17/2015	LCCMR7	St 6 5m	42.6	851
7/17/2015	LCCMR7	St 10 5m	42.6	851
7/17/2015	LCCMR7	St 11 5m	42.6	851
7/17/2015	LCCMR7	St 11 13m	43.2	863
7/17/2015	LCCMR7	St 11 60m	41.7	834
7/16/2015	LCCMR7	Check Std 40.0 mg/L CaCO3	39.4	787
9/8/2015	LCCMR8	St 4 (OS) 5m*	40.8	814
9/8/2015	LCCMR8	St 1 5m*	41.6	831
9/8/2015	LCCMR8	St 12 5m*	41.5	830
9/8/2015	LCCMR8	St 7 5m*	41.3	825
9/8/2015	LCCMR8	St 6 5m*	40.9	817
9/8/2015	LCCMR8	St 8 5m*	41.7	832
9/9/2015	LCCMR8	St 3 (WM) 5m*	41.3	824
9/9/2015	LCCMR8	St 3 (WM) 20m*	41.6	830
9/9/2015	LCCMR8	St 3 (WM) 120m	42.2	843
9/9/2015	LCCMR8	St 2 (CD1) 5m *	41.4	827
9/9/2015	LCCMR8	St 2 (CD1) 22m*	40.8	815
9/9/2015	LCCMR8	St 2 (CD1) 210m*	41.9	838
9/9/2015	LCCMR8	St BP 5m*	40.3	806
9/10/2015	LCCMR8	St 9 5m*	41.2	823
9/10/2015	LCCMR8	St 5 5m*	41.5	829
9/10/2015	LCCMR8	St 10 5m*	41.7	833
9/10/2015	LCCMR8	St 11 5m*	41.8	835
9/10/2015	LCCMR8	St 11 17m*	42.7	852
9/10/2015	LCCMR8	St 11 60m*	42.0	840
9/9/2015	LCCMR8	Check Std 40.0 mg/L CaCO3*	39.5	789

Table VI-9. Total inorganic carbon concentrations (mg L^{-1}; µmol L^{-1}) for Lake Superior western arm sampling stations for all depths sampled during LCCMR 2014 cruises.

Date	Cruise	Station	TIC (mg/L C)	TIC St. Dev. (mg/L C)	TIC (umol/L C)
6/3/2014	LCCMR1	St 4 (OS) 5m	10.0	0.15	836
6/3/2014	LCCMR1	St 1 5m	10.0	0.12	834
6/3/2014	LCCMR1	St 2 (CD1) 210m	11.4	0.16	951
6/3/2014	LCCMR1	St 2 (CD1) 35m	10.7	0.18	894
6/3/2014	LCCMR1	St 2 (CD1) 5m	10.8	0.13	896
6/4/2014	LCCMR1	St 3 (WM) 5m	10.2	0.07	852
6/4/2014	LCCMR1	St 3 (WM) 120m	9.8	0.25	815
6/4/2014	LCCMR1	St 3 (WM) 30m	10.3	0.19	861
6/5/2014	LCCMR1	St 8 5m	10.1	0.15	844
6/5/2014	LCCMR1	St 10 5m	10.5	0.10	871
6/5/2014	LCCMR1	St 11 20m	10.2	0.08	850
6/5/2014	LCCMR1	St 11 60m	10.2	0.14	848
6/5/2014	LCCMR1	St 11 5m	10.3	0.21	854
6/5/2014	LCCMR1	St 12 5m	9.6	0.11	800
6/5/2014	LCCMR1	St 9 5m	10.1	0.15	844
6/6/2014	LCCMR1	St 5 5m	10.3	0.07	856
6/6/2014	LCCMR1	St 7 5m	10.3	0.18	855
6/12/2014	LCCMR1	Check Std 11.13 mg/L C	11.3	0.14	941
7/22/2014	LCCMR2-3	St 4 (OS) 5m	10.3	0.05	858
7/22/2014	LCCMR2-3	St 1 5m	10.3	0.12	854
7/22/2014	LCCMR2-3	St 2 (CD1) 5m	10.7	0.15	888
7/22/2014	LCCMR2-3	St 2 (CD1) 35m	10.5	0.12	875
7/22/2014	LCCMR2-3	St 2 (CD1) 210m	10.5	0.11	872
7/23/2014	LCCMR2-3	St 3 (WM) 5m	10.4	0.11	866
7/23/2014	LCCMR2-3	St 3 (WM) 120m	10.7	0.17	891
7/23/2014	LCCMR2-3	St 3 (WM) 30m	10.4	0.13	865
7/24/2014	LCCMR2-3	St 8 5m	10.3	0.12	861
7/24/2014	LCCMR2-3	St 10 5m	10.4	0.15	865
7/24/2014	LCCMR2-3	St 11 5m	10.3	0.11	858
7/24/2014	LCCMR2-3	St 11 12m	10.6	0.19	879
7/24/2014	LCCMR2-3	St 12 2m	10.8	0.17	897
7/24/2014	LCCMR2-3	St 9 5m	10.6	0.21	879
7/25/2014	LCCMR2-3	St BP 5m	10.6	0.21	882
7/25/2014	LCCMR2-3	St 5 5m	10.5	0.14	870
7/25/2014	LCCMR2-3	St 7 2m	10.3	0.10	858
7/25/2014	LCCMR2-3	St 6 5m	10.6	0.16	885
8/29/2014	LCCMR2-3	Check Std 10.11 mg/L C	12.8	0.22	1063
8/16/2014	LCCMR4	St 1 5m	9.9	0.18	827
8/16/2014	LCCMR4	St 2 (CD1) 18m	10.0	0.17	830
8/16/2014	LCCMR4	St 2 (CD1) 210m	10.3	0.16	854
8/16/2014	LCCMR4	St 2 (CD1) 5m	9.9	0.10	827
8/16/2014	LCCMR4	St 4 (OS) 5m	10.0	0.11	833
8/17/2014	LCCMR4	St 3 (WM) 120m	10.2	0.06	852
8/17/2014	LCCMR4	St 3 (WM) 30m	10.1	0.19	845
8/17/2014	LCCMR4	St 3 (WM) 5m	10.0	0.13	835
8/18/2014	LCCMR4	St 10 5m	10.0	0.14	833
8/18/2014	LCCMR4	St 11 14m	10.2	0.14	849
8/18/2014	LCCMR4	St 11 5m	10.1	0.16	843
8/18/2014	LCCMR4	St 11 60m	10.4	0.10	869
8/18/2014	LCCMR4	St 12 5m	10.1	0.19	843
8/18/2014	LCCMR4	St 8 5m	10.0	0.13	831
8/18/2014	LCCMR4	St 9 5m	10.0	0.13	837
8/19/2014	LCCMR4	St BP 5m	10.0	0.10	831
8/19/2014	LCCMR4	St 5 5m	10.1	0.12	839
8/19/2014	LCCMR4	St 6 5m	10.1	0.13	844
8/19/2014	LCCMR4	St 7 5m	10.3	0.06	855
9/30/2014	LCCMR4	Check Std 10.07 mg/L C	9.8	0.12	819
9/24/2014	UNOLS Inspection	St 4 (OS) 25m	10.1	0.19	838
9/24/2014	UNOLS Inspection	St 4 (OS) 5m	10.3	0.15	859
9/30/2014	UNOLS Inspection	Check Std 7.78 mg/L C	7.9	0.09	661
9/30/2014	LCCMR5	St 2 (CD1) 5m	10.0	0.11	834
9/30/2014	LCCMR5	St 2 (CD1) 20m	10.0	0.17	831
9/30/2014	LCCMR5	St 2 (CD1) 210m	10.3	0.16	855
9/30/2014	LCCMR5	St 4 (OS) 5m	10.1	0.16	844
9/30/2014	LCCMR5	St 1 5m	10.2	0.11	852
10/1/2014	LCCMR5	St 3 (WM) 5m	10.1	0.13	838
10/1/2014	LCCMR5	St 3 (WM) 30m	10.1	0.11	841
10/1/2014	LCCMR5	St 3 (WM) 120m	10.3	0.11	861
10/1/2014	LCCMR5	St 8 5m	10.1	0.13	838
10/2/2014	LCCMR5	St 12 5m	10.1	0.13	841
10/2/2014	LCCMR5	St 11 60m	10.4	0.14	865
10/2/2014	LCCMR5	St 11 10m	10.1	0.13	839
10/2/2014	LCCMR5	St 11 5m	10.1	0.18	838
10/2/2014	LCCMR5	St 9 5m	10.1	0.16	843
10/2/2014	LCCMR5	St 10 5m	10.1	0.12	844
10/2/2014	LCCMR5	St 7 5m	10.2	0.18	850
10/2/2014	LCCMR5	St 6 5m	10.2	0.16	847
10/2/2014	LCCMR5	St 5 5m	10.2	0.06	850
10/14/2014	LCCMR5	Check Std 9.82 mg/L C	10.1	0.12	838

Table VI-10. Total inorganic carbon concentrations (mg L^{-1}; µmol L^{-1}) for Lake Superior western arm sampling stations for all depths sampled during LCCMR 2015 cruises.

Date	Cruise	Station	TIC (mg/L C)	TIC St. Dev. (mg/L C)	TIC (umol/L C)
2/8/2015	Bayfield Ice Road	Bayfield 10m	10.4	0.09	864
2/8/2015	Bayfield Ice Road	Bayfield 20m	10.3	0.09	861
2/9/2015	Bayfield Ice Road	Check Std 11.42 mg/L C	11.8	0.13	979
5/19/2015	LCCMR6	St 4 (OS) 5m	9.5	0.12	787
5/20/2015	LCCMR6	St 1 5m	9.5	0.03	790
5/20/2015	LCCMR6	St 12 5m	9.5	0.11	788
5/20/2015	LCCMR6	St 9 5m	9.5	0.13	788
5/20/2015	LCCMR6	St 7 5m	9.4	0.02	780
5/20/2015	LCCMR6	St 6 5m	9.3	0.06	776
5/21/2015	LCCMR6	St 3 (WM) 5m	9.2	0.03	763
5/21/2015	LCCMR6	St 3 (WM) 120m	9.2	0.01	769
5/21/2015	LCCMR6	St 3 (WM) 30m	9.3	0.06	772
5/21/2015	LCCMR6	St 8 5m	9.3	0.03	774
5/21/2015	LCCMR6	St 2 (CD1) 210m	9.3	0.03	777
5/21/2015	LCCMR6	St 2 (CD1) 20m	9.3	0.05	778
5/21/2015	LCCMR6	St 2 (CD1) 5m	9.3	0.03	772
5/21/2015	LCCMR6	St BP 5m	9.3	0.03	773
5/22/2015	LCCMR6	St 5 5m	9.3	0.05	778
5/22/2015	LCCMR6	St 10 5m	9.3	0.03	775
5/22/2015	LCCMR6	St 11 60m	9.6	0.09	797
5/22/2015	LCCMR6	St 11 25m	9.3	0.10	773
5/22/2015	LCCMR6	St 11 5m	9.3	0.04	777
6/22/2015	LCCMR6	Check Std 10.79 mg/L C	10.5	0.07	873
7/15/2015	LCCMR7	St 4 (OS) 5m	9.4	0.10	781
7/15/2015	LCCMR7	St 1 5m	9.5	0.18	789
7/15/2015	LCCMR7	St 12 5m	9.9	0.06	822
7/15/2015	LCCMR7	St 7 5m	9.5	0.10	793
7/15/2015	LCCMR7	St 8 5m	9.3	0.08	775
7/16/2015	LCCMR7	St 3 (WM) 5m	9.4	0.14	783
7/16/2015	LCCMR7	St 3 (WM) 30m	9.5	0.09	789
7/16/2015	LCCMR7	St 3 (WM) 120m	9.5	0.11	791
7/16/2015	LCCMR7	St 5 5m	9.6	0.11	797
7/16/2015	LCCMR7	St 2 (CD1) 5m	9.3	0.04	775
7/16/2015	LCCMR7	St 2 (CD1) 30m	9.5	0.08	795
7/16/2015	LCCMR7	St 2 (CD1) 120m	9.6	0.10	798
7/16/2015	LCCMR7	St BP 5m	9.2	0.16	770
7/17/2015	LCCMR7	St 9 5m	9.6	0.12	796
7/17/2015	LCCMR7	St 6 5m	9.5	0.09	792
7/17/2015	LCCMR7	St 10 5m	9.6	0.07	795
7/17/2015	LCCMR7	St 11 5m	9.6	0.05	797
7/17/2015	LCCMR7	St 11 13m	9.7	0.10	811
7/17/2015	LCCMR7	St 11 60m	9.8	0.07	814
7/20/2015	LCCMR7	Check Std 9.83 mg/L C	9.9	0.13	824
9/8/2015	LCCMR8	St 4 (OS) 5m	9.4	0.08	781
9/8/2015	LCCMR8	St 1 5m	9.6	0.20	800
9/8/2015	LCCMR8	St 12 5m	9.5	0.08	792
9/8/2015	LCCMR8	St 7 5m	9.4	0.05	785
9/8/2015	LCCMR8	St 6 5m	9.6	0.09	798
9/8/2015	LCCMR8	St 8 5m	9.4	0.09	779
9/9/2015	LCCMR8	St 3 (WM) 5m	9.5	0.06	790
9/9/2015	LCCMR8	St 3 (WM) 20m	9.5	0.08	790
9/9/2015	LCCMR8	St 3 (WM) 120m	9.8	0.05	815
9/9/2015	LCCMR8	St 2 (CD1) 5m	9.4	0.05	782
9/9/2015	LCCMR8	St 2 (CD1) 22m	9.7	0.11	806
9/9/2015	LCCMR8	St 2 (CD1) 210m	9.8	0.08	819
9/9/2015	LCCMR8	St BP 5m	9.4	0.10	779
9/10/2015	LCCMR8	St 9 5m	9.4	0.07	785
9/10/2015	LCCMR8	St 5 5m	9.5	0.12	794
9/10/2015	LCCMR8	St 10 5m	9.5	0.09	793
9/10/2015	LCCMR8	St 11 5m	9.6	0.11	799
9/10/2015	LCCMR8	St 11 17m	9.7	0.07	805
9/10/2015	LCCMR8	St 11 60m	10.1	0.13	838
9/14/2015	LCCMR8	Check Std 10.21 mg/L C	10.4	0.06	868
10/5/2015	LCCMR9	St 4 (OS) 5m	9.6	0.10	796
10/5/2015	LCCMR9	St 1 5m	9.6	0.09	801
10/5/2015	LCCMR9	St 12 5m	9.7	0.14	808
10/5/2015	LCCMR9	St 7 5m	9.5	0.09	794
10/5/2015	LCCMR9	St 8 5m	9.6	0.08	802
10/6/2015	LCCMR9	St 3 (WM) 120m	9.7	0.14	806
10/6/2015	LCCMR9	St 3 (WM) 25m	9.7	0.14	807
10/6/2015	LCCMR9	St 3 (WM) 5m	9.6	0.10	795
10/6/2015	LCCMR9	St 5 5m	9.7	0.11	804
10/6/2015	LCCMR9	St 2 (CD1) 210m	9.8	0.10	815
10/6/2015	LCCMR9	St 2 (CD1) 45m	9.6	0.06	800
10/6/2015	LCCMR9	St 2 (CD1) 5m	9.6	0.10	796
10/6/2015	LCCMR9	St BP 5m	9.6	0.08	798
10/7/2015	LCCMR9	St 9 5m	9.5	0.13	791
10/7/2015	LCCMR9	St 6 5m	9.5	0.10	791
10/7/2015	LCCMR9	St 10 5m	9.6	0.07	801
10/7/2015	LCCMR9	St 11 60m	9.7	0.08	804
10/7/2015	LCCMR9	St 11 10m	9.6	0.07	798
10/7/2015	LCCMR9	St 11 5m	9.6	0.10	796
10/9/2015	LCCMR9	Check Std 9.35 mg/L C	9.3	0.06	775
11/11/2015	Mooring	Mooring	9.3	0.07	775
11/13/2015	Mooring	Check Std 10.01 mg/L C	9.6	0.07	802

Table VI-11. pCO_2 values for all rivers sampled discharging to the western arm of Lake Superior within the Superior, Wisconsin and Duluth, Minnesota area.

Date	River	Station	pCO_2	Latitude (^oN)	Longitude (^oW)
9/11/2014	Amity Creek	AC 85	538.2	46.8402	92.007569
10/16/2014	Amity Creek	AC 86	330.0	46.8402	92.007569
11/13/2014	Amity Creek	AC 87	439.6	46.8402	92.007569
12/16/2014	Amity Creek	AC 88	594.7	46.8402	92.007569
3/24/2015	Amity Creek	AC 89	453.5	46.8402	92.007569
4/24/2015	Amity Creek	AC 90	351.1	46.8402	92.007569
6/3/2015	Amity Creek	AC 91	443.7	46.8402	92.007569
6/17/2015	Amity Creek	AC 92	514.8	46.8402	92.007569
7/29/2015	Amity Creek	AC 93	490.3	46.8402	92.007569
10/29/2014	Nemadji River	NR 01	1594.1	46.6979	92.03251
1/28/2015	Nemadji River	Nemadji R. L.W.R	1829.3	46.66602	92.06453
1/28/2015	Nemadji River	Nemadji R. Mouth	2021.8	46.69468	92.0369
4/29/2015	Nemadji River	NR 02	1428.2	46.6979	92.03251
7/1/2015	Nemadji River	NR 03	1817.3	46.6979	92.03251
8/20/2015	Nemadji River	NR 04	2075.5	46.6979	92.03251
11/6/2014	St. Louis River	SLB 01	969.1	46.653503	92.226505
1/29/2015	St. Louis River	SLR Boyscout Chann.	1280.3	46.653	92.22615
1/29/2015	St. Louis River	SLR Boyscout Bay	1941.8	46.35652	92.23378
5/6/2015	St. Louis River	SLB 02	829.8	46.653503	92.226505
7/7/2015	St. Louis River	SLB 03	1416.4	46.653503	92.226505
8/25/2015	St. Louis River	SLB 04	950.1	46.653503	92.226505
10/23/2014	St. Louis River	SLM 01	432.6	46.77848	92.09281
11/21/2014	St. Louis River	SLM 02	454.0	46.77848	92.09281
12/11/2014	St. Louis River	SLM 03	552.8	46.77848	92.09281
1/8/2015	St. Louis River	SLM 04	861.3	46.77848	92.09281
1/15/2015	St. Louis River	SLM 05	611.1	46.77848	92.09281
4/23/2015	St. Louis River	SLM 06	468.1	46.77848	92.09281
6/4/2015	St. Louis River	SLM 07	782.4	46.77848	92.09281
6/24/2015	St. Louis River	SLM 08	1191.4	46.77848	92.09281
8/4/2015	St. Louis River	SLM 09	423.0	46.77848	92.09281

Table VI-12. pH, blank corrected acid neutralizing capacity (unfiltered; mg L^{-1} and µeq L^{-1} as $CaCO_3$), organic carbon (mg L^{-1}) and inorganic carbon (mg L^{-1} and µmol L^{-1}) for all rivers sampled discharging to the western arm of Lake Superior within the Superior, Wisconsin and Duluth, Minnesota area.

Date	River	Station	pH	ANC (mg/L CaCO3)	ANC (ueq/L CaCO3)	DOC (mg/L C)	TOC (mg/L C)	POC (mg/L C)	TIC (mg/L C)	TIC (umol/L C)
9/11/2014	Amity Creek	AC 85	8.3	132.0	2637				29.2	2431
10/16/2014	Amity Creek	AC 86	8.446	111.3	2224				28.1	2338
11/13/2014	Amity Creek	AC 87	8.178	117.5	2347				27.5	2286
12/16/2014	Amity Creek	AC 88	7.851	81.9	1637				18.4	1535
3/24/2015	Amity Creek	AC 89	7.894	64.9	1298	6.41	6.49	0.08	14.9	1239
4/24/2015	Amity Creek	AC 90	8.051	64.1	1280	8.02	8.07	0.05	14.7	1223
6/3/2015	Amity Creek	AC 91	8.240	88.9	1777	8.41	8.70	0.28	19.8	1646
6/17/2015	Amity Creek	AC 92	8.316	113.5	2268	6.78	6.76	-0.02	26.0	2168
7/29/2015	Amity Creek	AC 93	8.470	128.0	2557	6.9	7.0	0.19	28.7	2388
10/29/2014	Nemadji River	NR 01	7.664	93.7	1873				22.4	1863
1/28/2015	Nemadji River	Nemadji R. L.W.R	7.554	112.9	2256		5.40		27.6	2296
1/28/2015	Nemadji River	Nemadji R. Mouth	7.521	113.2	2262		5.74		28.3	2352
4/29/2015	Nemadji River	NR 02	7.610	62.0	1239	12.92	12.83	-0.09	15.5	1287
7/1/2015	Nemadji River	NR 03	7.876	106.8	2133	10.78	11.66	0.88	25.0	2084
8/20/2015	Nemadji River	NR 04	7.711	93.3	1864	15.3	15.1	-0.23	22.0	1833
11/6/2014	St. Louis River	SLB 01	8.051	137.8	2754				34.1	2835
1/29/2015	St. Louis River	SLR Boyscout Chann.	7.660	97.1	1940		10.94		24.3	2022
1/29/2015	St. Louis River	SLR Boyscout Bay	7.477	99.5	1987		11.45		24.7	2056
5/6/2015	St. Louis River	SLB 02	7.955	76.3	1525	13.62	13.76	0.14	18.4	1529
7/7/2015	St. Louis River	SLB 03	7.747	71.4	1426	21.6	21.4	-0.21	15.6	1295
8/25/2015	St. Louis River	SLB 04	8.044	101.2	2022	12.6	12.8	0.18	22.5	1877
10/23/2014	St. Louis River	SLM 01	7.939	47.2	942				10.5	878
11/21/2014	St. Louis River	SLM 02	7.897	59.4	1188				13.4	1119
12/11/2014	St. Louis River	SLM 03	7.770	61.0	1218				13.6	1134
1/8/2015	St. Louis River	SLM 04	7.664	68.2	1362	6.3	6.3	0.07	16.5	1376
1/15/2015	St. Louis River	SLM 05	7.694	53.8	1075	2.59	2.85	0.26	12.6	1052
4/23/2015	St. Louis River	SLM 06	7.827	44.8	894	1.64	1.69	0.05	10.9	911
6/4/2015	St. Louis River	SLM 07	7.733	50.3	1005	17.73	18.81	1.08	10.7	894
6/24/2015	St. Louis River	SLM 08	7.679	56.5	1128	12.60	12.95	0.35	12.5	1040
8/4/2015	St. Louis River	SLM 09	8.058	51.2	1023	4.6	4.7	0.10	11.2	932

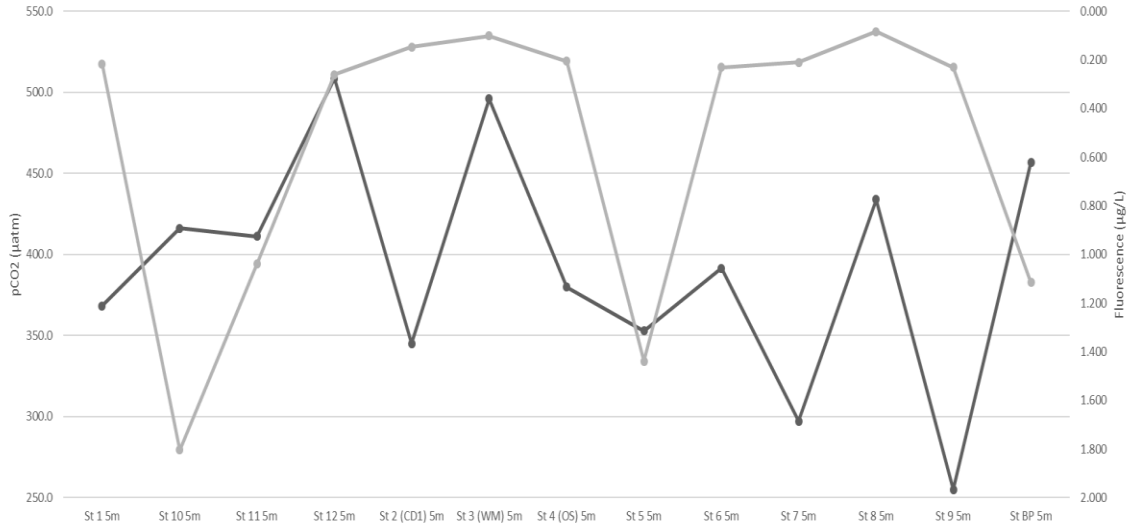

Figure VI-1. Standard plot of mean lake surface pCO_2 (µatm; black) and chlorophyll fluorescence (µg L^{-1}; grey) at all western arm sampling stations during LCCMR7 (July 2015).

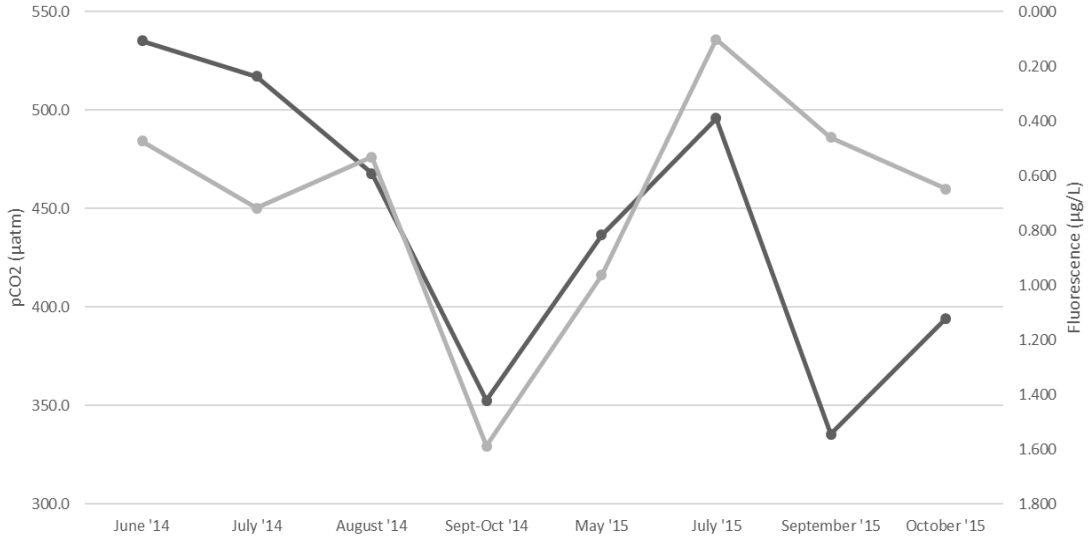

Figure VI-2. Standard plot of mean lake surface pCO_2 (µatm; black) and chlorophyll fluorescence (µg L^{-1}; grey) at Station 3 (WM) for all LCCMR cruises. All surface water samples taken at 5 m depth.

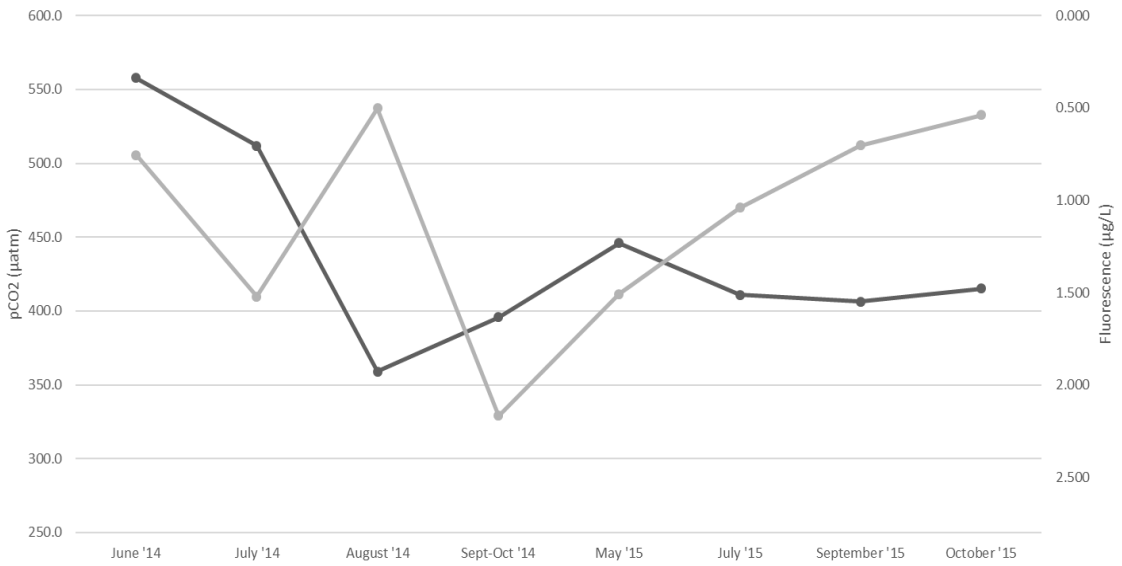

Figure VI-3. Standard plot of mean lake surface pCO_2 (µatm; black) and chlorophyll fluorescence (µg L^{-1}; grey) at Station 11 for all LCCMR cruises. All surface water samples taken at 5 m depth.

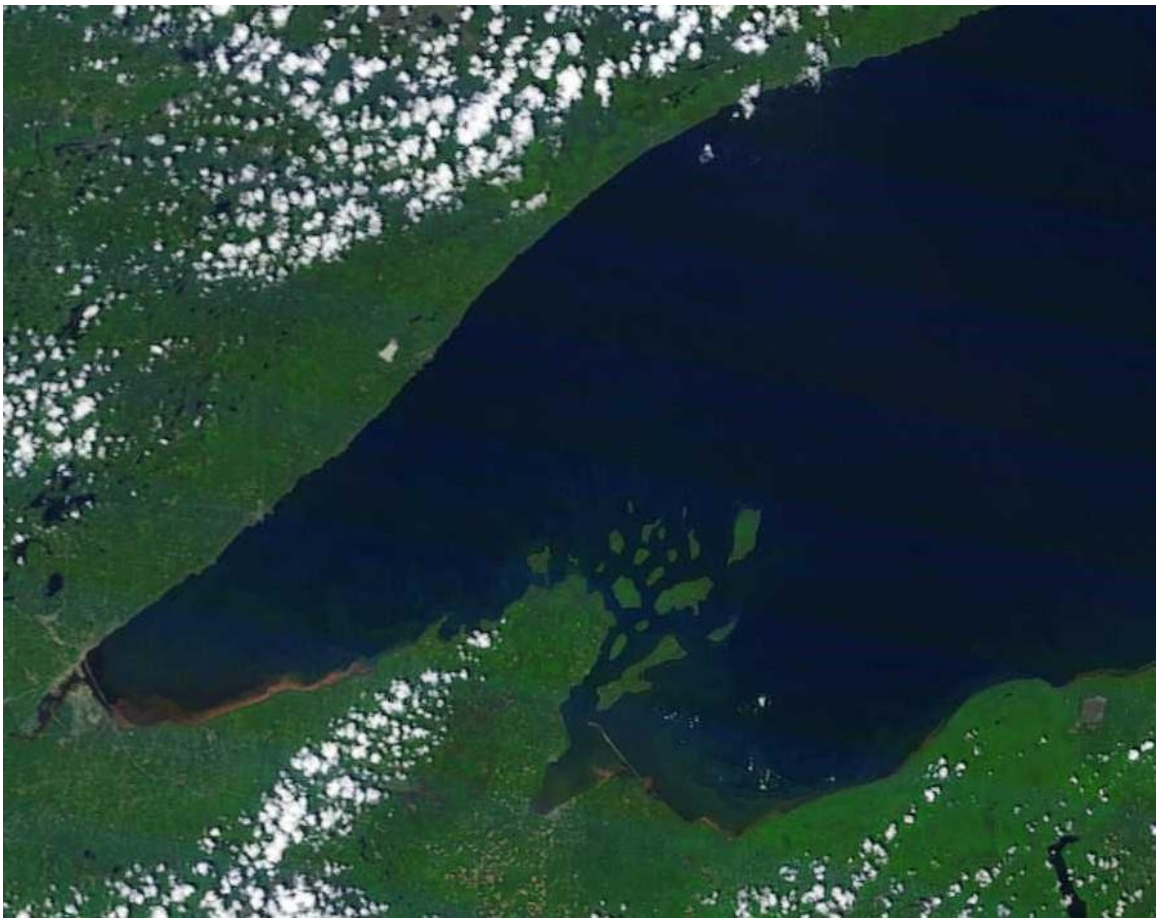

Figure VI-4. MODIS satellite image (16:44; 6/4/2014) of the western arm of Lake Superior corresponding to LCCMR1 cruise dates (6/3/2014 – 6/6/2014).

Figure VI-5. MODIS satellite image (18:59; 7/23/2014) of the western arm of Lake Superior corresponding to LCCMR2-3 cruise dates (7/22/2014 – 7/25/2014).

Figure VI-6. MODIS satellite image (19:11; 8/15/2014) of the western arm of Lake Superior corresponding to LCCMR4 cruise dates (8/16/2014 – 8/19/2014).

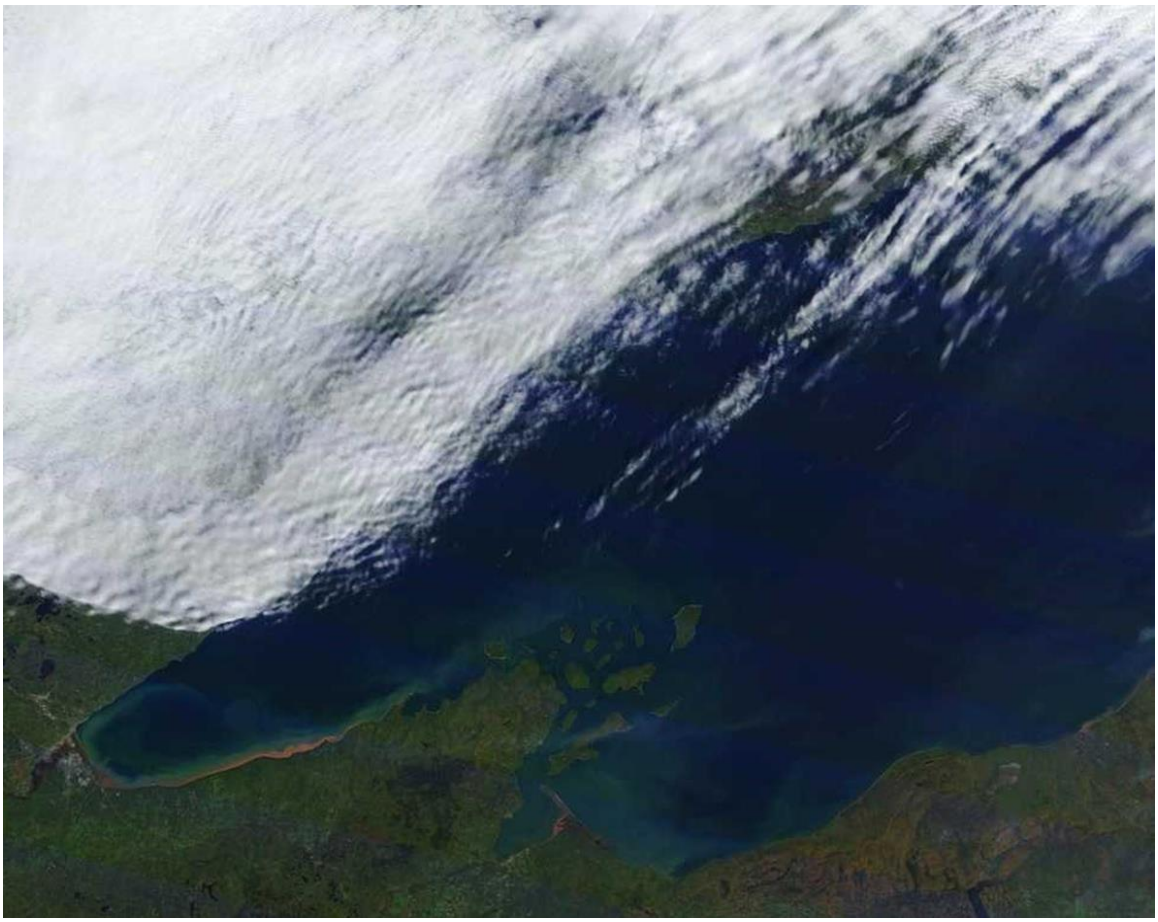

Figure VI-7. MODIS satellite image (17:05; 10/6/2014) of the western arm of Lake Superior corresponding to LCCMR5 cruise dates (9/30/2014 – 10/2/2014).

Figure VI-8. MODIS satellite image (19:13; 5/21/2015) of the western arm of Lake Superior corresponding to LCCMR6 cruise dates (5/19/2015 – 5/22/2015).

Figure VI-9. MODIS satellite image (19:06; 7/17/2015) of the western arm of Lake Superior corresponding to LCCMR7 cruise dates (7/15/2015 – 7/17/2015).

Figure VI-10. MODIS satellite image (16:50; 9/9/2015) of the western arm of Lake Superior corresponding to LCCMR8 cruise dates (9/8/2015 – 9/10/2015).

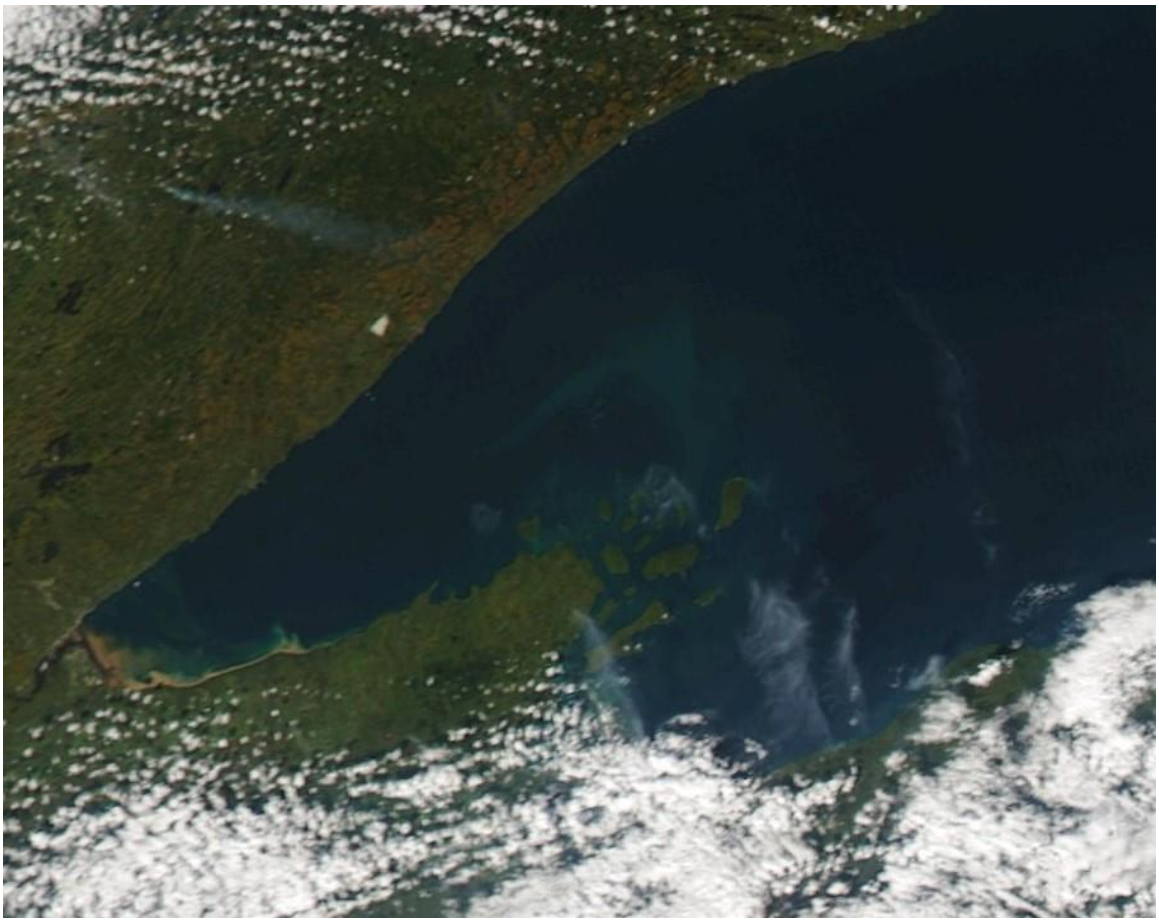

Figure VI-11. MODIS satellite image (18:12; 10/6/2015) of the western arm of Lake Superior corresponding to LCCMR9 cruise dates (10/5/2015 – 10/7/2015).